

**SEQUENTIAL DELIVERY OF ANGIOGENIC GROWTH FACTORS FROM POROUS
HOLLOW FIBER MEMBRANES**

by

Jillian Erin Tengood

B.S. in Chemical Engineering, Lehigh University, 2004

Submitted to the Graduate Faculty of
Swanson School of Engineering in partial fulfillment
of the requirements for the degree of
Doctor of Philosophy

University of Pittsburgh

2011

UNIVERSITY OF PITTSBURGH
SWANSON SCHOOL OF ENGINEERING

This dissertation was presented

by

Jillian Erin Tengood

It was defended on

November 23, 2010

and approved by

Alan Russell, PhD, University Distinguished Professor, Departments of Surgery,
Bioengineering and Chemical Engineering

William Wagner, PhD, Professor, Departments of Surgery, Bioengineering and Chemical
Engineering

Alan Wells, MD DMSc, Thomas Gill Professor, Departments of Pathology and
Bioengineering

Dissertation Director: Steven Little, PhD, Assistant Professor, Departments of Chemical
Engineering, Bioengineering and Immunology

Copyright © by Jillian Erin Tengood

2011

SEQUENTIAL DELIVERY OF ANGIOGENIC GROWTH FACTORS FROM POROUS HOLLOW FIBER MEMBRANES

Jillian Erin Tengood, PhD

University of Pittsburgh, 2011

Angiogenesis, often thought of as the first step of wound healing, is an organized series of events, beginning with vessel destabilization, followed by endothelial cell proliferation and migration, ending with vessel maturation. Vascular endothelial growth factor (VEGF) and basic fibroblast growth factor (bFGF) have been shown to be important in vascular permeability and endothelial cell proliferation, and migration (early stage angiogenesis), while platelet derived growth factor (PDGF) and sphingosine 1-phosphate (S1P) have been shown to stimulate vascular stability (late stage angiogenesis). For this reason, it was hypothesized that inducing angiogenesis by sequentially delivering angiogenic growth factors, controlling their presence and absence, would better mimic the temporal role of each factor during the progression of native angiogenesis *in situ*. To this end, we utilized a delivery system based on porous cellulose hollow fibers that, for the first time, permits sequential delivery of an early stage factor followed by a late stage growth factor *in vivo*, where previous attempts have only resulted in different rates of delivery. Our delivery system addresses the idea that factors involved in one stage of angiogenesis may inhibit other stages of angiogenesis, causing absence of one factor to be just as important as the presence of another factor. Using a modified murine Matrigel plug model, it is apparent that delivery strategies where VEGF alone is delivered before S1P alone as well as delivery strategies where bFGF alone is delivered before PDGF alone, not only lead to greater recruitment of endothelial cells, but also higher maturation index of associated vessels.

Sequential delivery was also optimized by examining varying delivery schedules. Additionally, the hollow fiber delivery system, was analyzed for its transport properties, where it was discovered that transport from the lumen of the hollow fiber to the surrounding environment was not only based on diffusion of the factor, but osmosis-driven convection as well. Sequential delivery strategies such as this one have potential to improve wound healing strategies involving angiogenesis as well as other types of tissue formation that occur in a series of organized stages.

TABLE OF CONTENTS

PREFACE.....	XV
1.0 INTRODUCTION.....	1
1.1 WOUND HEALING STAGES	1
1.2 CLINICAL WOUNDS AND TREATMENTS.....	3
1.2.1 Wound types	3
1.2.2 Current treatment options	5
1.3 TISSUE ENGINEERING AS A TREATMENT FOR WOUNDS	6
2.0 NEOVASCULARIZATION	9
2.1 ANGIOGENESIS.....	9
2.2 VASCULOGENESIS.....	10
2.3 VASCULOGENESIS AS A THERAPY	12
2.4 BLOOD VESSEL WIDENING, SPLITTING AND EXPANSION	13
3.0 ANGIOGENESIS.....	14
3.1 ANATOMY OF A BLOOD VESSEL	14
3.1.1 Endothelial Cells	14
3.1.2 Mural Cells	15
3.1.3 Basement Membrane	16
3.2 ANGIOGENIC GROWTH FACTORS.....	17

3.2.1	Vascular endothelial growth factor	17
3.2.2	Basic fibroblast growth factor	18
3.2.3	Platelet derived growth factor	19
3.2.4	Sphingosine 1-phosphate	20
3.2.5	Other growth factors involved in angiogenesis	21
4.0	ANGIOGENESIS THERAPIES FOR TISSUE REGENERATION	23
4.1	INDUCTION VIA GROWTH FACTORS	23
4.2	CONDUCTION VIA BIOENGINEERED SCAFFOLDS	26
4.3	CELL TRANSPLANTATION (CELL THERAPY)	29
5.0	CONTROLLED GROWTH FACTOR DELIVERY	31
5.1	PROOF OF CONCEPT MODELS	33
5.2	HINDLIMB ISCHEMIA MODELS	34
5.3	MYOCARDIAL INFARCTION MODELS	35
5.4	ANIMAL MODEL TRANSLATION	36
6.0	STAGE-WISE ANGIOGENESIS	37
6.1	EARLY ANGIOGENESIS	37
6.2	LATE ANGIOGENESIS	38
6.3	PHYSIOLOGIC GROWTH FACTOR TIMING	39
6.4	GROWTH FACTOR INTERACTIONS	41
7.0	SEQUENTIAL DELIVERY	42
7.1	INTRODUCTION	42
7.2	COMBINED RELEASE SYSTEMS	44
7.3	LAYER BY LAYER FILMS	52
7.4	MICROCHIP TECHNOLOGY	60

7.5	EMERGING RELEASE TECHNOLOGY – TUNABLE MICROPARTICLES	64
7.6	CONCLUSIONS	68
8.0	SEQUENTIAL DELIVERY OF VEGF AND S1P	70
8.1	INTRODUCTION.....	70
8.2	MATERIALS AND METHODS	72
8.2.1	Hollow fiber fabrication and characterization.....	72
8.2.2	<i>In vitro</i> release	73
8.2.3	Murine Matrigel plug assay	73
8.2.4	Immunofluorescence.....	74
8.2.5	Statistical analysis.....	74
8.3	RESULTS	75
8.3.1	Hollow fiber fabrication	75
8.3.2	Sequential delivery of molecules of relevant size	76
8.3.3	Endothelial cell recruitment and vessel formation	79
8.3.4	Vascular maturation index.....	85
8.4	DISCUSSION	89
8.5	CONCLUSION	96
8.6	SUPPLEMENTAL INFORMATION.....	97
8.6.1	Methods: Tubular formation assay.....	97
8.6.2	Results: Endothelial cell tubular formation following angiogenic factor release from hollow fibers through Matrigel <i>in vitro</i>	97
9.0	SEQUENTIAL DELIVERY OF BASIC-FGF AND PDGF	100

9.1	INTRODUCTION.....	100
9.2	MATERIALS AND METHODS	102
9.2.1	Hollow fiber fabrication and characterization.....	102
9.2.2	<i>In vitro</i> release	102
9.2.3	Murine Matrigel plug assay	103
9.2.4	Immunofluorescence.....	104
9.2.5	Statistical analysis	104
9.3	RESULTS	105
9.3.1	Sequential bFGF and PDGF release from cellulose hollow fibers	105
9.3.2	Recruitment of endothelial cells to Matrigel plugs in response to various treatment schedules.....	106
9.3.3	Vessel maturation in response to various treatment schedules	109
9.3.4	Integration of neovasculature with native vasculature	111
9.4	DISCUSSION	114
9.5	CONCLUSION	120
10.0	MODELING RELEASE FROM POROUS HOLLOW FIBERS	121
10.1	INTRODUCTION.....	121
10.2	THEORY AND MODEL DEVELOPMENT	123
10.2.1	Diffusion.....	123
10.2.2	Osmotic and hydrostatic pressure.....	125
10.2.3	Model.....	126
10.3	METHODS AND MATERIALS	130
10.3.1	Hollow fiber fabrication	130

10.3.2	Hollow fiber image analysis and characterization.....	130
10.3.3	Release studies.....	132
10.3.4	Osmolality determination.....	132
10.4	RESULTS	133
10.4.1	Hollow fiber characteristics	133
10.4.2	Osmolality	134
10.4.3	Model predictions and release data.....	135
10.4.4	Model prediction for long term release.....	141
10.5	DISCUSSION	142
10.6	CONCLUSION	146
11.0	SUMMARY AND CONCLUSIONS	148
12.0	FUTURE WORK.....	150
	BIBLIOGRAPHY.....	152

LIST OF TABLES

Table 1. Hollow fiber fabrication conditions.....	131
Table 2. Hollow fiber model parameters.	134

LIST OF FIGURES

Figure 1. Vessel cross section.....	16
Figure 2. Growth factor involvement in angiogenesis events. ¹	40
Figure 3. Cumulative release of VEGF and PDGF from a combined polymeric scaffold. ⁶⁷	46
Figure 4. Total release of VEGF and PDGF from a layered polymeric scaffold. ²¹³	48
Figure 5. VEGF ₁₆₅ and PDGF-BB release from alginate hydrogels of varying molecular weight. ²¹⁴	49
Figure 6. <i>In vitro</i> release kinetics of pre-encapsulated PDGF and VEGF from alginate fabricated from poly lactide-co-glycolide. ²¹⁶	51
Figure 7. Layer-by-layer film fabrication technique. ²¹⁹	52
Figure 8. COS expression of temporal delivery of DNA. ²²⁸	57
Figure 9. Release of heparin and dextran sulfate from LBL film. ¹⁹³	58
Figure 10. Pulsatile release of a single substance from a microchip device. ²³²	61
Figure 11. Cumulative percent of initial loading released from microchip device <i>in vitro</i> . ²²³	62
Figure 12. <i>In vivo</i> release profiles (urine measurements) of mannitol release from a silicon microchip. ²³⁶	63
Figure 13. Degradation kinetics of large pore and small pore silicon particles. ²³⁹	65
Figure 14. Schematic of triphasic release from microparticle systems.	67
Figure 15. Scanning electron images of cellulose hollow fiber.....	76

Figure 16. Release profile of sequentially delivered VEGF and Fluorescein.....	78
Figure 17. H&E images of murine Matrigel plugs where VEGF and/or S1P are delivered.....	81
Figure 18. CD31 Matrigel plug staining where VEGF and/or S1P are delivered.	83
Figure 19. CD31 quantification where VEGF and/or S1P are delivered.....	84
Figure 20. CD31 and α SMA Matrigel plug staining where VEGF and/or S1P are delivered.	87
Figure 21. Maturation index where VEGF and/or S1P are delivered.....	88
Figure 22. Projected <i>in vivo</i> release when injections occur daily.	91
Figure 23. H&E of Matrigel plug loaded with 100ng VEGF, 10x.	91
Figure 24. Tubular formation assay with HUVECs and S1P.	99
Figure 25. Cellulose hollow fiber image and sequential release of bFGF and PDGF.....	106
Figure 26. CD31 Matrigel plug staining where bFGF and/or PDGF are delivered.....	108
Figure 27. CD31 quantification where bFGF and/or PDGF are delivered.	109
Figure 28. CD31 and α SMA Matrigel plug staining where bFGF and/or PDGF are delivered.....	110
Figure 29. Maturation index where bFGF and/or PDGF are delivered.	111
Figure 30. H&E images of murine Matrigel plugs where bFGF and/or PDGF are delivered.	113
Figure 31. Vessel integration quantification when bFGF and/or PDGF are delivered.....	114
Figure 32. Hollow fiber schematic and model theory.....	124
Figure 33. Hollow fiber fabrication schematic.	131
Figure 34. Representative fiber characterization images.	133
Figure 35. Osmolality of VEGF, bFGF and PDGF, as a function of concentration.....	135

Figure 36. Effect of injection volume on release.	136
Figure 37. Effect of micropore/macropore fractions on release.	137
Figure 38. Effect of wall thickness on release.	137
Figure 39. Model prediction and <i>in vitro</i> data.	138
Figure 40. Model prediction and <i>in vitro</i> data for bFGF release from Fiber I, Fiber II and Fiber III.	139
Figure 41. Model prediction and <i>in vitro</i> data for VEGF, bFGF and PDGF, release from Fiber III.	140
Figure 42. Long term release predictions for VEGF, with varying injection volume (V_{hf}).	142

PREFACE

This work represents the result of many years of research in the collaborative environment of the McGowan Institute for Regenerative Medicine at the University of Pittsburgh Department of Bioengineering. During these years, I had the fortune of meeting a number of people that have either been instrumental for my scientific, professional or personal growth. First, I would like to thank my advisor, Dr. Steven Little, for his never ending support – I have learned so much from him and will forever be grateful. Dr. Little has provided me with guidance when designing experiments, preparing manuscripts, creating presentations and writing grant applications, and most importantly, when serving as a mentor for junior scientists. Without Dr. Little and the members of the Little Laboratory, the completion of this research would not be possible. I would also like to thank Dr. Alan Russell, Dr. William Wagner and Dr. Alan Wells, for serving on my dissertation committee, helping me troubleshoot and providing advice. I have benefitted from their instruction and comments and each of them have provided a unique perspective on my research. Thank you also to Dr. William Federspiel who assisted me in the development of the transport model described in this dissertation. An additional thanks to Dr. Richard Bodner, who helped me develop my animal model and Dr. Jianjun Guan, who taught me how to make hollow fibers. I would also like to thank the members of the Center for Biologic Imaging (especially Christina Goldbach) and the members of the Division of Laboratory Animal Resources for their expertise and assistance in helping my research advance. Thank you to the graduate and

undergraduate students of the Little Laboratory, both past and present, that have assisted me in my experiments, lent a hand whenever possible and helped me talk out ideas and problems. I am grateful to have worked with people who have such an enthusiasm for research and are so generous with their time. Thank you to Dr. Sanjeev Shroff and the Cardiovascular Bioengineering Training Program for providing both financial and intellectual support during my graduate career. Lastly, I would like to thank Dr. Harvey Borovetz and the graduate committee for accepting me into the Bioengineering graduate program and allowing me to participate in the PhD program.

On a personal note, I would like to thank my family and friends for all of their love and support over the last 27 years. Thank you to my parents for every opportunity that they have given me, for without those opportunities, I would not have been able to achieve everything that I have achieved. My parents have always believed in me and I am forever appreciative. Thank you to my sister, Tara, for being there for me as a great friend under any circumstances. She was always someone who could make me laugh and forget about whatever was going on in the world around me. Thank you to my childhood friends in Philadelphia and the new friends I have made in Pittsburgh for helping me to escape my work and enjoy everything life has to offer. Finally, I would like to thank my husband, Anthony, who has been more than understanding through my entire academic career. He has always pushed me to succeed and held my hand through every high and low. I look forward to our future together.

1.0 INTRODUCTION

In 2010, a major aim of medicine is to generate or regenerate functional tissues to replace lost or compromised tissues and organs.¹ The process of wound repair during injury, whether traumatic or surgical, is paramount to human survival.² Diabetic ulcers and burn and trauma wounds are among the type of wounds receiving attention in the field of wound healing and tissue engineering, “an interdisciplinary field that applies the principles of engineering and life sciences towards the development of biological substitutes that restore, maintain or improve tissue function or a whole organ”.³ Many biomedical implants and scaffolds lack vasculature or an integrated delivery system, making the most significant barrier to wound healing and three-dimensional regeneration a lack of delivery of nutrients, oxygen and growth factors beyond the limits of diffusion.⁴⁻⁵ Engineering large and/or complex tissues requires development of a stable vascular network, capable of perfusing the implant, which remains the primary limitation to engineering tissue of clinically relevant sizes.⁶

1.1 WOUND HEALING STAGES

Healing of any wound involves a complex, carefully regulated series of overlapping processes, organized into four stages: hemostasis (the cessation of bleeding), inflammation, proliferation (generation of granulation tissue) and scar formation or remodeling.⁷⁻⁸ During this process,

many growth factors and signals are presented to the healing tissue, coming from nearby cells and microvasculature.⁶ The temporal presence (and consequent absence) of these growth factors and signals are imperative to the healing process.

Immediately following an injury, tissue factor is released from activated endothelial cells, initiating the blood coagulation phase of healing.⁹⁻¹⁰ This phase is characterized by disruption of blood vessels as well as endothelial-endothelial cell contacts¹¹, vasoconstriction¹², formation of a hemostatic plug and platelet activation.¹⁰ Platelet activation occurs when inflammatory growth factors (VEGF, bFGF, PDGF, TP, EGF, HGF, TGF- β and Ang-1) or extracellular matrix components of blood vessel basement membrane are exposed.⁹ Activated platelets then release the contents of their alpha and dense granules, leading to endothelial cell activation, along with inflammatory cell recruitment, resulting in the release of more cytokines and growth factors.^{9-10, 12-13} The coagulation phase of wound healing results in the formation of a fibrin clot, which serves to provide a provisional extracellular matrix for cellular migration.^{9, 11}

Beginning about one hour after injury, the inflammation phase lasts for a few days, where a specialized cell group known as leukocytes (white blood cells) accumulate at the site of injury and clean out the wound.¹⁰ First neutrophils, a sub-group of leukocytes, passively collect at the wound site, making up about 50% of the cells present, playing a role in wound debridement and bacterial killing.^{10, 12-13} Neutrophils eventually migrate to the surface of the wound, making room for bone marrow derived monocytes.¹³ These monocytes differentiate into macrophages, another sub-group of leukocytes¹⁰, which bind to the extracellular matrix via integrin receptors¹¹ and secrete growth factors that facilitate the next phase of healing.¹²

The proliferative phase of healing begins around the third day following an injury and lasts for about three weeks.¹⁰ This phase is marked by the production of collagen and scar tissue

(to replace fibrin, provisional matrix and granulation tissue) by fibroblasts.¹⁰⁻¹¹ As collagen is produced, wound contraction occurs and tissue integrity is restored by fibroplasias, neovascularization and re-epithelialization.¹² Neovascularization is very important during this phase, as the formation and integration of new blood vessels allows oxygen and nutrient delivery to the healing tissue, which is necessary for cellular metabolism.^{4-5, 11} Without neovascularization, healing tissue becomes necrotic and the wound will not heal.

The last phase of wound healing, the remodeling phase is a slow, dynamic process (can last up to six months), characterized by equilibrium between collagen synthesis and destruction, giving the scar its tensile strength.^{10, 12} The degradation of collagen in the wound is controlled by several proteolytic enzymes (matrix metalloproteinases), which are secreted by macrophages, fibroblasts and endothelial cells.¹¹ Wound sites typically only gain about 20% of their final strength in the first three weeks following an injury and may never reach 100% of the original strength prior to the injury.¹⁴

1.2 CLINICAL WOUNDS AND TREATMENTS

1.2.1 Wound types

The need for an improvement in clinical wound treatment is evidenced by the 8 million patients per year that present with a significant wound, including burn wounds and skin ulcers caused by pressure, venous stasis or diabetes, where there is no “gold standard” treatment.^{11, 15} With burn wounds accounting for 1.25 million of these patients¹⁶, another specific area of trauma wounds that is the focus of wound treatment research is battle field wounds. Battlefield injuries are at

their highest, despite the fact that battlefield fatalities are less than half of what they have been for previous wars.¹⁷⁻¹⁸ These injuries are typically associated with profuse bleeding, pain, inflammation and infection, leading to increased pressure, reduced blood flow (ischemia) and eventually a condition known as compartment syndrome.^{3, 16} Proper re-establishment of blood flow in a wound has potential to eliminate compartment syndrome and set the stage for regeneration.

Skin ulcers, a type of non-traumatic wound, are also a cause for wound treatment. These wounds are prevalent in the diabetic population and are the major cause of non-traumatic lower-extremity amputations – a diabetic patient loses a foot or a leg to a diabetic ulcer every 30 seconds in the world.¹² Diabetic patients commonly experience a reduction in growth factor and receptor expression, as well as peripheral arterial disease.^{12, 19-21} This combination leads to neuropathy, ischemia and poor nutrient supply, depriving patients of sensation, causing unrecognized trauma.^{10, 12} These resulting infection is associated with abnormal or reduced growth factor expression, leukocyte abnormality and microangiopathy, which all lead to poor wound healing.^{10, 12}

Ulcers of the skin can also be caused by insufficiency of the venous valves, known as venous stasis, causing blood to pool and hydrostatic pressure to increase. The pressure on the capillary beds causes the gap junctions between the endothelial cells to widen. The widening of the gap junctions causes a decrease in oxygen, nutrient and cytokine levels, leading to tissue breakdown, ulceration and infection.¹⁰ Skin ulcers tend to be chronic, resulting from impeded neovascularization and a high bacterial burden,¹⁰ and more than half of chronic wounds that persist for more than a year remain resistant to traditional therapies.²²⁻²³

Another type of skin ulcer is an arterial ulcer, caused by poor distal perfusion to a limb. These ulcers often lead to progressive hypoxia, ischemia, necrosis and skin breakdown, and are prevalent in patients with peripheral artery disease, where the hypoxia feedback loop responsible for initiating blood vessel growth when oxygen levels are low does not perform properly.²⁴ Patients without normal angiogenic capacity could benefit from clinical wound healing methods designed to stimulate angiogenesis.

1.2.2 Current treatment options

Currently, a common treatment for non-healing surface wounds is skin grafting,^{16, 22} but in many cases the skin and underlying tissue is so greatly damaged that there is no available site from which autologous tissue can be taken. In the case of non-surface wounds, a clinically accepted therapy is transplantation, but the need for transplants is far greater than the supply.²⁵ Allografts and xenografts typically lead to immunorejection and/or pathogen transmission and subsequent complications associated with immunosuppressive therapies.⁴ Another common treatment is sharp debridement of the wound to healthy, well-vascularized tissue, combined with removal of necrotic debris, foci of infection and edema. This treatment helps to reestablish the dynamic process of normal wound healing.^{10, 12} In 1997, the use of Regranex® (Ortho-McNeil Pharmaceutical), or becaplermin gel, was approved by the Food and Drug Administration as a topical wound ointment for the use of healing ulcerations (in conjunction with standard wound healing practices) in the feet of chronic wounds.¹⁰ To date, becaplermin gel has also been used on irradiated wounds and chronic orbital ulcers after extirpation.² The ointment, applied once daily, contains platelet derived growth factor (PDGF) at a concentration of 100µg/g gel,¹² promoting chemotactic recruitment and proliferation of cells involved in wound repair.¹⁰ More

recently, becaplermin gel has also been shown to induce bone healing in craniofacial wounds.² Additionally, cell-based therapies such as a human fibroblast-derived dermal substitute, a human fibroblast-derived temporary skin substitute and an allogenic bilayered cultured skin equivalent, are commercially available tissue engineered solutions to chronic wounds.²⁶ Although there have been many recent advances, randomized trials and studies that evaluate the efficacy of these advancements have been less than ideal, leaving the “gold standard” for wound healing yet to be discovered.²⁷⁻²⁹ The desire to create more effective and practical therapies for tissue loss and functional deficits have inspired the field of tissue engineering.²⁵

1.3 TISSUE ENGINEERING AS A TREATMENT FOR WOUNDS

The most recent definition of tissue engineering, as defined by Williams in 2006, is the creation of new tissue for the therapeutic reconstruction of the human body by the deliberate and controlled stimulation of selected target cells through a systematic combination of molecular and mechanical signals.³⁰ Although tissue engineering is a viable solution to many problems in healing, there are many limitations that prevent these therapies from becoming clinically relevant. Mainly, these limitations are biocompatibility and a lack of blood supply, where restoration of new blood vessel growth is important in all regenerative processes.^{1, 4-5, 31} In an effort to address the lack of blood supply, many researchers have attempted grow or assemble vessels ex-vivo and then implant them into the body. While large (>1mm diameter) and intermediate vessels (50-150 μ m diameter) are sometimes possible to engineer³²⁻³³, smaller vessels such as capillaries are notoriously difficult to engineer, due to their required degree of self assembly and self-organization.³⁴ One example of research in this field is the co-culture of

endothelial and mural cells with the overall goal of inducing cells to form a functional vascular network ex-vivo that will promote survival of the implanted tissue.³⁵⁻³⁶ However, this attempt, as well as other similar attempts have led to immature vessels that have a limited potential to integrate with host vasculature³⁷ and are prone to regression.³⁸ These vessels have also been shown to be more fragile, leaky and lead to edema after implantation.³⁹ Additionally, the implantation of a foreign cell population, when the patient's own cells cannot be used, invariably leads to immunological responses, causing thrombosis and occlusion upon implantation.¹⁶ Overall, success of prevascularization on the capillary level has not been achieved beyond 1mm, thus not challenging oxygen and nutrient diffusion limitations.³⁴

In an effort to avoid immune response, some researchers are attempting to promote invasion of host vasculature into an implant by combining a scaffold with drug release, functional matrices or surgical techniques. One method is the creation of channels similar in size to microvasculature and favorable for endothelial attachment with the idea that endothelial cells will invade and line the channels, forming vessels. An example of this uses microelectrochemical systems (MEMs) to etch channels into a silicon wafer, which can then be used as a mold for a poly(glycerol sebacate) scaffold. When the scaffolds are bonded together, capillary networks are created which can then be endothelialized *in vitro* under flow conditions. However, these flow conditions are not present upon implantation *in vivo*.⁴⁰ Another example involves the seeding of endothelial cells onto collagen gels that are molded around stainless steel needles. The vessels formed as a result of this technique show normal microvascular functions including reactivity to cytokines, but they lack a basement membrane, which is necessary for maintenance of vessel integrity once implanted *in vivo*.³² Microchannels have also been created in a polyethylene diacrylate hydrogel, resulting in host tissue infiltration within the actual

channels of the implant. Additionally, VEGF localization to the host derived tissue was observed, but host tissue infiltration into the hydrogel itself was not seen.⁴¹ Tissue engineering of implants larger than 1mm requires development of a stable vascular network, capable of perfusing the implant. This challenge remains the primary limitation to engineering tissue of clinically relevant sizes.⁶

2.0 NEOVASCULARIZATION

Formation of new blood vessels, or neovascularization, is essential to wound healing and tissue growth, specifically so that the oxygen and nutrient supply can be reestablished to the wounded or growing tissue.^{10, 42-45} Additionally, inflammatory cells that are necessary for wound repair require the interaction with and transmigration through the blood vessel basement membrane to enter the site of injury.⁴⁶ It is believed that techniques to promote and accelerate this process will have a tremendous impact on public health.⁴⁷ As just a few examples, therapeutic induction of neovascularization can be used to treat ischemic left ventricular dysfunction (as a result of coronary artery disease)⁴⁷, battlefield wounds¹⁷⁻¹⁸, diabetic ulcers and tissue defects.⁴⁸

2.1 ANGIOGENESIS

Perhaps the most well known and well studied type of neovascularization is angiogenesis, which is defined as the growth of new blood vessels from pre-existing vessels.⁴⁹ Angiogenesis can be either physiological or pathological, where physiological angiogenesis is a normal and vital process in growth and development as well as wound healing and pathological angiogenesis is a fundamental step in the transition of tumors from a dormant state to a malignant one.⁵⁰ The cells and biological structures that make up blood vessels, as well as the biomolecules involved in the process of physiological angiogenesis will be discussed further in Chapter 3.0

Healing of any wound, other than non-excisional wounds, cannot occur without neovascularization, which is generally considered to occur during the proliferative phase of wound healing. Clinically, new capillaries first become visible 3-5 days following an injury.⁵¹ However, many signals that initiate angiogenesis also occur in the inflammatory phase.⁴⁶ As new blood vessels form, endothelial cells that line the vessels control oxygen and nutrient transport across the vessel wall to the healing tissue,⁴⁶ as well as organize and regulate healing. These endothelial cells also provide the provisionally matrix necessary for the proliferative phase of healing,⁵¹ where blood vessels represent 60% of the mass of granulation tissue.⁵² Impaired granulation tissue formation is a hallmark of chronic non-healing wounds.

2.2 VASCULOGENESIS

Another way that vessels are formed in the body is through vasculogenesis, which is defined as *de novo* formation of immature cords from the differentiation of progenitor cells. These cords go through tubulogenesis and mature into vessels.¹⁰ The process of vasculogenesis is essential in adult neovascularization as well as fetal vessel formation. Fetal vasculature formation begins with primitive cells of mesoderm origin (hemangioblasts) that form blood islands, which eventually differentiate into endothelial cells.¹⁰

Circulating endothelial progenitor cells derived from bone marrow (marked by CD133 expression), thought to be involved in adult vasculogenesis, were isolated for the first time in 1997.¹⁰ These cells were shown to contribute to the re-endothelialization of injured vessels and ischemia-induced neovascularization, improving endothelial cell function.⁵³ These cells represent an important endogenous repair mechanism by which the body maintains vessel

function, where several clinical studies have shown a decreased number of these cells in some pathological conditions, specifically coronary artery disease.^{10, 53} Various stimuli, such as vascular trauma, cause the mobilization of these cells from the bone marrow into circulation.⁵³ Once at the site of injury, the progenitor cells exert their function by activating the local endothelial cells and/or differentiating into mature endothelial cells that integrate the damaged vessels, thereby contributing to endothelial repair.^{8, 53} Studying adult vasculogenesis allows researchers to make decisions about how to induce endothelial progenitor cell migration in a wound site.

Mobilization from the bone marrow into circulation is thought occur via cytokine mediated pathways, specifically in response to VEGF, as observed in burn and coronary artery bypass grafting patients.⁵³ *In vitro*, multipotent adult progenitor cells (CD133 positive), isolated from the bone marrow differentiate into endothelial cells, marked by CD34 and VEGF-R2 expression. when cultured on high density fibrinogen with VEGF.¹⁰ Additionally, an increase in VEGF correlates with a rise in circulating early endothelial progenitor cells within six hours of burn and coronary artery bypass patients, returning to normal within 48-72 hours.¹⁰ Once at the site of vascularization, early progenitor cells become late progenitor cells by losing expression of the transmembrane glycoprotein CD133 and gaining another membrane protein CD31, the glycoprotein Von Willebrand factor and transmembrane vascular endothelial cadherin expression.¹⁰ Finally, there is also evidence the vasculogenesis is contributed to by circulating endothelial progenitor cells, which naturally home and integrate into sites of physiological vessel formation *in vivo*.⁵⁴

2.3 VASCULOGENESIS AS A THERAPY

Vascular and cardiac diseases encompass a variety of pathological, structural and functional changes in the cellular architecture of blood vessels and heart muscle.⁵⁵ Traditional approaches to such pathologies have been pharmacological agents or surgical intervention, but with regenerative medicine at the front of therapeutic medical research, a paradigm shift has occurred, moving focus to other approaches such as cell therapy.⁵⁶ Animal studies have provided evidence of the role of endothelial progenitor cells in postnatal vasculogenesis and their potential to treat complications associated with tissue ischemia.⁵⁶⁻⁵⁷ Bone marrow-derived progenitor cells that are phenotypically CD34 and Flk1 positive, as well as CD133 positive cells, have been reported to contribute to tissue repair by differentiating into both endothelial cells and vascular smooth muscle cells, as well as other cell types.⁵⁸ These cell types have been evaluated for their benefits in treating acute myocardial infarction, limb ischemia⁵⁹⁻⁶² and dilated cardiomyopathy.⁵⁸⁻⁶⁰ Various studies have been performed to test the clinical efficacy of endothelial progenitor cells in patients with cardiovascular disease. These include the mobilization of these cells with pharmacologic agents in patients with heart disease and harvesting of cells from the circulation and bone marrow for autologous reinfusion in affected patients.⁵⁸ Results from these trials have been mixed and not as successful as animal studies, likely due to the variation in the definition of human endothelial progenitor cells and the resulting heterogeneity in cell populations used in the treatments.⁵⁸

2.4 BLOOD VESSEL WIDENING, SPLITTING AND EXPANSION

Other methods the body uses to react to decreased blood flow is arteriogenesis, the development of collateral circulation by the widening of small vessels¹⁰ and intussusceptions (splitting) of one vessel into two.⁹ Arteriogenesis is induced following the occlusion of a major artery and consequent hemodynamic and mechanical effects on the collateral vessel wall. These effects occur with increasing blood flow velocity due to the low pressure at the reentrant site of the collateral vessel.⁶³ A variety of different cytokines act by stimulating endothelial and smooth muscle cell proliferation and monocyte migration or recruitment and activation (MCP-1, bFGF, TGF- β , VEGF, and GM-CSF).⁶³ Several clinical trials have been published in that field to suggest the feasibility and safety of treatment with such cytokines or their genes. However, the results indicate that further studies are needed before proarteriogenic therapies are ready for clinical application.⁶³

All of these processes are essential in both embryogenesis and wound healing, but also play a role in several pathological processes such as tumor vascularization, diabetic retinopathy, psoriasis and rheumatoid arthritis.⁹ Perhaps the most common form of neovascularization in adults is angiogenesis, the process by which endothelial cells sprout from preexisting blood vessels and then migrate and proliferate to form a cord-like structure.¹⁰

3.0 ANGIOGENESIS

Angiogenesis is an organized series of events, beginning with vessel destabilization, followed by endothelial cell proliferation and migration, and lastly vessel maturation.⁹ During these events, different angiogenic growth factors become important at different points in time,⁶⁴ forming a set of stage-specific “instructions” to guide the process. Chapter 6.0 will describe this process in greater detail. The following sections describe the cells and proteins that make up blood vessels, as well as the growth factor involved in angiogenesis.

3.1 ANATOMY OF A BLOOD VESSEL

3.1.1 Endothelial Cells

Blood vessels are complex structures comprised of endothelial cells, mural cells and a basement membrane (Figure 1). Endothelial cells are the cells that line the interior surface of blood vessels, serving as the interface between the blood and the rest of the vessel wall from the largest artery to the smallest capillary. As a monolayer, these cells control the passage of molecules and the transport of white blood cells into and out of the bloodstream. These cells can come from other endothelial cells or endothelial progenitor cells that circulate in the bone marrow or blood and are often identified by CD31, and/or von Willebrand factor.⁵⁴ In quiescent vessels,

endothelial cells are polarized with a luminal and abluminal surface, acting as a barrier and a non-thrombogenic surface.¹⁰ Endothelial cells express VEGF receptors, which bind VEGF produced by vascular pericytes, as well as secrete anti-apoptotic factors. Both of these actions are essential to their survival.^{9, 65-66}

3.1.2 Mural Cells

Mural cells associated with blood vessels can be vascular pericytes (on smaller vessels) or smooth muscle cells (on larger vessels).⁶⁵ These cells serve to reinforce tubular endothelial networks, stabilize vessels by enhancing endothelial cell-cell contact, produce extracellular matrix proteins and regulate luminal diameter.¹⁰ Normal pericytes are embedded into the basement membrane of capillaries as either solitary cells or a single cell layer.⁶⁵ In veins and arteries, vascular smooth muscle cells form a single or multiple cell layer around the vessel to mediate vascular tone and contraction.⁶⁵ Vascular mural cells are commonly identified by alpha smooth muscle actin, regulator of G protein signaling 5 and platelet derived growth factor receptor. Mural cells that associate with vasculature are necessary for vessel maturation, stabilization and quiescence.⁶⁵ Therefore, mural cells are inherently scarce at the site of developing vascular sprouts and are recruited to the site of newly forming vessels by biomolecules such as PDGF and sphingosine-1-phosphate.⁶⁵ Contacts made with neighboring endothelial cells help coordinate intracellular signaling to prevent vessel leakage and inhibit proliferation.⁶⁵

3.1.3 Basement Membrane

The basement membrane serves as a physical barrier conferring adhesion and stability of the vessel. Collagen IV and laminin 1 comprise a large portion of the extracellular matrix proteins present in the basement membrane, which is also a reservoir for heparin binding growth factors such as VEGF and bFGF.⁹ When the basement membrane is degraded, for example following an injury, sequestered growth factors are released, creating space for endothelial cells to migrate and secrete new basement membrane.⁹

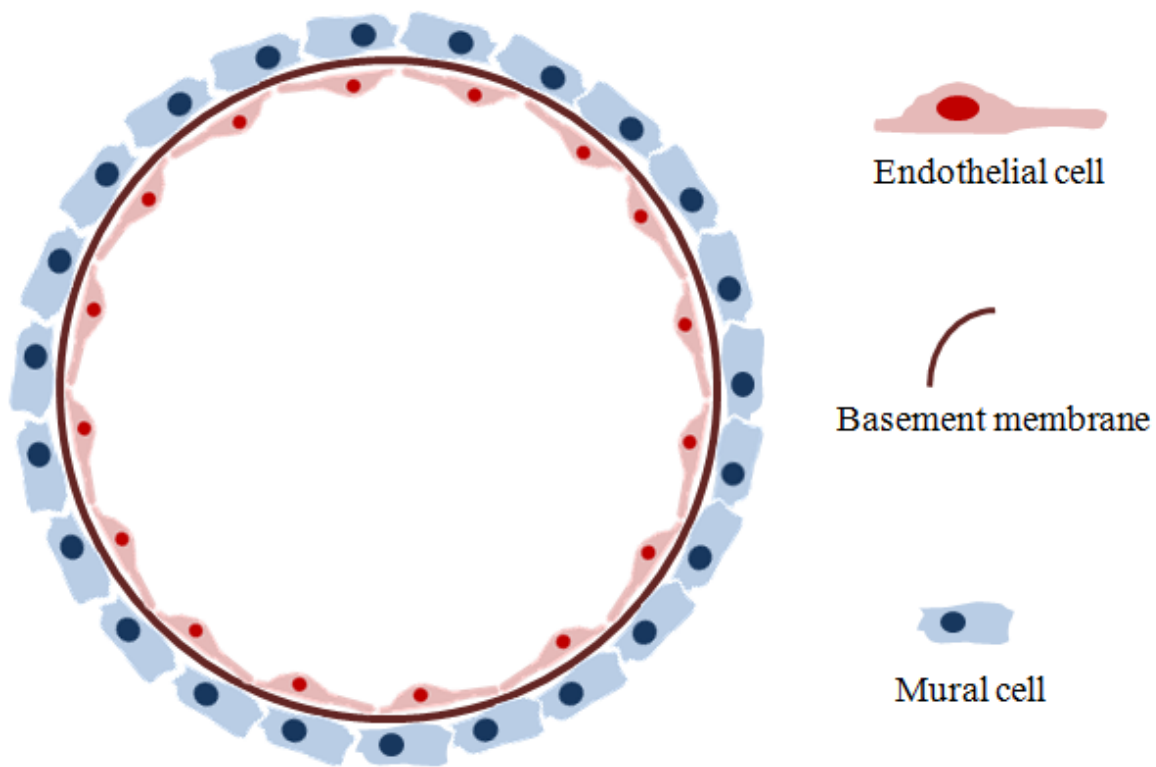


Figure 1. Vessel cross section.

3.2 ANGIOGENIC GROWTH FACTORS

There are many growth factors involved in the process of angiogenesis, which constitute a complex family of polypeptide molecules and exert specific biologic reactions through the act of binding to cell surface receptors.¹

3.2.1 Vascular endothelial growth factor

Vascular endothelial growth factor (VEGF) is a 34-46kD secreted, heparin-binding⁸ glycoprotein with a disulphide homodimer bond, with VEGF165 being the predominant isoform in humans.⁹ VEGF was first discovered when isolated from tumor lysates, and shown to be involved in the initiation of angiogenesis⁶⁷ and endothelial cell proliferation,^{65, 68} and is one of the most widely studied angiogenic growth factors.⁶⁹ Specifically, VEGF promotes angiogenesis, providing chemotactic factors for inflammatory cells, recruiting endothelial progenitor cells from the bone marrow and upregulating other angiogenic factors.⁸ It is released from activated platelets as well as activated macrophages following an injury.⁸ The VEGF/VEGF-receptor signaling system (5 VEGFs, 3 VEGFRs) on endothelial cells is perhaps the most important signaling system for angiogenesis.¹⁰ It has been shown that blocking the action of VEGF (with a monoclonal antibody to either VEGF or its receptor) blocks the process of angiogenesis.⁹ Additionally, under hypoxic conditions, VEGF production by vascular pericytes is upregulated⁸ from a baseline maintenance level.⁶⁵ This upregulation leads to dissociation of the endothelial cells and vascular pericytes, allowing angiogenesis to initiate.⁶⁵ Other angiogenesis actions in which VEGF is involved include vasodilation and increased permeability of the endothelial barrier^{8, 65}

In vitro, VEGF has been shown to explicitly stimulate the proliferation of human umbilical vascular endothelial cells (HUVECs) and not smooth muscle cells,⁸ displaying the specificity in the action of VEGF. Additionally, VEGF has been shown to induce upregulation of matrix metalloproteinase-1 from smooth muscle cells,⁸ which in turn leads to basement membrane degradation. *In vivo*, VEGF has improved skin graft survival in rats⁸ and also reduced pericyte coverage on nascent vascular sprouts through inhibition of PDGFR signaling in mural cells.⁶⁵ A reduction in pericyte coverage leads to less mature and less stable vessels. In combination with bFGF, VEGF has increased angiogenesis in a rabbit hindlimb ischemia model.⁸ However, it has also been shown that angiogenesis induced by the delivery of exogenous VEGF leads to leaky, immature vessels,⁹ indicating that perhaps other growth factors are necessary for complete angiogenesis. The importance of VEGF in development has been documented, showing that a 50% reduction in VEGF expression results in embryonic lethality.⁷⁰

3.2.2 Basic fibroblast growth factor

Basic fibroblast growth factor (bFGF) is an 18kD protein that, like VEGF, is released into a wound site from activated platelets and macrophages.⁸ As a strong mitogen for many cell types, bFGF plays a role in neuronal signaling, inflammation, hematopoiesis, tumor growth and invasion, as well as angiogenesis.⁹ Basic FGF is also found bound to heparin sulfate proteoglycans in the extracellular matrix and is released during ECM-breakdown.⁹ In addition to inducing angiogenesis as a result of its chemoattraction effect on smooth muscle and endothelial cells, bFGF aids in the proliferation of fibroblasts and epithelial cells.⁸ Specific to endothelial cells, bFGF induces proliferation, chemotaxis and urokinase type plasminogen activator activity, VEGF and VEGFR2-upregulation, all the while inducing a pro-angiogenic phenotype.^{9, 71-72}

Furthermore, monoclonal antibodies against bFGF has been shown to inhibit angiogenesis in a similar fashion as antibodies to VEGF.⁹

In vitro, bFGF seems to have important interactions with VEGF, where bFGF activity has been shown to be regulated by the upregulation of VEGF.⁹ Additionally, bFGF has been shown to upregulate VEGF expression in rabbit vascular smooth muscle cells in a concentration dependent manner.⁸ *In vivo*, bFGF has been shown to enhance collateral blood flow when administered to ischemic coronary artery⁷², limb and heart.⁷³ Additionally, four weeks following removal of the right femoral artery in rabbits, an increased number of arterioles, tissue perfusion and vascular density were observed.⁸

3.2.3 Platelet derived growth factor

Found at the surface of healing wounds², platelet derived growth factor, a 30kD dimer, is a prominent cytokine active in all stages of the healing process¹⁰ and one of the most potent inducers of angiogenesis.⁹ It is a known powerful chemoattractant and mitogen, exerting action on fibroblasts, neutrophils, monocytes, smooth muscle cells and endothelial cells.^{2, 12} PDGF is mainly secreted by the platelets' alpha granule⁷⁴, but also produced by other cells involved in healing (macrophages, endothelial cells, fibroblasts, keratinocytes)^{9, 12}, stimulating mitogenicity and chemotaxis of more fibroblasts, neutrophils and macrophages². More specifically, PDGF, stimulates macrophages to produce and secrete other growth factors for various phases in the healing process and fibroblasts to upregulate production of fibronectin, collagen, proteoglycans, hyaluronic acid and collagenase.²

PDGF exerts its cellular effects by binding and activating PDGF receptors, leading to stimulation of cell growth as well as changes in cell shape and motility.² This action induces

reorganization in the actin filament system and stimulates chemotaxis.² PDGF receptors can be found on many cell types (fibroblasts, smooth muscle cells, microvascular endothelial cells), leading to cellular proliferation and migration, when bound to PDGF (ex: PDGF homodimer PDGF-BB binding the β form of the receptor).⁹ Genetic deletion of PDGF-BB in mice has been shown to lead to a reduction in pericyte coverage of blood vessels, resulting in defective endothelial cell junction, endothelial hyperplasia, microvascular leakage, vessel dilation, poor capillary flow and hemorrhage.⁶⁵ It is believed that PDGF is responsible for the promotion and stabilization of mature blood vessels through the recruitment and support of mural cells.^{67, 75-76} This action is thought to occur via the activation of the stromal derived factor-1A/CXCR4 axis.⁶⁵ Because of its evident pluripotency, PDGF has become the first growth factor to be used clinically for the healing of wounds, specifically diabetic foot ulcers, known as becaplermin gel.

3.2.4 Sphingosine 1-phosphate

Sphingosine-1 phosphate (S1P), a pleiotropic autocrine and paracrine signaling sphingolipid⁷⁷, is stored in platelets and released upon activation, following an injury.⁷⁸ S1P is produced intracellularly in organelles and the plasma membrane, and is then secreted.⁷⁹⁻⁸⁰ It is also known for recruiting vascular pericytes to a vessel wall,⁶⁵ thus promoting vessel stabilization *in vivo*.^{74, 78} As an endogenous lipid, S1P exerts pleiotropic effects including cell migration, cell proliferation, and cell survival in diverse cell types (including endothelial cells) through specific G-protein-coupled receptors.⁸¹⁻⁸² Endothelial cells largely express the S1P receptors S1P1, S1P2 and S1P3, which mediate stimulation of endothelial cell proliferation, migration, and capillary-like tube formation *in vitro*.⁸³⁻⁸⁴ These receptors appear in varying ratio, depending on what vessel type on which the endothelial cell appears (arteries, capillaries, veins, lymphatics).⁸⁵ S1P

has been shown to stimulate endothelial proliferation, migration and angiogenesis, protect against apoptosis and control vascular permeability.⁸⁶⁻⁸⁷ *In vitro*, S1P induces endothelial cell proliferation as well as serves as a potent chemoattractant for endothelial cells.⁸⁸ Also *in vitro*, S1P has been shown to reduce endothelial cell permeability⁸⁵, likely due to the ability of S1P1 and S1P3 to strengthen endothelial cell junctions.⁸⁹⁻⁹¹ It has also been shown to promote directed migration, vascular differentiation and formation of capillary networks, on complex extracellular matrices.^{83,92}

The S1P1 receptor on endothelial cells has been shown to be imperative in the recruitment of vascular pericytes, ensuring vessel maturation.⁹² When endothelial cells are exposed to S1P *in vitro*, their angiogenic effects (migration, proliferation and tube formation) are mostly due to the inability of pericytes and smooth muscle cells to form the vascular sheath and thus stabilize the nascent vessel. Remarkably, this process is controlled by the endothelial S1P1 and not smooth muscle S1P1 because both the global and endothelial-specific S1P1 knockout exhibit the same lethal phenotype caused by vascular hemorrhage.⁹³ S1P1-deficient mice have a marked endothelial-cell defect that diminishes the structural integrity of their blood vessels and results in embryonic lethality.⁷⁷ *In vivo*, S1P has a beneficial effect on ischemia-induced myocardial damage through inhibiting leukocyte infiltration and apoptosis.⁹⁴

3.2.5 Other growth factors involved in angiogenesis

Other growth factors that are involved with angiogenesis include placenta growth factor (PlGF), epidermal growth factor (EGF), Angiopoietin-1 (Ang-1) and Angiopoietin-2 (Ang-2). PlGF is expressed in placenta as well as tumors and binds with VEGF. It has been shown to control the bioactivity of both VEGF and bFGF *in vivo*.⁹ EGF is secreted by platelets, macrophages and

monocytes, but does not seem to have a direct effect on vascular endothelium. However, EGF plays a role in tumor proliferation, metastasis, apoptosis, angiogenesis and wound healing.⁹ Angiopoietin-1 (Ang-1) binds the cell surface receptor TIE2, which is expressed exclusively on endothelial cells. In highly vascularized tissues, Ang-1 is constitutively and widely expressed, where it binds extracellular matrix proteins and is released when endothelial cell binds at the same site. Ang-1 can induce endothelial cell adhesion, spreading, focal contact formation and migration, but cannot trigger angiogenesis alone. It is involved in vessel maturation and quiescence, and inhibits activating effects of VEGF on endothelial cells.⁹ Ang-2 is a natural antagonist of Ang-1 with similar binding affinity to the cell surface receptor TIE2. It is expressed in the ovary, placenta and uterus, which are all organs with constant blood vessel growth and regression. Ang-2 can be up-regulated by VEGF, bFGF and hypoxia, while down-regulated by Ang-1, TGF- β and itself. Like Ang-1, Ang-2 cannot trigger angiogenesis alone.⁹

There are also a number of growth factors responsible for inhibiting angiogenesis and blood vessel growth.⁹⁵⁻⁹⁶ These factors can be found circulating in the bloodstream or stored in the extracellular matrix. In normal conditions, these factors govern blood vessel homeostasis, but when an injury occurs, angiogenic stimulators are released, favoring blood vessel growth.⁹⁶

4.0 ANGIOGENESIS THERAPIES FOR TISSUE REGENERATION

Impaired circulation (clogged or lack of vasculature) is an underlying pathological feature in peripheral arterial disease, ischemic heart disease and chronic wounds. Patients exhibiting these maladies, combined with burn and trauma wound patients, create a need for angiogenic therapies to help regenerate tissue, restore perfusion, reverse ischemia and accelerate repair. Three common strategies, or fundamental “tools”, are often employed when addressing the problem of tissue regeneration and engineering of any tissue or organ.¹ The first strategy, *induction*, entails delivery of growth factors that promote a specific, desired host effect. The second strategy, *conduction*, involves the implantation of an acellular biomaterial or scaffold that provides structural support for the ingrowth of the desired healthy host cells. The third strategy is *transplantation of cells* that participate in tissue-specific regeneration. These strategies, known as the “tissue engineering triad” can be used alone or in combination with each other.⁹⁷ Coordinated interactions with soluble growth factors, other cells and extracellular matrices define a local microcellular environment that cells sense, regulating their cellular processes.²⁵

4.1 INDUCTION VIA GROWTH FACTORS

Cell fate is influenced largely by the biomolecules they sense in their local environment through cell surface receptors. Biomolecules known as growth factors are soluble-secreted signaling

polypeptides capable of instructing specific cellular responses in a biological environment. Triggering responses can result in a very wide range of cell actions, including cell survival, and control over migration, differentiation or proliferation of a specific subset of cells.⁹⁸ It is widely accepted that the incorporation of growth factors can facilitate proper growth in tissues that cannot heal on their own.⁹⁹ It is increasingly clear that growth factors are typically multimodal, exhibiting different mechanisms of action, depending on the concentration, exposure time and phenotype of the target cells.²⁵

Growth factors action is initiated by binding to specific transmembrane receptors on the surface of target cells that facilitate communication from outside of the cell to its cytoplasm and nucleus. The typical response to growth factor binding to its receptor is receptor activation by phosphorylation of the intracellular portion of the receptor, followed by signal transduction through molecular pathways in the cell cytoplasm to the nucleus. The level of expression of these receptors partially controls the level of response from the cell.¹⁰⁰

As regulators of chemotactic, mitogenic, morphogenic, apoptotic and metabolic effects, growth factors play a crucial role in information transfer between a cell population and their microenvironment.^{25, 101} With an improved understanding of the critical pathways involved in angiogenesis, the role of growth factors can be used to advance therapies in the clinic. Delivery of either bFGF or VEGF has shown limited success, ultimately leading to weak, leaky vessels.⁹ Specifically, VEGF delivery has been shown to be insufficient for the formation of complex, mature vasculature, lacking pericyte coverage and stability.¹⁰²⁻¹⁰³ Also, bFGF induced tubules tend to regress over time, in the absence of other angiogenic signals,¹⁰⁴ likely due to the fact that bFGF only acts on the formation of tubular structures and not the supporting anatomy.¹⁰⁵

However, individual growth factor based therapeutics for angiogenesis induced wound healing has had limited success.^{43, 106}

The limitations associated with delivery of growth factors include a short half-life in vivo, temperature sensitivity and the need for refrigerated storage. An alternative approach to growth factor delivery is gene therapy, where a plasmid DNA encoding for the desired protein is injected into the wound bed temporarily increases the local expression of the protein. While protein delivery relies on the delivery and activity of the protein, gene delivery also relies on cellular production and secretion of the encoded protein.¹ This process results in delayed availability of the protein, when compared to protein delivery and effectiveness for only three weeks¹⁰⁷, but solves the problem of protein destabilization when incorporated with a polymer. The biggest challenge in this approach is to overcome the low efficiency of transfection, which results in low levels of protein production.¹⁰⁸

Some clinical trials have been performed that are based on either delivery of recombinant growth factors or genes that encode for those growth factors. In a non-viral gene therapy for peripheral arterial disease patients, a gene encoding for human VEGF was used.¹⁰⁹ Plasmid was injected into the calf or distal thigh twice: once at the initiation of the study, and again four weeks later.¹⁰⁹ These injections led to an increase in VEGF gene expression levels, collateral vessel development, distal blood flow and healing.¹⁰⁹ Recombinant bFGF has been studied when delivered via an intra-arterial diffusion to the legs of peripheral arterial disease patients.¹¹⁰ A trend of increased walking time, ankle-brachial index and quality of life, was observed in patients receiving treatment compared to the placebo, but a statistical difference was not observed.¹¹⁰

Treatment of delayed and chronic wounds has also been explored. VEGF has been reported to enhance healing and angiogenesis in ischemic ulcers, but capillaries are immature and leaky,¹⁰ similar to the delivery of exogenous VEGF in the protein form. Recombinant human keratinocyte growth factor-2, which stimulates endothelial cells, was administered as a topical spray to venous insufficiency ulcers, in conjunction with standard compression therapy in a phase II clinical trial.¹¹¹ A statistical difference was observed when growth factor treated ulcers were compared to ulcers only treated with compression therapy.¹¹¹ In 1997, becaplermin gel was the first growth factor based therapy for the promotion of angiogenesis in non-healing wounds, specifically full thickness diabetic foot ulcers. Becaplermin gel has also been used in an off-label fashion to treat venous stasis ulcers, arterial insufficiency ulcers, burns, ischemic ulcers, trauma wounds and pressure ulcers.¹¹² To date, becaplermin gel still stands alone, however it is only effective in 30% of the wounds it is used to treat.¹⁰

4.2 CONDUCTION VIA BIOENGINEERED SCAFFOLDS

Polymer systems used for angiogenic conduction attempt to mimic key aspects by which the extracellular matrix interacts with the cells. Synthetic polymers are readily available and exhibit well-defined chemical and physical characteristics, allowing for reproducibility of scaffold properties.¹ These polymer systems are often combined with growth factor delivery or induction approaches so that the cells are attracted to the site, but also have structural support for migration and attachment. Polymer matrices with relevant modifications for growth factor presentation and release are attractive platforms for delivery substrates. Bioactive growth factors can be chemically immobilized or physically encapsulated into polymer matrices, preventing

denaturation. Their release is then controlled by the degradation rate of the scaffold, their diffusion through the polymer or external triggers.¹¹³⁻¹¹⁴ Controlling the degradation kinetics of polymer-based delivery systems enable one to control the release profile of growth factors, resulting in optimized concentrations of growth factors, which is one of the main goals of these systems.⁹⁸

In addition to designing scaffolds that release growth factors to control chemotactic responses of cells, the physical properties of the scaffold itself can contribute to subsequent cellular growth factor secretion and related cell signalling.⁶⁷ Research shows that physical parameters, such as shape, elasticity, hardness, stiffness, pore size, elastic reversibility and degradation rate of matrices, can alter cellular processes.¹¹⁵⁻¹¹⁶

Some bioengineered scaffolds include prevascularization, where endothelial cells are seeded *ex vivo* and implanted. Prevascularization of tissue involves co-culturing endothelial and mural cells with the overall goal of inducing cells to form a functional vascular network *ex vivo* that will promote survival of the implanted tissue. For instance, when skin-like tissues are constructed *in vitro* with endothelial cells along with fibroblasts and keratinocytes, there is more expedient integration with host vasculature than when endothelial cells are not included.³⁵⁻³⁶ However, these skin-like constructs were less than 1mm thick and did not challenge oxygen and nutrient diffusion through the tissue (one of the primary limitations to tissue engineering vascularized constructs³⁴). A major limitation of prevascularization strategies is vessel phenotype heterogeneity, maturation and stabilization.³⁴ It has been shown that immature vessels have a limited potential to integrate with host vasculature³⁷ and are prone to regression.³⁸ Further, these vessels have been shown to be more fragile, leaky and can lead to the formation of edema after implantation.³⁹ Additionally, the implantation of a foreign cell population invariably

leads to immunological responses leading to thrombosis and occlusion upon implantation.¹⁶ In contrast, an acellular, non-allogenic implant would allow for an off-the-shelf product which could prove invaluable for emergency situations such as burn and trauma wounds. However, without some sort of vasculature or integrated delivery system, the most significant barrier to wound healing and three-dimensional regeneration is a lack of delivery of nutrients, oxygen and growth factors, beyond the limits of diffusion.^{4-5, 23} Prevascularization provides one means to solve this problem from the time of implantation. However, prevascularization has been met with limited success due to retraction and inability to integrate with native vasculature.^{32, 34, 37-38, 40}

The simplest way to promote invasion of host vasculature is to create channels similar in size to microvasculature and favorable for endothelial cell attachment. One attempt has been by etching capillary patterns using microelectromechanical systems (MEMS) techniques into a silicon wafer, which served as a micromold for a poly(glycerol sebacate) scaffold.⁴⁰ These scaffolds were bonded together, creating capillary networks that could be endothelialized under flow conditions *in vitro*. Although *in vitro* results seem promising⁴⁰, it is unclear how this system will behave *in vivo*, where ideal flow conditions are not met. Another example of *in vitro* perfusion of microvascular tubes is seen when endothelial cells are seeded onto collagen gels molded around stainless steel needles.³² Although these tubes show normal microvascular functions including reactivity to cytokines, they showed a lack of basement membrane formation, which would likely be responsible for maintaining vessel integrity once implanted *in vivo*. Finally, microchannels have also been created in a polyethylene glycol diacrylate (PEGDA) hydrogel⁴¹ and tested both *in vitro* and *in vivo*. Although these microchannels resulted in host tissue infiltration within the actual channels of the implant and VEGF localization to the

host derived tissue, there was no evidence of host tissue infiltration into the hydrogel itself.⁴¹ Hence, in order to promote endothelial cell recruitment *in vivo*, it has become a common strategy to combine angiogenic growth factor delivery with these scaffolds.

4.3 CELL TRANSPLANTATION (CELL THERAPY)

Cell therapy is also being explored as a treatment to promote angiogenesis. Local injection of bone marrow derived progenitor cells have been used to replace the senescent fibroblasts and endothelial cells found in the ischemic wound.¹⁰ Also, bone marrow derived mononuclear cells containing the endothelial progenitor cell fraction implanted into ischemic limbs have been shown to promote collateral vessel formation with incorporation of endothelial progenitor cells into new capillaries.¹⁰ Some researchers are attempting to develop therapies that mimic the natural attraction of circulating endothelial progenitor cells, which have been shown to contribute to neovascularization in a hind-limb ischemia model in an immune-compromised mouse, improving perfusion and capillary density.⁵⁴

Administration of cells is a promising approach for therapeutic angiogenesis due to their ability to produce angiogenic cytokines and participate in vascular regeneration.¹¹⁷⁻¹¹⁹ One major obstacle is the retention of viable cells following transplantation. Evidence indicates that the vast majority of transplanted cells neither survive for long after injection nor remain within the implanted location.¹²⁰⁻¹²² Research shows that material-based deployment of cells using hydrogels improves efficacy, especially in the case of endothelial progenitor cells.¹²³ Hydrogels are attractive materials to serve as cell and drug carriers, as well as tissue matrices, due to their ability to absorb water and permeate solutes within the swollen matrices.¹²⁴ Examples of natural

materials that have been explored for this purpose are collagen¹²⁵, fibrin¹²⁶, alginate¹²⁷, gelatin¹²⁸, and hyaluronan.¹²⁴

Bone marrow mononuclear cells and hematogenous stem cells are both capable of synthesizing and releasing VEGF and bFGF as well as other factors that induce endothelial cell proliferation.¹²⁹⁻¹³⁰ When bone marrow mononuclear cells were implanted in a canine abdominal aortic replacement model, endothelialization of an artificial blood vessel was observed.¹³¹ This cell type was also shown to increase collateral blood flow when injected in an ischemic myocardium rat model.¹³² The first clinical report using bone marrow mononuclear cells as angiogenic therapies describes increased ankle brachial pressure index, treadmill exercise tolerance and collateral blood flow without complications.⁵⁹

Embryonic stem cells are another cell source for cell-based angiogenic therapies. Due to their pluripotency, embryonic stem cells have the ability to differentiate into any lineage, under the correct environmental conditions and cues. For example, in the case of myocardial regeneration, conventional needle-based intramyocardial injections of embryonic stem cells may be less effective than the epicardial delivery of cellularized biomaterials, due to the cell-cell and cell-matrix interactions.¹³³ A composite cell sheet made of cardiac progenitors derived from nonhuman primate ESC (for new cardiomyocytes) and adipose tissue-derived stromal cells (for trophic support) were used in a nonhuman primate model of myocardial infarction.¹³³ These composites led to enhanced survival of implanted cells (compared to a sham), however, due to study limitations, they were only able to show improved cardiac function in small infarctions.¹³³ Recent clinical trials have explored the feasibility and safety of autologous stem cell therapy, specifically for peripheral artery occlusive disease.^{61, 134-136} The long-term results of these clinical studies remain undetermined and the potential for tumor formation is a concern.¹³⁷⁻¹³⁸

5.0 CONTROLLED GROWTH FACTOR DELIVERY

Advances in the field of growth factor delivery for angiogenesis will greatly depend on our growing understanding of the mechanisms that regulate tissue level neovascularization.¹⁰ These mechanisms often involve the presentation of cytokines and growth factors, however, the manner in which they are presented are likely to be just as important as the molecule itself. Specific to healing, the main growth factors involved include PDGF, FGF, VEGF, IGF, EGF and TGF- β .¹² These factors can be easily encapsulated, injected or incorporated, into a scaffold and delivered in combination with each other as well as other factors.^{9, 12, 67, 139-140} Unfortunately, delivery and administration of growth factors currently lacks the sophistication required to orchestrate a stage-wise series of events.

At present, growth factors are commonly applied in solution form via bolus injection.¹ This method of delivery is high in cost and often results in negative side effects at non-target sites, such as promotion of disease.^{99, 101} Additionally, due to short half lives of growth factors, following hydrolysis by enzymes (bFGF half life = 3-10 minutes¹⁴¹, VEGF half life < 30 minutes¹⁴²) the bioavailability of the bolus injection is often low. Taken together, bolus injections of growth factors can result in non-functional tissue, which translate to leaky blood vessels in the case of angiogenesis.¹ Sometimes, a high concentration of growth factor that compensates for the loss of bioavailability leads to toxicity at the site of injection.²⁵ In order to

be an effective therapy, a growth factor has to reach the site of injury without degradation and remain at the target site long enough to exert its action.²⁵

In the case of peripheral vascular disease, which affects 15% of the adult population¹⁴³, obstruction of the blood supply reduces blood flow to the upper and lower limbs. It is believed that therapies that enhance angiogenesis can improve blood flow and relieve symptoms.¹⁴⁴ Although bolus injection of VEGF showed promising results in animal peripheral vascular disease studies¹⁴⁵⁻¹⁴⁷, no significant improvement was observed in phase II clinical trials.¹⁴⁸⁻¹⁴⁹

There is increasing evidence that enabling growth factors to exert their biological function efficiently requires the design and development of release technologies that provide controlled delivery, while preventing unwanted side effects.²⁵ Controlled release polymer systems and liposomes have shown to improve protein safety and efficacy.¹⁵⁰ Encapsulation of a growth factor in a delivery system (or attaching a growth factor to a polymer carrier) has been demonstrated to hold a great deal of promise for growth factor based therapies.²⁵ This method of protecting a protein allows delivery of unaltered proteins and is useful for chronic administration, leading to treatments for a number of diseases.¹⁵⁰⁻¹⁵¹ This strategy has found widespread use in wound healing and tissue regeneration, allowing for improved bioavailability, reduced frequency of administration, minimized release to non-target sites and more effective routes of administration. Carriers and delivery systems act as depots or reservoirs for high concentrations of growth factors while providing a protective environment. Delivery of specific cues to the proper site may allow for the regulation of the phenotype of host cells and thus guide tissue formation, healing or regeneration.²⁵ Sometimes, the carrier or delivery systems can also serve as an artificial extracellular matrix for cellular migration, while maintaining space in which tissue regeneration can occur.²⁵ An ideal delivery system should: 1) consist of a non-cytotoxic

and biodegradable carrier material, 2) have a feasible preparation method that does not affect protein activity, 3) retain a high loading efficiency and a controlled release profile, 4) target and be retained at the desired site of action, and 5) restrict the protein conformational mobility and protect the protein from physical and chemical degradation.²⁵ A broad range of biomaterial-based delivery technologies are being discovered and have the ability to control release kinetics of varying biological cues for diverse biomedical applications. There is great potential for applications in immunology, oncology and tissue engineering, where sustained growth factor release from a scaffold would be desired.¹⁵¹

Poly(lactide-co-glycolide), or PLG, is an attractive choice for controlled delivery of growth factors, as it degrades by hydrolysis to lactic and glycolic acid and has been used for over thirty years in a variety of medical devices. Microspheres can be readily made using a double emulsion technique, a process that can easily incorporate growth factors, where growth factor delivery is coupled to the degradation of the polymer.¹⁵² Over the years, other polymers and delivery systems (including microspheres) have also been explored for growth factor delivery, specifically with angiogenic growth factors.

5.1 PROOF OF CONCEPT MODELS

As proof of concept of local growth factor administration, bFGF was loaded into resin-based microspheres in a non-disease model, where microspheres were injected directly into the coronary artery.¹⁵³ Local delivery of bFGF, specifically to the heart and no other organs, was shown when compared to non-loaded microspheres, resulting in an increase in proliferating cells.¹⁵³ Basic FGF has also been loaded into heparin immobilized PLG microspheres and

injected into the subcutaneous space on the dorsal side of a mouse.¹⁵⁴ After one week, the skin surrounding the areas of bFGF-loaded microspheres showed an increase in capillary density, a response which was enhanced by heparin immobilization.¹⁵⁴ In addition, when VEGF was loaded into PLG microspheres for release over 21 days in a rat corneal implant model, an increase in angiogenic area was seen as a dose-dependent response to the amount of VEGF loaded.¹⁵⁵

5.2 HINDLIMB ISCHEMIA MODELS

Localized delivery of angiogenic growth factors that overcome the limitations of bolus injections has led to the exploration of angiogenic growth factor delivery in a number of disease models. In the case of a mouse ischemic hindlimb model, controlled release of VEGF from a poly (lactide-co-glycolide) scaffold for 28 days was able to improve tissue perfusion, capillary density and incidence of mature vessels compared to a blank scaffold or no treatment at all.¹⁴⁴ In another mouse ischemic limb model, VEGF loaded PLG nanoparticles were injected into the ischemic thigh adductor muscles, and VEGF was released over a 4 day period.¹⁵⁶ When compared to untreated ischemic limbs, VEGF nanoparticle treated limbs showed a significant increase in blood vessel volume.¹⁵⁶ In a similar study, where VEGF is released from a PLG scaffold over a longer period of time, PLG-VEGF scaffolds resulted in improved tissue perfusion, greater capillary density and more mature vasculature, compared to the controls over a 28 day period.¹⁴⁴

Alternatively, the release of bFGF was explored in similar models. Ionic gelatin-based hydrogels have been shown to release bFGF for 28 days.¹⁵⁷ When these bFGF-releasing hydrogels were applied to the quadriceps in a mouse hindlimb ischemia model, reperfusion was

significantly higher than a bolus injection of bFGF.¹⁵⁷ In a rat ischemic hindlimb model, a fibrin-based scaffold, loaded with heparin, VEGF and bFGF, was implanted between the superficial abductor and semi-membranous membrane.¹⁵⁸ After 14 days, a statistical increase was observed in perfusion of the limb and capillary number when compared to a blank scaffold.¹⁵⁸

Lastly, an injectable hydrogel has been proposed as a feasible option for VEGF delivery, due to its ability to be injected in a minimally invasive procedure.¹⁵⁹ Specific attention has been given to alginate, a naturally occurring polysaccharide, given its biocompatibility and availability.¹⁶⁰⁻¹⁶¹ In a mouse ischemic limb study, an injectable biodegradable alginate hydrogel, allowing sustained and localized release of VEGF, demonstrated release at a desirable concentration for extended periods of time and significant improvement in blood vessel density and restored blood flow when compared to bolus injection or hydrogel alone.¹⁴³

5.3 MYOCARDIAL INFARCTION MODELS

Left coronary artery ligation has been employed as a model for myocardial infarction, allowing for post-infarction treatment studies.¹⁶² A chitosan hydrogel has been employed as a growth factor delivery vehicle in a rabbit myocardial infarction model.¹⁶² In this model, the hydrogel is UV-crosslinked after it is applied to the infarct site.¹⁶² Left ventricle systolic pressure as well as endothelial cell presence was statistically higher in bFGF loaded hydrogel when compared to the blank hydrogel or no treatment at all.¹⁶² A gelatin hydrogel microsphere system has also been shown to release bFGF in a myocardial infarct model.¹⁶³ Four weeks following coronary artery ligation in rats, infarcts treated with bFGF loaded microspheres were shown to increase

myocardial blood flow as a result of myocardial angiogenesis, as well as improve the left ventricular systolic and diastolic function.¹⁶³ Another gelatin hydrogel microsphere system was explored where bFGF-loaded microspheres were injected in a myocardial infarct model and observed in dogs for 17 days.¹⁶⁴ These microspheres were able to improve left ventricle function as well as microvessel density, when compared to a saline injection.¹⁶⁴

5.4 ANIMAL MODEL TRANSLATION

Although much success has been seen in the animal models mentioned above, very few of these therapies show promising results in clinical trials. One explanation for this is that the animals used in these models enter the study as healthy individuals. Many patients, especially peripheral artery and myocardial infarction patients, have other associated medical conditions that can contribute to their response to certain therapies. Also, in some cases, such as a myocardial infarction model, application of the therapeutic treatment immediately following the medical condition is not clinically possible.¹⁶⁴ Lastly, these strategies are being explored in animal models, which will behave differently than they will in humans. Alternatively, the treatments explored in these models do not account for the stage-wise characteristics of the angiogenesis cascade.

6.0 STAGE-WISE ANGIOGENESIS

Angiogenesis occurs through a series of distinct steps, vessel destabilization, endothelial cell proliferation, endothelial cell migration and finally culminates in vessel maturation.⁹ This process is often referred to as stage-wise angiogenesis or the angiogenesis cascade.¹⁶⁵⁻¹⁷⁰ Each step along the way requires the presence (and sometimes absence) of different factors.⁶⁴

6.1 EARLY ANGIOGENESIS

Vessel destabilization is the natural response to stimulus such as injury, inflammation, hypoxia and neoplastic transformation,¹⁰ which are all scenarios in which blood vessel growth is needed. Soluble growth factors, cytokines and both cell-cell and cell-matrix interactions, all play a role in activating endothelial cells to begin angiogenesis.¹⁰ Once activated, endothelial cells attract leukocytes and blood platelets that release a multitude of pro- and anti-angiogenic factors.⁹ Endothelial cells begin to loosen their contacts with each other, as well as the supporting basement membrane and pericytes, leading to increased vascular permeability and deposition of fibrin.^{9, 65} Degradation of the basement membrane of an existing vessel, controlled by enzymes expressed at the tips of the capillaries (urokinase plasminogen and matrix metalloproteinases), must occur to allow for formation and advancement of a capillary sprout.^{8, 10} Angiogenic growth factors involved in initiation of angiogenesis include VEGF and TGF- β , allowing the local

resident endothelial cells to invade and migrate through the ECM, proliferate and form new immature tubules.¹⁰

Activated endothelial cells migrate on the fibrin scaffold (provided by fibroblasts) and invade towards the angiogenic stimulus, contributing to the next phase of proliferation and migration.⁹⁻¹⁰ Fibroblasts are a rich source of angiogenic cytokines, which are responsible for angiogenic stimulus. These cytokines have been shown to induce endothelial cells to form capillary-like networks *in vitro*, an action that cannot be completely inhibited by VEGF antibodies.¹⁰ As endothelial cells receive signals to proliferate, they form an immature capillary lumen.⁹⁻¹⁰ Migrating endothelial cells follow a cytokine gradient and rely on adhesion molecules and integrins (especially alpha-v/beta-3) to mediate their cell-matrix interactions.¹⁰ Migration is assisted by the degradation of the extracellular matrix, which in turn is driven by matrix metalloproteinases (MMPs). Each MMP exists for a specific extracellular matrix protein. MMP gene transcription is induced by growth factors and cytokines, released as proenzymes and cleaved by proteinases.¹⁰ As endothelial cells migrate into the area of neovascularization, they further proliferate, forming cytoplasmic vacuoles, which later become immature, leaky tubules.¹⁰

6.2 LATE ANGIOGENESIS

The final step of angiogenesis is the maturation of the new vessel via the recruitment of smooth muscle cells and pericytes that cover the vessel and stabilize it, allowing blood to flow without leaking.⁸ Endothelial cell proliferation and migration are inhibited and new basement membrane is secreted.⁹ Simultaneously, endothelial cells re-form their contacts with each other as well as the basement membrane proteins.⁹ Pericytes are recruited to an immature vessel by PDGF and

S1P, where they can differentiate into mural cells.^{9, 65} Factors that are present at this stage of angiogenesis inhibit endothelial cell proliferation, but still provide signals to promote survival of endothelial cells to endothelial cells.⁶⁵ In wound angiogenesis, when normoxia is restored and inflammation subsides, the levels of growth factors that promote angiogenesis decline.¹⁷¹

6.3 PHYSIOLOGIC GROWTH FACTOR TIMING

Angiogenesis is stimulated early in the wound healing process, with VEGF acting as one of the main initiators.¹⁷² A summary of individual factor involvement can be seen in Figure 2, reproduced from Fischbach, et al.¹ While much is known about the “wound healing cascade” or the profile of growth factors involved at various stages of wound healing, researchers are just beginning to learn about the “angiogenesis cascade”, where not only is there a time-dependent growth factor concentration profile, but also the expression of their receptors.²⁵ Following wound induction in an animal model, VEGF upregulation has been shown to occur as early as three days and last up to seven days.¹⁷³ An even more immediate response is seen with the upregulation of bFGF because bFGF is released immediately from the extracellular matrix of damaged tissue.¹⁷⁴ Additionally, it has been shown that in following hernia repair in humans, both VEGF and bFGF are upregulated over the first 4 days post-surgery, where bFGF already shows decreasing values by day 4.¹⁷⁵ Thrombin, the clot that forms during the first hour of the wound healing cascade, has been shown to upregulate the expression of the VEGF receptor, enhancing the effects of VEGF.¹⁷⁶

With respect to the later stage of angiogenesis, binding of Ang-1 to the Tie2 receptor on endothelial cells has been shown to upregulate PDGF production by endothelial cells.¹⁷⁷⁻¹⁷⁸ It

has been shown that an absence of PDGF during this stage leads to poorly-formed and immature blood vessels.¹⁷⁹ Additionally, when VEGF is present for long periods of time, the result is small, over-branched, leaky vessels, similar to those of tumor vessels.¹⁷³ It has also been found that diabetic patients with chronic non-healing ulcers have high levels of circulating VEGF and low levels of PDGF.^{19, 180} At the end of angiogenesis, growth factor levels decrease, and vascular pericytes secrete TGF- β , which acts to inhibit vascular proliferation.¹⁸¹

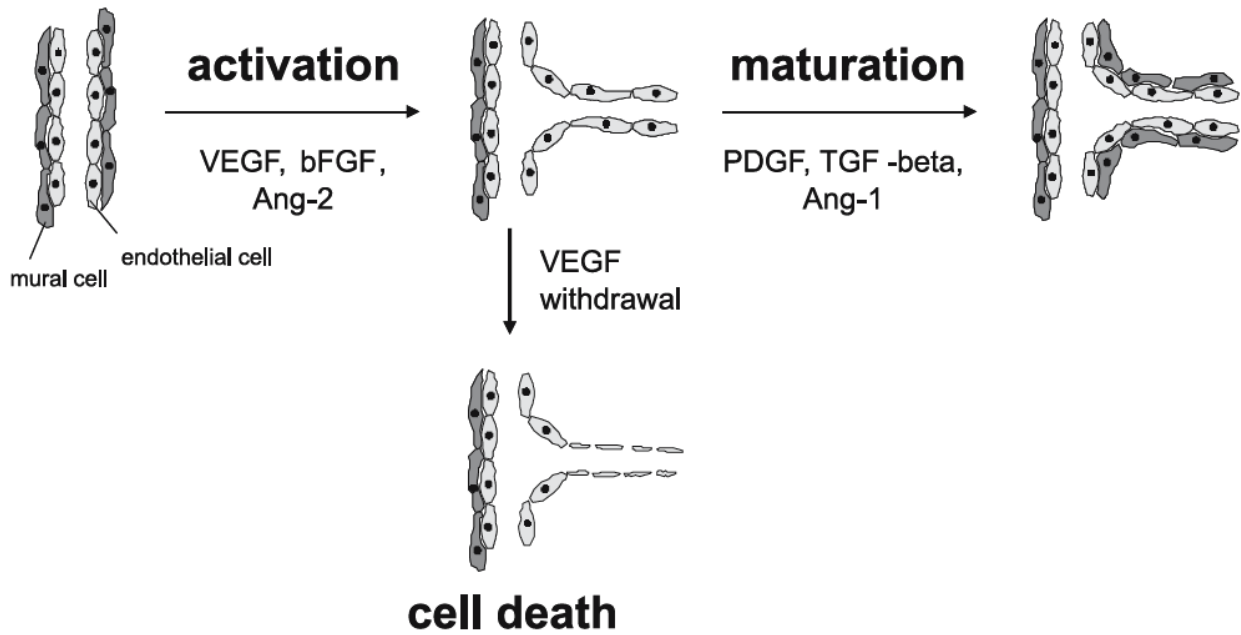


Figure 2. Growth factor involvement in angiogenesis events.¹

6.4 GROWTH FACTOR INTERACTIONS

Given the limited success of delivering only one angiogenic factor, as well as the multitude of factors that are involved with various stages of angiogenesis, some investigators have hypothesized that a combination of angiogenic growth factors might be the key to inducing functional angiogenesis that integrates with native vasculature.^{9, 67, 139-140} However, some combinations of factors has shown to inhibit certain steps of angiogenesis, while other combinations of factors have shown to inhibit each other. For example, it has been shown that PDGF inhibits the angiogenic effects of bFGF, when the two factors were presented to bovine aortic endothelial cells.⁷¹ Similarly, S1P inhibits the task of human umbilical vein endothelial cell recruitment¹⁸², a task thought to be performed by VEGF.⁹ It is also known that VEGF upregulates S1P receptors on endothelial cells,¹⁸³ indicating that it would be necessary to present VEGF before S1P for the purpose of growing new blood vessels. The evidence that dual delivery of growth factors does not solve the problem of generating functional, integrated vasculature *in vivo*, suggests that angiogenic growth factors should be presented in profile in which they are presented during native angiogenesis.

7.0 SEQUENTIAL DELIVERY

7.1 INTRODUCTION

Decades of research have revealed that surface-bound and secreted biomolecules displayed and exchanged by cells form an organized “message” that can be accentuated or even inverted depending upon the temporo-spatial organization of the stimuli. It is becoming apparent that combinations of these various biomolecules can form organized sets of “instructions” that can be accentuated or even inverted depending upon the temporo-spatial organization of the stimuli (e.g. see examples from adaptive immunity¹⁸⁴, immunological tolerance¹⁸⁵, pancreatic insulin regulation¹⁸⁶, lipolysis¹⁸⁷, and osteocoupling¹⁸⁸ as just a few emerging examples). The complex processes of cell migration, differentiation and proliferation are typically dependent on both the presence/absence of specific growth factors and their time-dependence.⁹⁸ Growth factor signaling plays a significant role in the sequence of events responsible for both the development and regeneration of tissues, where the timing and order of presentation is crucial to the downstream signaling events.¹ Consequently, it is not surprising that the complexity of these biological processes dwarfs the complexity of current treatments intending to direct, accelerate or repair them. A prominent example of a biological process that is currently over-simplified by existing treatments is angiogenesis (the growth of neovasculature from existing vasculature). VEGF, FGF and angiopoietin-2, are required to disrupt the structure of preexisting blood vessels

and to promote the proliferation and migration of new cells to form new immature vessels. Angiopoietin-1 and PDGF are required to stabilize these newly formed blood vessels.¹⁸⁹⁻¹⁹¹ Another example where specific release kinetics would be desired is the release of gonadotropin releasing hormone, where a pulsatile release profile is desirable.¹⁹² Sustained release of this hormone does not result in increased fertility. Polymer systems capable of distinct release kinetics for growth factors may be critical to control biological processes.

It is thought that mimicking the natural sequence of “instructions”, as opposed to providing multiple “instructions” simultaneously, is the key to successful therapeutic angiogenesis.⁹ An appropriate system for delivery would not only exert control over the presence over factors but the absence as well, with the overall goal of mimicking physiological signaling and achieving biological functionality.¹ Creating an environment that mimics the multifactorial cascade of events that naturally occur in the body to accelerate or exploit the inherent capability of tissue growth is one goal of the regenerative medicine field. This process requires recapitulation of at least several of the spatial and temporal microenvironments presented naturally in the healing process. A number of approaches have been explored to achieve site specific and time-controlled delivery of therapeutics. However, many of these current approaches still have limited clinical utility, due to the challenging requirements for the delivery of multiple therapeutic agents in the proper time frame required for many biological events.¹⁹³

7.2 COMBINED RELEASE SYSTEMS

Only recently has delivery technology developed to the point where engineers are capable of varying the rate of multiple biological “instructions” with respect to one another.¹⁹⁴⁻¹⁹⁶ One method to control the delivery of growth factors in a way that can approximate the way in which they are presented naturally is to combine multiple release systems (gels, polymer microparticles, scaffolds, etc.) with two different release profiles, so that the growth factors are released at two different rates.^{67, 139-140} For example, one factor can be pre-encapsulated in polymeric microspheres and then mixed into a polymer scaffold during the fabrication process.⁶⁷ Proteins are most easily encapsulated using a double emulsion procedure that utilizes an internal aqueous (protein solution) phase during processing. The double emulsion process of microsphere fabrication begins with a protein solution being added to and heavily mixed with a polymer solution, where the solvents are immiscible, forming the first emulsion. This emulsion is poured into the immiscible solvent of the polymer solution and stirred, forming the second emulsion. The resulting double emulsion is poured into a polyvinyl alcohol solution, where the polymer solvent evaporates, leaving behind solid microparticles with encapsulated protein.¹⁹⁷

Polymer scaffolds can be fabricated by a variety of processes. One of these processes is solvent-casting particle-leaching in which salt particles are added to a polymer solution of specific diameter to produce a uniform suspension.¹⁹⁸⁻¹⁹⁹ As the solvent evaporates, the polymer matrix is left behind with salt particle embedded throughout.¹⁹⁹ When this matrix is immersed in water, the salt leaches out, producing a porous structure. Another method for scaffold fabrication involves gas foaming, where a biodegradable polymer is saturated with carbon dioxide at high pressures.²⁰⁰ As pressure is returned to atmospheric levels, the solubility of the gas in the polymer decreases, resulting in nucleation and growth of gas bubbles in the

polymer.¹⁹⁹ A third method of scaffold fabrication involves non-woven scaffolds have been produced from polyglycolic acid and polylactic acid,²⁰¹ which led to the development of a fiber bonding technique, where the resulting scaffold has increased mechanical properties.²⁰² Additional methods of scaffold fabrication include, but are not limited to: phase separation²⁰³, melt molding²⁰⁴, freeze drying²⁰⁵⁻²¹¹ and solution casting²¹². All of these methods allow for the incorporation of polymer microspheres, resulting in a combination of two release systems.

Theoretically each polymeric system allows (individually) for tuning of spatial and temporal delivery of growth factors (discussed in Chapter 5.0), allowing for spatially and temporally controlled delivery of growth factors.¹ In the method discussed here, the factor that is expected to act early is incorporated into a rapidly releasing phase, and the growth factor expected to act later in the process is incorporated into a phase with more sustained release. Even though both factors are released simultaneously, if the rates of release are different enough to capture the distinctions between the various stages in the healing cascade (amounts, time-frames of biological events), it should serve the healing process to a greater degree than administration of both factors at the same rate.

An example that employs this technique, and the first attempt of dual angiogenic growth factor delivery through a polymeric system, is adding polylactic co-glycolic acid microspheres that have been loaded with PDGF to a VEGF loaded scaffold and implanting into the subcutaneous pocket of a rat.⁶⁷ In this example, VEGF largely associates with the surface of the scaffold, allowing for rapid release, but PDGF is more evenly distributed through the scaffold. The scaffold as a whole results in temporal release of VEGF and PDGF (Figure 3).⁶⁷ When compared to bolus injections of the same factors individually, a statistical significantly difference in vessel density was observed at four weeks.⁶⁷

In a similar technique, PDGF was encapsulated in polylactic co-glycolic acid microspheres and mixed into a VEGF-containing alginate gel in a layered fashion, resulting in VEGF and PDGF release at different rates from one layer and VEGF release alone from the second layer (Figure 4).²¹³ These layered scaffolds were implanted into mice in a hindlimb ischemia model. Although the PDGF and VEGF layer scaffold was able to induce angiogenesis to great extent than a blank scaffold, as well as show varying degrees of angiogenesis in the two layers, the layer with both PDGF and VEGF did not induce angiogenesis to a great degree than PDGF alone. Additionally, it is shown that when VEGF is present without PDGF, there is an increased blood vessel density.

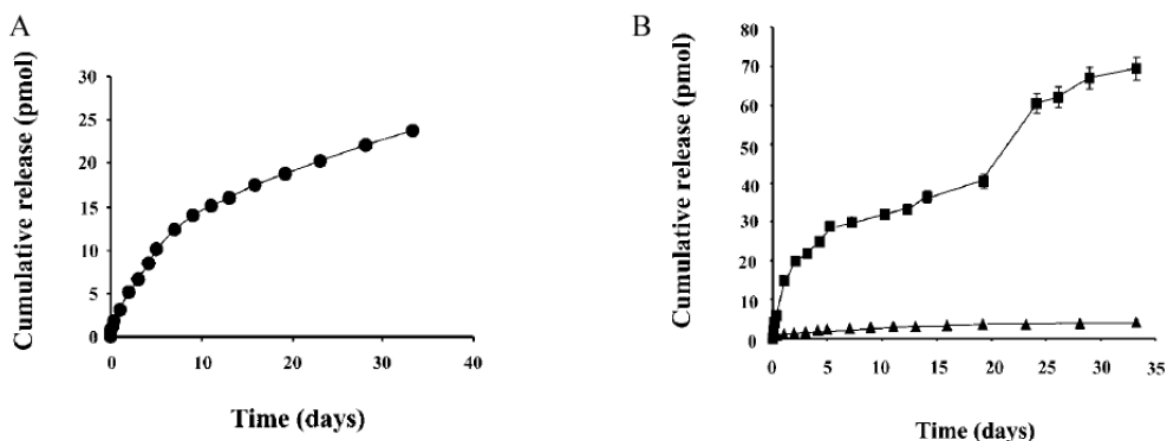


Figure 3. Cumulative release of VEGF and PDGF from a combined polymeric scaffold.⁶⁷ *In vitro* release kinetics. (A) *In vitro* release kinetics of VEGF from scaffolds fabricated from PLG (85:15, lactide:glycolide), measured using ¹²⁵I-labeled tracers. (B) *In vitro* release kinetics of PDGF pre-encapsulated in PLG microspheres (triangle - 75:25; box - 75:25), before scaffold fabrication. Data represent the mean ($n = 5$), and error bars represent standard deviation (error bars not visible are smaller than the symbol).

A third example of VEGF and PDGF delivery that has been explored is the combination of low molecular weight and high molecular weight alginate hydrogel for release of VEGF and PDGF at different rates, where VEGF release is quicker at first, followed by an increase in release of PDGF (Figure 5).²¹⁴ This gel was injected into rats following left anterior descending coronary artery ligation in a myocardial infarction model. While an increase in alpha smooth muscle positive vessels were observed when both VEGF and PDGF were delivered, there was no statistical difference in vessel density or left ventricular function when the VEGF and PDGF group was compared to delivery of PDGF alone.

Sequential delivery of growth factors has also been approached using the development of a composite system consisting of gelatin microspheres that have been incorporated into a synthetic hydrogel matrix.²¹⁵ This system was designed to release IGF-1 and TGF- β for the purpose of articular cartilage healing, using a non-invasive injectable therapy.²¹⁵ In this study, factors such as crosslinking extent and polymer density, were used to control the rate of release of each factor.²¹⁵

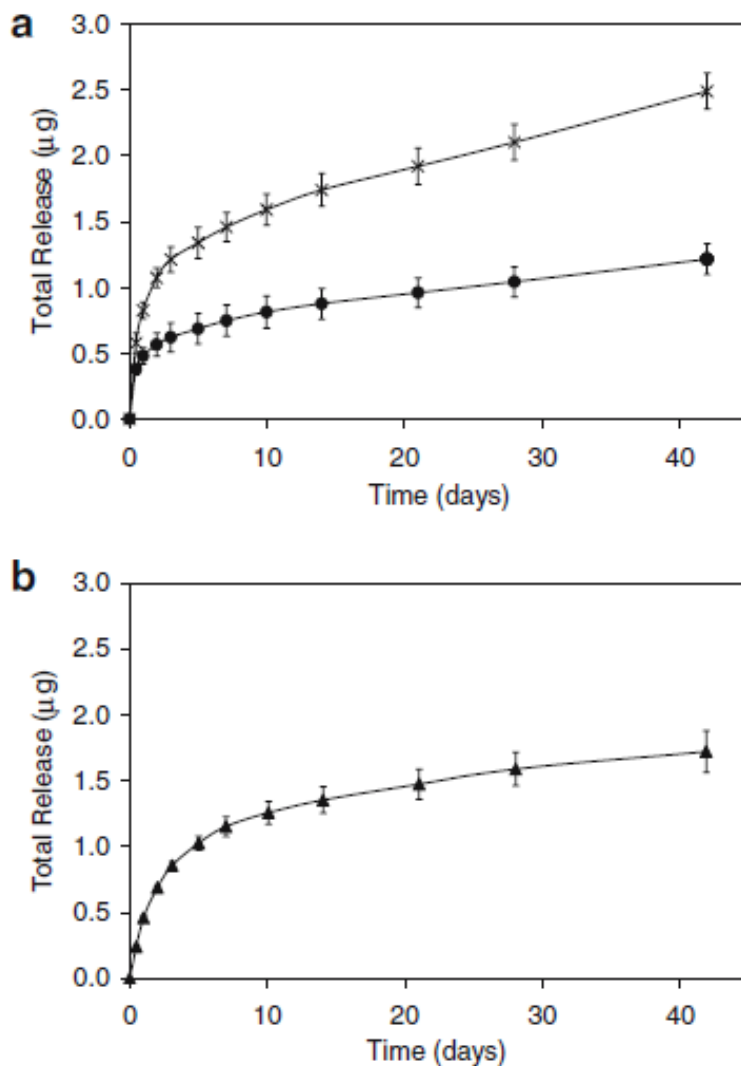


Figure 4. Total release of VEGF and PDGF from a layered polymeric scaffold.²¹³

VEGF (a) and PDGF (b) release from layered scaffolds was determined using radiolabeled growth factor ($n = 4$). The overall release profile of VEGF (a) is similar in layer 1 (cross) and layer 2 (circle) with an initial burst of VEGF followed by a steady release. Pre-encapsulation of PDGF in PLG microspheres slowed its release from layer 1 of scaffolds (b). The quantity of VEGF and PDGF released was proportional to the total mass of growth factor incorporated in each layer (1.5 mg VEGF and/or 3 mg PDGF in layer 1; 3 mg VEGF in layer 2). Values represent mean and standard deviation.

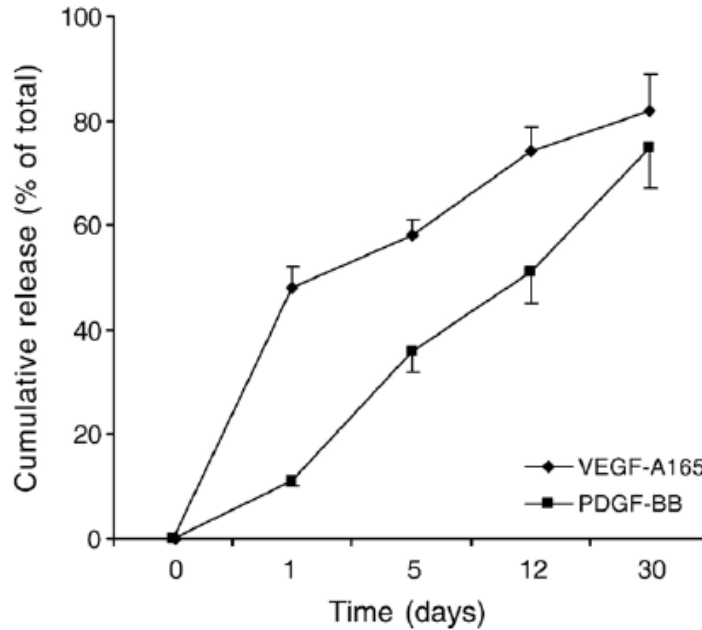


Figure 5. VEGF₁₆₅ and PDGF-BB release from alginate hydrogels of varying molecular weight.²¹⁴

The cumulative release of VEGF-A₁₆₅ and PDGF-BB from alginate hydrogels *in vitro* following incubation in PBS at 37 °C. Values are given as mean ±SEM, n=4 at each data point.

Additionally, alginate and poly lactide-co-glycolide were combined to create a release system, capable of releasing VEGF and PDGF.²¹⁶ This system is capable of delivery of multiple angiogenic factors with distinct kinetics (Figure 6).²¹⁶ Release kinetics were confirmed *in vivo* in a mouse hindlimb ischemia model, where PDGF release was detected until 42 days, but VEGF content was only detected until 28 days.²¹⁶ In this model, sequential delivery of VEGF followed by PDGF resulted in the formation of mature (alpha smooth muscle actin positive) vessel formation.

Systems in which release systems are combined for the temporal delivery of growth factors will need to be optimized for each particular treatment, formulation, growth factor and

delivery strategy, in order to be effective. Optimization would include identification of key growth factors, the mode of factor delivery, method of system fabrication and desired release kinetics for each particular tissue injury or disease.²¹⁶ Additionally, when combining two release systems, the resulting release profile is often constant release of both factors, simply at different rates. This may not be optimal for processes that, if occurring simultaneously, may conflict with one another. In this case, it might be beneficial to temporally separate the signals that promote each individual processes, as discussed in Chapter 6.0. In these cases, the release of one or more of the factors would need to be delayed for a predetermined amount of time (according to what happens physiologically), while an initial factor is released. These systems require further investigation before reaching the point where delayed release is a possibility.

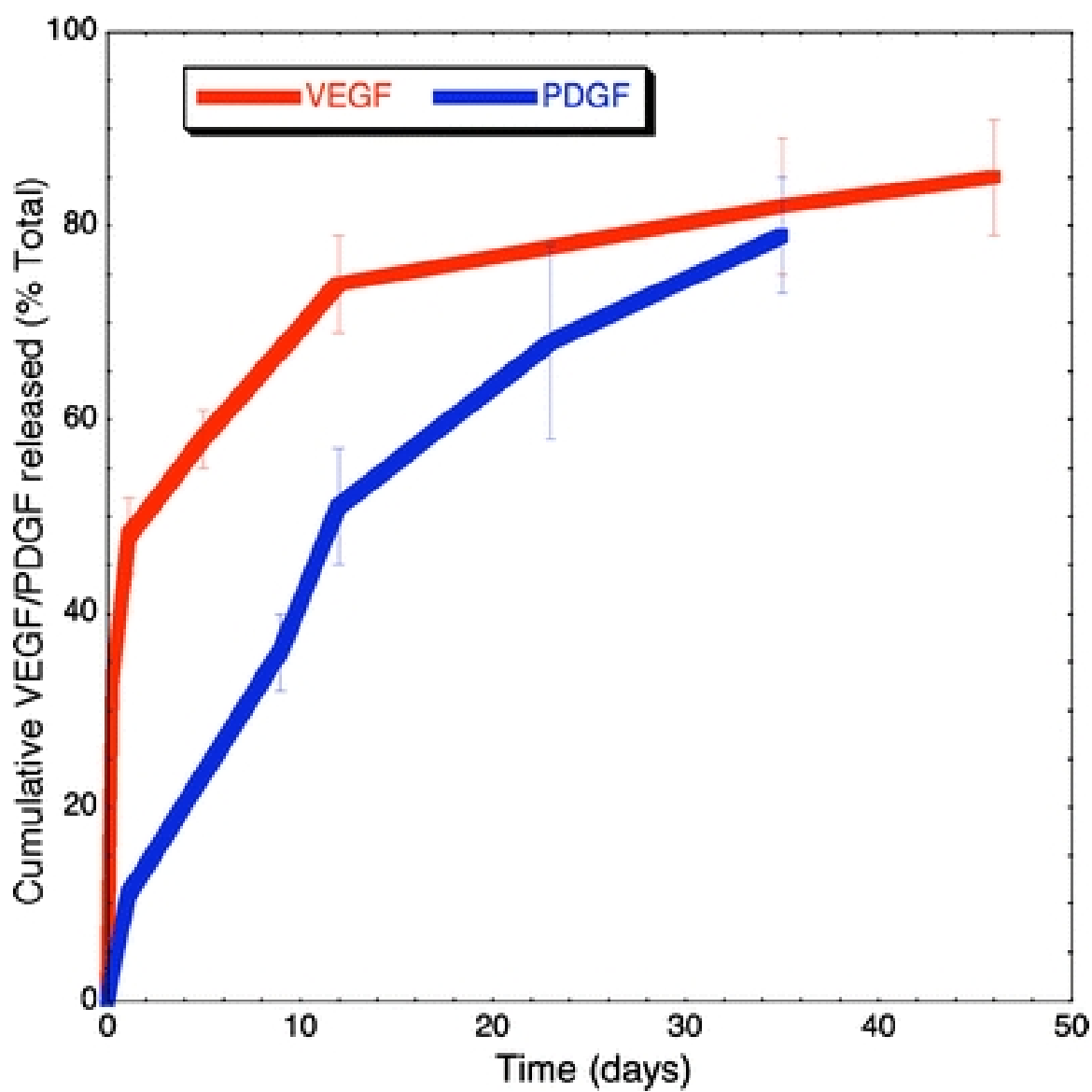


Figure 6. *In vitro* release kinetics of pre-encapsulated PDGF and VEGF from alginate fabricated from poly lactide-co-glycolide.²¹⁶

7.3 LAYER BY LAYER FILMS

One strategy that attempts to overcome the hurdle of factor release overlap is the use of stratified systems such as layer-by-layer (LBL) films. LBL films consist of electrostatic layer-by-layer assembly with a cationic polyelectrolyte and anionic particles such as protein molecules.²¹⁷ The fabrication process entails sequential adsorption on monolayers of oppositely charged polymers, colloids or other materials onto a solid substrate to form a cohesive, ionically crosslinked thin film, with the idea that films will surface-erode in a fashion that releases factors in the opposite order to which they are loaded into the stratified system.²¹⁸ This technique takes advantage of the attractive electrostatic forces between charged polymers and oppositely charged surfaces (See Figure 7).²¹⁹ Multilayers can be deposited rapidly and inexpensively atop large area surfaces of any geometry while allowing for nanometer-scale control over a range of physical properties.²¹⁸

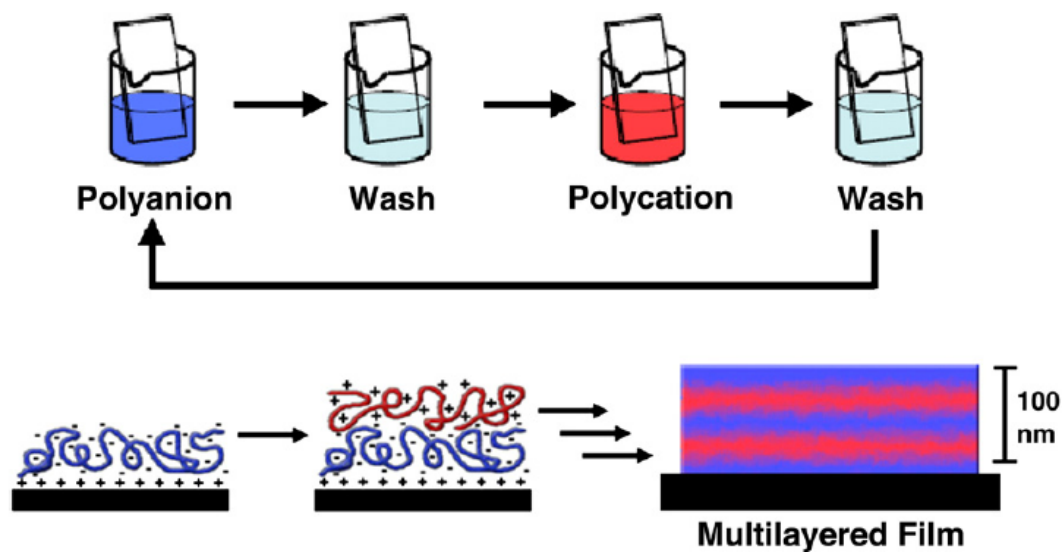


Figure 7. Layer-by-layer film fabrication technique.²¹⁹

Polyelectrolyte multilayers have attracted much interest for their versatility, ease of preparation and ability to coat virtually any substrate (titanium, ceramic, polymer, glass).²²⁰⁻²²¹ This assembly technique allows for absolute control over the order in which multiple functional elements are incorporated into a growing film. Because an LBL film is an erodible multilayer that deconstructs in aqueous conditions via disassembly and/or breakdown of the constituent polymers, it is being explored as a potential controlled release delivery system.²²¹ By employing degradable polyelectrolytes as building blocks, the ability to tune the degradation kinetics of multilayer assemblies has been demonstrated and used to control the release kinetics of compounds embedded in these films (examples: antimicrobial, anti-inflammatory, drug-releasing stents),²²¹ while allowing for the incorporation of sensitive biomolecules (proteins) and DNA (due to mild aqueous conditions during fabrication).²¹⁸ Hydrolytically degradable LBL thin films can be constructed from any molecular species that is either intrinsically charged or that can be encapsulated in a charged “carrier”.²²² A main feature of this technique is its ability to small features, nonplanar surfaces and microparticles, while still being able to build complex special architectures.²²²⁻²²⁴

Early drug release experiments with LBL films using hydrogen bonded-based interactions showed films that fall apart rapidly at near neutral pH, resulting in instantaneous method of drug release.²²⁰ A second approach was to pre-construct LBL films from inert polymers with drug loaded into the permeable network for diffusive or pH induced release, allowing for sustained release of small molecules.²²⁵ However, in this approach, large molecules such as proteins remained trapped. A hydrophobic, and thus slowly degrading, poly(β -aminoester) has been used as a cationic polymer, with either heparin sulfate or chondroitin

sulfate as an polyanion, for LBL film fabrication, allowing for release of a growth factor (large protein) without rapid degradation of the film.²²⁰ These films demonstrated sustained controlled release of bFGF (over 12 days) from a synthetic, biodegradable polymer LBL drug delivery system, where release is tunable through the polycation, polyanion and number of layers used to construct the film.²²⁰ Basic FGF released from the film exhibits enhanced ability to promote proliferation in pre-osteoblast cells compared with exogenous supplementation.²²⁰ Another example of the use of the cationic poly(β -aminoester) for the fabrication of LBL films is demonstrated in a transcutaneous drug delivery model, using a model protein.²²¹ In this model, researchers have demonstrated that protein antigen released from multilayer patches can be acquired by immune cells in the skin within hours of application of the film.²²¹ Additionally, they show that two molecules (antigen and adjuvant) can be loaded together and released with distinct kinetics, as may be desirable for temporally controlling the induction of a therapeutic response.²²¹

One example of LBL films being used in an animal disease model is the delivery of gentamicin to a rabbit bone infection model, using titanium implants.²²⁶ Typical treatment of infection following orthopedic surgery is a two stage surgical procedure and several weeks of intravenous antibiotics.²²⁷ In this study, thin films with antibiotic functionality were constructed using the LBL technique by alternating the deposition of a hydrolytically degradable poly(β -amino ester), biocompatible poly(acrylic acid), and the therapeutic gentamicin.²²⁶ With a burst release followed by zero-order sustained release for over a week, the films fabricated in this study demonstrate the release of one molecule by two release mechanisms, combining to match a desired release profile.²²⁶ In this study, implants significantly decreased the viable bacteria count compared to the uncoated implant, allowing for a one-stage re-implantation procedure

after an infected arthroplasty.²²⁶ In another example, when heparin was loaded into a degradable LBL film, distinct non-linear release that can be predicted within 10% at various pH conditions was observed.²²² It is believed that the distinct release regimes observed correspond with the degradation of individual layers of the film.²²² A technique similar to the ones described here could be utilized for the delivery of two different factors as well. These results are an important step forward in the effort to develop complex release architectures where a specific release profile is desired.

The techniques employed in the previously mentioned studies can be applied not only to the precise control over delivery of one protein, but the combined, temporal or sequential, delivery of two or more molecules. A system made from LBL poly(L-glutamic acid) (PLGA) and poly(L-lysine) (PLL) films into which cationic CD [pyridylamino- β -cyclodextrin (pCD)] and DNA have been embedded was employed for the delivery of two different DNA plasmids.²²⁸ Expression of both genes was tracked over an eight hour period on attached COS cells. SPT7 expression was detected as early as two hours following exposure, while expression of EGFP was not observed until four hours after exposure (Figure 8).²²⁸ When the placement of the plasmids in the thin film was reversed, so was the timing of expression.²²⁸

A multi-agent LBL film, capable both charged macromolecule and uncharged small hydrophobic drug delivery was developed, where release was controlled by the hydrolytic degradation of a poly(β -amino ester).¹⁹³ The intrinsic properties of the multilayer, the drug components and the layering agents in the film, all contribute to the release profiles of each component.¹⁹³ Release of heparin occurred over a 50 hour period, where 50% release occurred at 6 hours, while release of dextran sulfate occurred over a 120 hour period, where 50% release occurred at 37 hours (Figure 9).¹⁹³ These results demonstrate distinct release profiles of two

different molecules from the same biomaterial, where release profiles were largely controlled by the selection of layering agent.¹⁹³

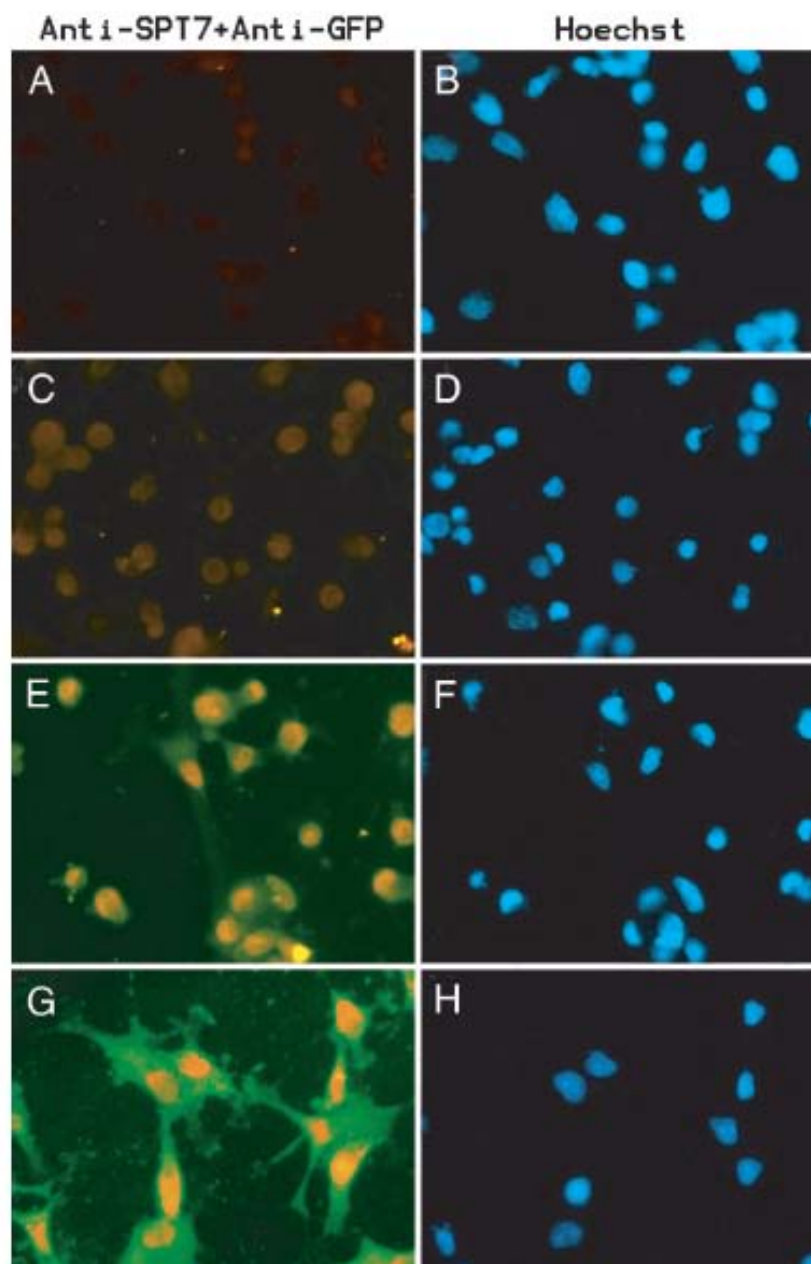


Figure 8. COS expression of temporal delivery of DNA.²²⁸

Expression of SPT7 and EGFP in COS cells grown on the surface of multilayered films (A and B) for 2 h (C and D), 4 h (E and F) and 8 h (G and H). The expression of SPT7 (red) and GFP (green) was detected with antibodies (A, C, E, and G). Nuclei were visualized by Hoechst 33258 staining (B, D, F, and H).

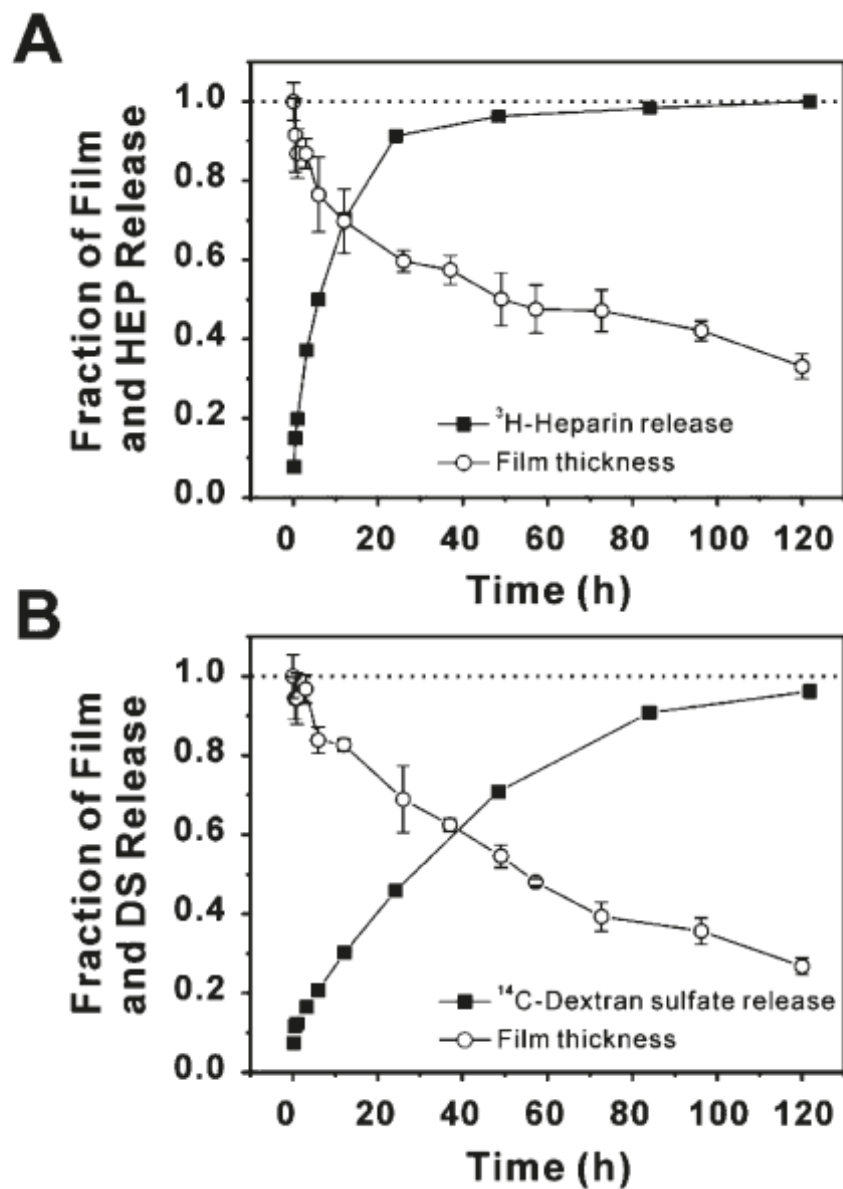


Figure 9. Release of heparin and dextran sulfate from LBL film.¹⁹³

Release profiles of radiolabeled anionic polysaccharide and film thickness changes for (top) the HEP film and (bottom) the DS film.

When considering the ability to finely tune release from an LBL, it is necessary to consider interlayer mixing, as this will have a negative effect on the ability to sequentially release factors. Current research involves adding physical barrier layers between layers to control interlayer diffusion following hydration.²¹⁸ Successfully achieving sequential delivery in these systems will require a balance of adding enough layers to decrease intermixing, while minimizing scaffold thickness, as to avoid bulk (internal, heterogeneous) erosion throughout the polymer layers. Another approach to decrease interlayer mixing and diffusion is covalently crosslinked barriers (instead of ionically crosslinked barriers) that lead to compartmentalized structures.²¹⁸ LBL films are also limited by the inability to control the relative positions and distributions of multiple species residing within a single film, resulting in highly disorganized architectures.²¹⁸ Over the years, many modifications have been developed, including the use of colloidal particles, where the colloidal core is destructed, leading to hollow particles. Additionally, the use of porous templates such as anodic alumina pores leads to tubular objects and sacrificial substrates, and eventually self-standing films.²²⁹

Results from the fabrication of LBL films are an important step forward in the effort to develop complex release architectures that combine more than one release agent for optimized, multi-drug release. LBL films can be applied to the surface of many implant materials, such as titanium orthopedic implants or cardiovascular stents. In many biomaterial implants, the need for sequential delivery of more than one agent would be desirable. LBL films is an emerging and developing area of research and can benefit from the interdisciplinary work of researchers in biology, medicine and the pharmaceutical sciences.²¹⁹

7.4 MICROCHIP TECHNOLOGY

In situations where precise control over drug release is imperative, due to a small therapeutic window for therapeutic concentration, or a therapeutic concentration that changes with time, microfabrication techniques may be ideal.²³⁰ The microprocessing techniques employed for drug releasing microchips are the same techniques used to make microprocessors for computers and other microelectric devices. Some examples of these are micropumps or microvalves, however, these both have limits on reliability and the types of solutions that can be used.²³¹ The first demonstration of a microchip used for drug delivery was developed in 1999, where solid-state silicon microchip reservoirs were loaded with sodium fluorescein and released in a pulsatile manner over several days (Figure 10).²³² Each reservoir is covered on one end by a thin gold membrane that serves as an anode in an electrochemical reaction.²³⁰ The reservoirs can be filled with any combination of drug or drug mixtures in the solid, liquid or gel state, by inkjet printing or microinjection.²³⁰ When release is desired, a voltage is applied between the anode membrane and a cathode, causing the anode to dissolve and the drug to be released from the reservoir.²³⁰ It was demonstrated that release from each reservoir could be controlled individually, creating a possibility for achieving many complex release patterns.²³²

A resorbable polymeric microchip was created from poly(L-lactic acid) (PLA), chosen for its slow degradation, allowing for complete release before degradation of the microchip, as well as its biocompatibility.^{223, 233-235} PLA microchips were fabricated with 36 reservoirs, each with a volume of 120-130nL.²²³ When four reservoirs were loaded with either heparin or dextran, release of each molecule was distinct (Figure 11).²²³

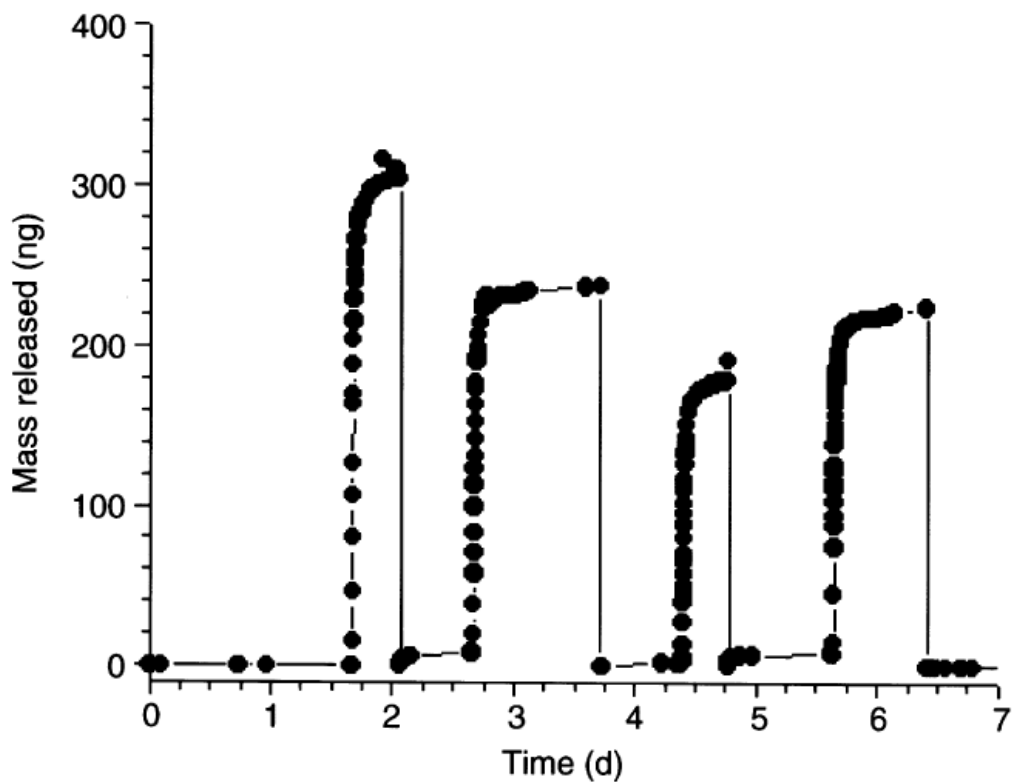


Figure 10. Pulsatile release of a single substance from a microchip device.²³²

The total mass of sodium fluorescein released into PBS over a period of several days is shown for each of four reservoirs. This release study was conducted in PBS stirred with a magnetic stirring bar at room temperature. The device was submerged in the PBS for >36 h before the first release to ensure that there was no leakage from any of the loaded reservoirs.

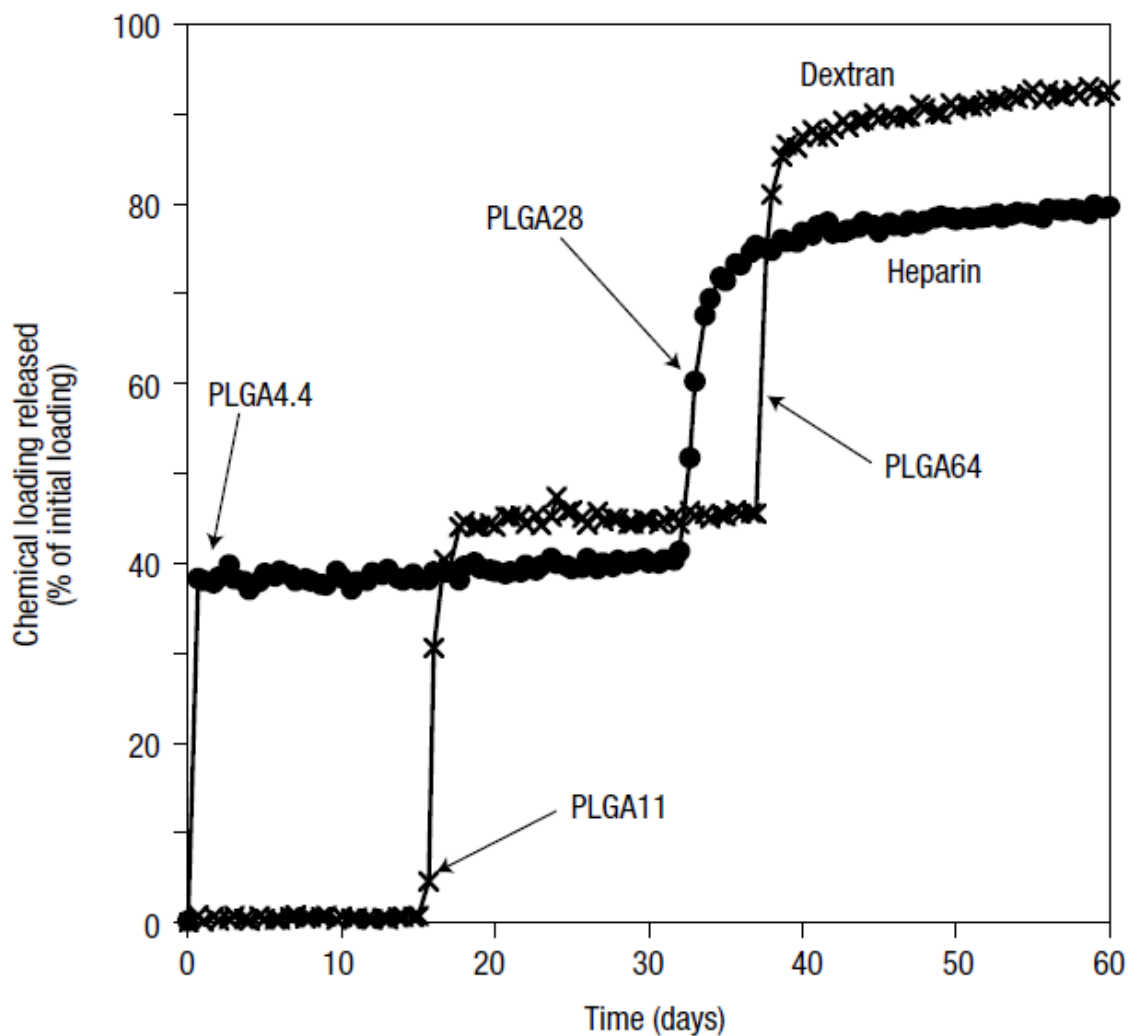


Figure 11. Cumulative percent of initial loading released from microchip device *in vitro*.²²³ Release results are shown for a representative device that was loaded with both ¹⁴C-dextran (crosses) and ³H-heparin (circles).

An *in vivo* study was carried out using a fully implantable silicon microchip, containing 24 reservoirs that were filled with mannitol.²³⁶ These microchips were placed into a stainless steel housing and implanted in the dorsal subcutaneous space of rats.²³⁶ Mannitol release was measured from urine samples, demonstrating that reservoirs successfully release on average 85% of its contents on demand (Figure 12).²³⁶

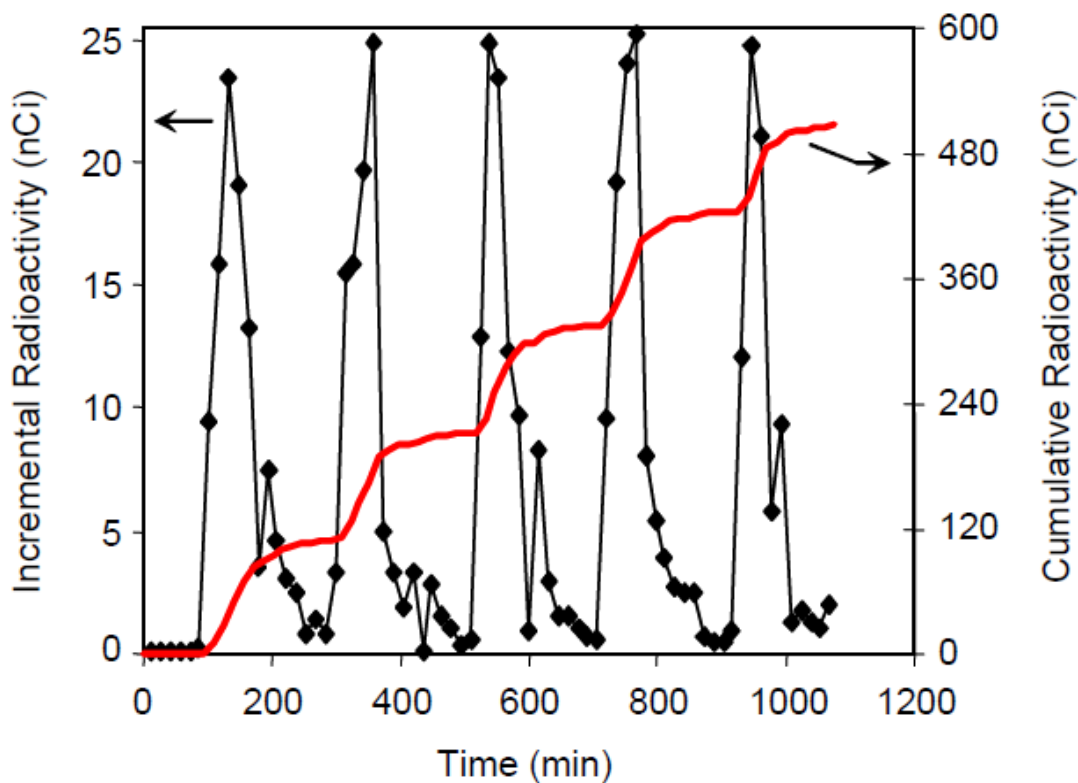


Figure 12. *In vivo* release profiles (urine measurements) of mannitol release from a silicon microchip.²³⁶

Advantages of this technique include its versatility, small size, quick response times and lower power consumption²³², where release is controlled by the size and polymer of the device, number and volume of reservoirs and thickness and material of the membrane.²²³ However, in

some instances, the small volume of the reservoir becomes a limitation of the device.²³⁷ Potential applications for devices such as these include implantable devices with patterned delivery of multiple drugs or an oral delivery device.²²³

7.5 EMERGING RELEASE TECHNOLOGY – TUNABLE MICROPARTICLES

The ability to precisely program a release profile into a degradable microparticle delivery system (such as the ones described in Section 7.2), through manipulation of physical properties and fabrication conditions, could lead to flexible and injectable sequential delivery systems. In most hydrolytically labile polymer release systems, the release of large encapsulated agents (proteins, nucleic acids) is dictated primarily by the degradation and erosion of the polymer.^{196, 238} If a clear correlation between release of an agent and degradation/erosion of a delivery system can be derived, it may be possible to dictate the release profile of the agent. For instance, one method for controlling release kinetics is PEG-based surface modification of porous silicon microparticles.²³⁹ Incorporation of high molecular weight PEG into the backbone of the polymer was able to delay degradation of the silicon microparticles.²³⁹ Although controlling release by chemical modification is a viable way to influence release behavior, this strategies may be limited to circumstances where polymer structure is of little importance to the desired formulation.

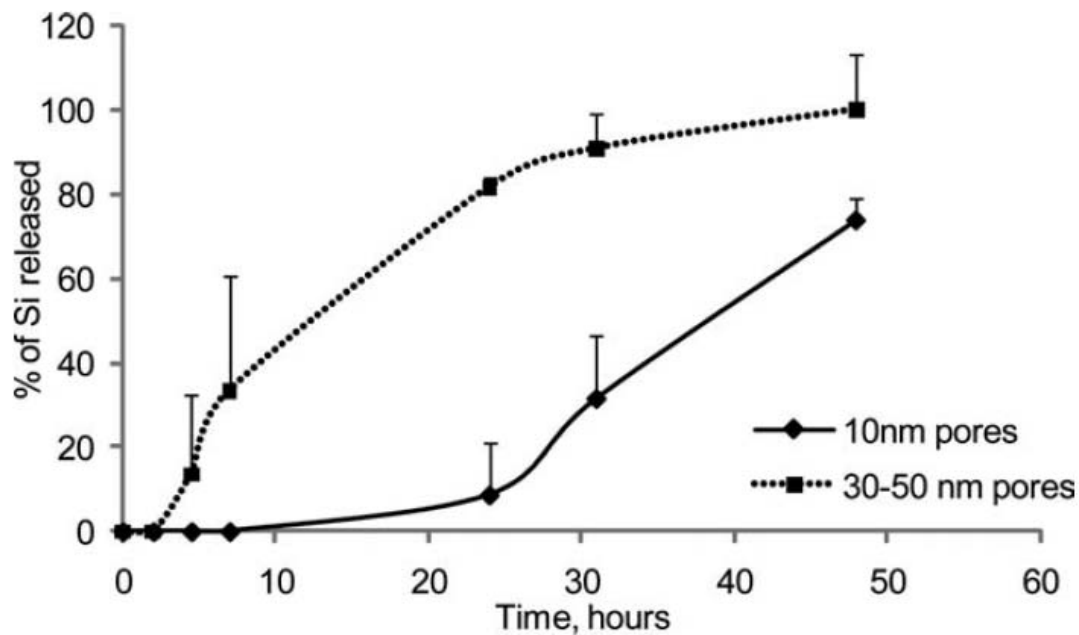


Figure 13. Degradation kinetics of large pore and small pore silicon particles.²³⁹

Degradation kinetics of large pores (30–50 nm) and small pores (10 nm) silicon microparticles as evaluated by inductively coupled plasma atomic emission spectrometer. The degradation kinetic profile is expressed as a percentage of the total silicon contents released to the degradation medium.

A more comprehensive understanding of how release is dictated by the processes occurring in degrading release systems would permit both flexibility and precision while tuning release of biological agents.¹⁹⁵⁻¹⁹⁶ It is widely known that bulk eroding polymer matrices can range from linear release, to four-phase release: initial burst, lag phase, secondary burst, terminal release.¹⁹⁵ The degradation mechanism of the polymer, matrix crystallinity and physical properties of what is being release all play a role in the release profile²⁴⁰, but most attempts to predict this behavior focus on a dominant erosion behavior. In a non-degradable matrix, *in vitro* release studies show that matrix porosity controls the diffusion of protein through the matrix.²⁴¹ When the rate hydrolysis is much faster than the rate of water diffusion through the polymer

matrix, surface erosion is prominent.²⁴² When water diffusion is so fast that the particle is completely hydrated before significant diffusion occurs (in the case of PLGA microspheres), bulk erosion occurs.

Recently, a model that describes up to three phases of release (burst-lag-burst, Figure 14) for agents ranging in size from small molecules to viruses¹⁹⁵ (and extended to matrix implants and hydrophobic agents¹⁹⁶) has been developed. This model takes five readily attainable parameters (polymer initial molecule weight, polymer degradation rate, microparticle size, initial drug distribution, drug molecular weight) into account when predicting release from a degradable microparticle system.²⁴³ These parameters are used to determine a new parameter known as the molecular weight of release (M_{wr}), which described the average polymer molecular weight that permits diffusion of the encapsulated agent and is dependent upon the size of the agent being released.¹⁹⁵ Using these values, the magnitude of initial burst and release kinetics of subsequent stages could be predicted in a regression free manner.¹⁹⁵ A modification to the model was made to include predictions that account for matrix hydration and dissolution kinetics.¹⁹⁶ These new considerations allow this model to be extended to surface eroding systems, as well as surface eroding systems that transition to bulk eroding systems.¹⁹⁶ These finding allow for the tuning of the magnitude of initial burst, the lag phase and the final rate of release, so that a particular microparticle formulation could be conceived given a desired release profile and application.²⁴³

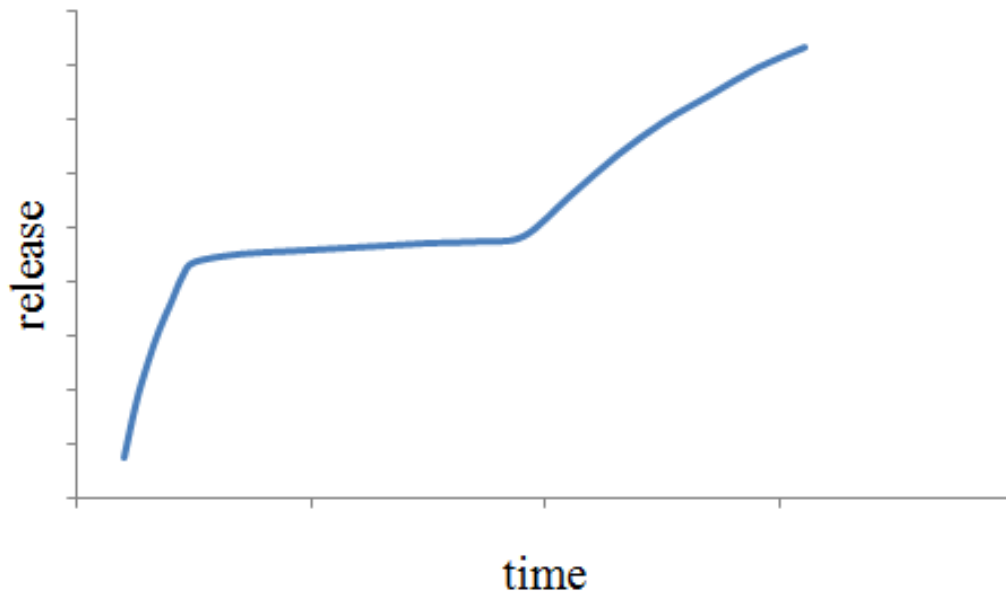


Figure 14. Schematic of triphasic release from microparticle systems.

Overall release time of a microparticle system is determined by the degradation rate of the polymer, however, it was found that each of the phases can be individually tuned. It has been determined that the initial burst can be adjusted by changes in the initial drug distribution as well as the matrix size.²⁴³ Similarly, it has been determined that the lag phase can be adjusted by changing the polymer molecular weight and degradation rate.²⁴³ Lastly, the terminal release can be adjusted by changing the copolymer ratio.²⁴³ Development of a model that could predict the behavior of any microparticle set would allow for rapid development of tunable microparticles.

Using this model as a tool, it can be envisioned that degradable particles that release factor 1 for a predetermined amount of time can be combined with separate degradable particles that are designed to “wait” until the other formulation has completed its release prior to the onset of factor 2 release. If possible, such would represent an extremely attractive way to sequentially

deliver two growth factors in the same injectable system. In the same way, it is possible that any number of other physiologically relevant release profiles, such as pulsatile kinetics, could be achieved through rational design of the degradable release formulations.

Research is currently being performed, where microparticles that release an early stage angiogenic factor are combined with microparticles that exhibit delayed release, or no initial burst, followed by release of a late stage angiogenic factor according to delivery schedules discussed in Chapters 8.0 and 9.0 . This combination of microparticles would produce a combined release profile of sequentially delivered angiogenesis promoting factors, and thus an injectable therapeutic alternative to current angiogenesis promoting treatments.

7.6 CONCLUSIONS

Release systems capable of unique and finely tuned release kinetics have potential in the fields of angiogenesis²⁴⁴, bone healing^{213, 245-248}, hormone therapy¹⁹² and tissue regeneration^{98, 101, 249}. Although many release systems are becoming increasingly relevant towards the development of temporal release systems that can mimic physiological processes, it is also important to determine the “ideal” release kinetics to achieve the desire response. The remaining chapters will discuss how porous cellulose hollow fiber membranes can be used to gain a better understanding of four angiogenesis promoting factors and their involvement in each angiogenic stage. This system allows for the exploration of many release profiles without fabrication of complex release systems. Equipped with this information, the emerging delivery systems

described above can be “programmed” with the appropriate sequential release time-frames for specific biological applications.

8.0 SEQUENTIAL DELIVERY OF VEGF AND S1P

8.1 INTRODUCTION

As discussed previously (Section 4.1), some progress has been made towards the promotion of angiogenesis *in vivo* by delivery of various angiogenic growth factors. Yet, delivery of a single factor alone (such as vascular endothelial growth factor, VEGF), is known to be associated with weak and leaky vessels.⁹ Consequently, it has been hypothesized that a combination of angiogenic growth factors might be the key to inducing functional, mature angiogenesis that integrates with the existing vasculature.⁹ Yet, the process of angiogenesis is an organized series of events, beginning with vessel destabilization, and followed by endothelial cell proliferation and migration, and lastly vessel maturation (Chapter 6.0).⁹ During these events, it is thought that different angiogenic factors become important at different points in time.⁶⁴

Certain factors have already been identified as playing a roles in a specific stage of angiogenesis, such as endothelial cell migration and proliferation⁹, vascular network maturation⁷⁵ and induce a proangiogenic phenotype in endothelial cells.⁷¹ Of these factors, VEGF and sphingosine-1-phosphate (S1P) are two with well documented and distinctive roles. Although VEGF is known to mediate the recruitment of endothelial cells⁹, it has been observed that S1P (an angiogenic factor shown to stabilize intracellular junctions and decrease permeability of endothelial cells²⁵⁰⁻²⁵¹), inhibits the recruitment of these endothelial cells. Furthermore, an

examination of S1P and VEGF signaling in endothelial cells suggests that there is a preferred sequence of factor presence and absence during the formation of mature vasculature^{102-103, 183, 252}. In light of these data, it is reasonable to speculate that the logical strategy to stimulate growth of neovasculature would be to first induce recruitment of endothelial cells through VEGF (without inhibition from S1P), followed by the onset of endothelial cell arrangement and mural cell recruitment due to subsequent presence of S1P (without inhibition from VEGF). In other words, exhibiting control over the absence of a given angiogenic factor may be just as important as control over the presence of that factor in a given stage of angiogenesis. VEGF and S1P are an example of factors in which their temporal presence may affect their action on a particular physiological process.

Controlled release is one viable strategy for achieving temporal presentation of small molecules and proteins in a format that can be applied therapeutically. Yet, to date, achieving such a complex release profile has proven elusive (Chapter 7.0).^{67, 139-140} For instance, dual delivery of basic fibroblast growth factor (bFGF) and VEGF²⁵³ as well as angiopoietin-1 and VEGF²⁵⁴ have been explored previously. In these studies, angiogenic growth factors were loaded into the same scaffold so that release of these factors occurs simultaneously (e.g. dual delivery). In addition, several attempts have been made to adjust the release of two factors independently (VEGF and PDGF), where each growth factor is loaded into a different scaffold (i.e. each factor is provided its own “resistance” to release over time). Accordingly, VEGF and PDGF were released at different rates, leading to some observable differences in response.^{67, 213} Yet, to study systems where the function of a growth factor may inhibit the function of another (e.g. angiogenesis), it would be desirable to develop a model where temporal separation of biomolecule release can be easily tuned.

Here, we describe a sequential delivery model based upon a porous hollow fiber that extends into an acellular site (*in vitro* or *in vivo*), permitting external control over presence and absence of angiogenic factors at any time. In this model, a hollow fiber membrane separates the angiogenic factor “reservoir”, which resides in the lumen of the fiber, from a scaffold for cellular infiltration. Due to the ease of accessibility to the hollow fiber lumen, this system is extremely modular, allowing for a quick change in factor delivery at any point in time. The fiber wall microstructure can be controlled through the hollow fiber fabrication process to ensure that large proteins can be effectively released over time to the surrounding matrix.²⁵⁵⁻²⁵⁸ We have used this model to study the hypothesis that the sequence and delivery schedule of VEGF and S1P will impact the significance and maturity of angiogenesis, based on evidence that the presence of one factor might inhibit the performance of another factor.

8.2 MATERIALS AND METHODS

8.2.1 Hollow fiber fabrication and characterization

Cellulose acetate hollow fibers were prepared using a double injection nozzle (14G/20G) and two syringe pumps (Braintree Scientific). Twenty percent cellulose acetate (30kD, Aldrich) in a DMSO/acetone/isopropanol/water [49:15:15:1 weight%] was pumped through the outer core of the nozzle at 1.5mL/min and deionized water was pumped through the center core at 10mL/min. The cellulose solution and deionized water were extruded into a deionized water bath where the cellulose solution precipitates in the form of a porous hollow fiber, as previously described²⁵⁹, creating a flexible hollow fiber membrane capable of implantation into an animal. Hollow fibers

were sterilized with UV light and stored in deionized water for future use. Lyophilized hollow fiber cross sections were sputter coated with 3.5nm of gold-palladium and imaged at 5kV using a JEOL 9335 SEM.

8.2.2 *In vitro* release

Wells of a 6-well cell culture plate were filled with 3mL Dulbecco's phosphate buffered saline, or PBS (Invitrogen) and a cellulose hollow fiber was cut to fit the well and injected with 10 μ L of rmVEGF (R&D Systems) and Fluorescein (Sigma) using a 28½G insulin syringe (1/2 cc Lo-Dose U-100 insulin syringe, Becton Dickinson and Co.). Hollow fibers were injected first with VEGF (100 μ g/mL) and subsequent release into a PBS bath was measured by sampling the supernatant and measuring using a VEGF ELISA kit (R&D Systems). After 24 hours, the fiber was rinsed five times with PBS and lumen contents were replaced with an aqueous solution of fluorescein (1800 μ M). Again, release was measured by sampling the supernatant and measuring fluorescence emissions every hour on a plate reader (SpectraMaxM5, Molecular Devices).

8.2.3 Murine Matrigel plug assay

Growth factor reduced Matrigel (500 μ L) was injected into the subcutaneous space on the dorsal side of C57BL/6 mice (8-10 weeks old, Charles River) on both the left and right flank, following anesthesia with 2-3% inhaled isoflurane. After five minutes (to permit gelling), a 12G needle was used to thread cellulose hollow fibers through the skin and Matrigel plugs. Hollow fibers were fixed in place using tissue glue and an Elizabethan collar was used to prevent mice from extracting the hollow fiber. On the day of implantation and every day for the next 6 days, hollow

fibers on the left side were injected with sterile saline, as an internal negative control, and hollow fibers on the right side were injected with 10 μ L of an angiogenesis promoting factor: 100 μ g/mL VEGF (R&D) and/or 1800 μ M S1P. For mice in the sequential delivery groups, factor switching occurred on the third day after implantation, following five rinses with saline. Seven days post-implantation, implants were extracted, fixed in 2% paraformaldehyde for 5 hours and 30% sucrose overnight and snap-frozen in liquid nitrogen. Frozen sections (8 μ m) were stained with Hemotoxylin and eosin (H&E) and analyzed for endothelial cell migration and vessel formation.

8.2.4 Immunofluorescence

Frozen Matrigel Plug sections (8 μ m) were incubated with primary antibodies rabbit anti-CD31 (Abcam) and Cy3-conjugated mouse anti- α -smooth muscle actin (Sigma) and secondary antibody goat anti rabbit Alexa Fluor 488[®] (Jackson Immuno). Sections were also counterstained with Hoechst (Sigma) to identify all mononuclear cells. Images of CD31 labeled cross-sections were taken at 40x. These images were analyzed using threshold analysis on Metamorph to quantify the percent of each image occupied by CD31 staining. These values were averaged to obtain a representative percent for each cross-section and normalized to the internal positive control in which only saline was delivered.

8.2.5 Statistical analysis

ANOVA was performed when assays contained more than one experimental group, as in the tubular formation assay (n=3) and Murine Matrigel plug assay (n=3). Pilot studies and a power analysis were performed to determine N for *in vivo* experiments. Subsequently, a post hoc

multiple comparison test was performed to compare means of different experimental groups (Holm-Bonferroni, $\alpha=0.05$, $k=4$).

8.3 RESULTS

8.3.1 Hollow fiber fabrication

To test our hypothesis, we required a delivery system capable of true, sequential release. A hollow fiber based system (in which both ends extend out from the site of delivery) would effectively accomplish this task as long as the wall porosity was made large enough to facilitate protein delivery. Given that commercially available fibers typically have smaller pores that do not permit protein delivery over the required time scales, we chose to fabricate fibers in-house using a double injection extrusion/precipitation method. Cellulose was chosen as a non-biodegradable, but biocompatible material. An SEM image of the hollow fiber wall shows the complicated pore structure consisting of both macropores ($>10\mu\text{m}$) and micropores ($<1\mu\text{m}$), where the micropores (being the rate limiting portion of delivery) control the rate of delivery from the lumen of the fiber to the surrounding environment (Figure 15a). A higher magnification SEM image shows the interconnected pore structure (less than $1\mu\text{m}$) of the cellulose hollow fibers (Figure 15b). The hollow fiber wall thickness was $114\pm 11\mu\text{m}$ and the inner diameter was $863\pm 67\mu\text{m}$.

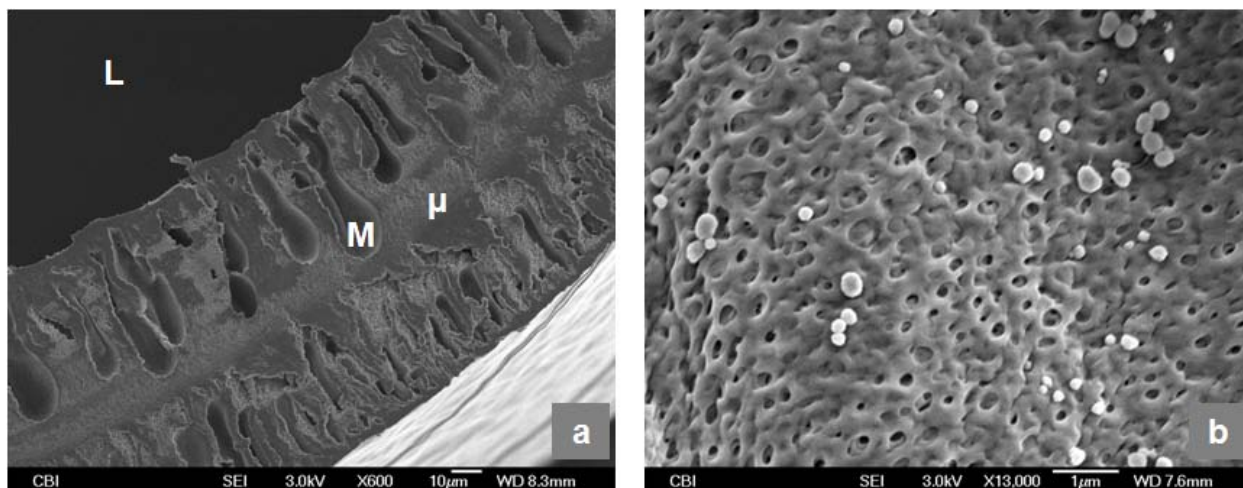


Figure 15. Scanning electron images of cellulose hollow fiber.

Double extrusion nozzle (14G/20G) extruded 20% cellulose at 1.5mL/min and water flowing at 10mL/min. (a) Hollow fiber wall depicting porous structure of hollow fiber from lumen (L) outward. The edges of the wall display macropores (denoted as M) around 10 μ m in width and 30-50 μ m in length. (b) The microporous voids (denoted as μ) of the remaining scaffold are less than 1 μ m.

8.3.2 Sequential delivery of molecules of relevant size

A hollow fiber-based release system was chosen to present factors sequentially because of the precision afforded through external regulation of the lumen contents over time. For the purpose of ensuring that fibers are capable of sequential control, we chose to modulate the presence/absence of two factors in the lumen of the fibers over time: 1) vascular endothelial growth factor (VEGF, 45kDa) and 2) Fluorescein (376Da) as an easily detectible molecule of similar size and solubility to S1P (379Da). Specifically, porous fibers were loaded with VEGF for an initial period of release, rinsed and then subsequently loaded with fluorescein. Egress of these molecules through the fibers and into a surrounding saline solution is represented in Figure 16. Importantly, when factors are exchanged (corresponding with saline flushing prior to

administration of a new factor, depicted by the dotted line), VEGF release decreases and fluorescein is subsequently detectable in the supernatant. These results suggest that our fibers are readily capable of release of a growth factor sized protein as well as sequential delivery of two factors, as determined empirically.

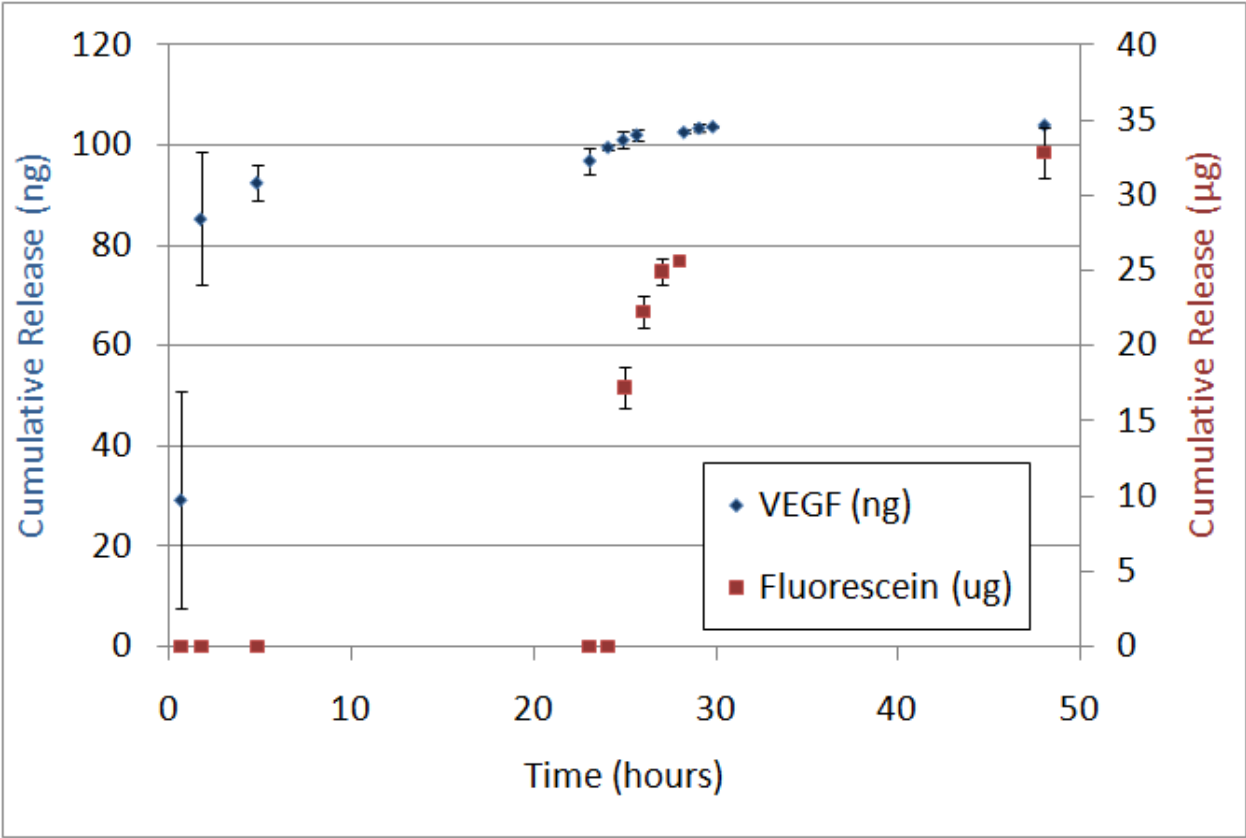


Figure 16. Release profile of sequentially delivered VEGF and Fluorescein.

Release profile from a cellulose hollow fiber, where dotted line represents the time at which fiber was rinsed. Following injection of VEGF (100µg/mL), release is sustained for 24 hours before the fiber is rinsed five times with PBS. VEGF release drops after rinsing at 24 hours. Injection of Fluorescein (1800µM) occurs at 24 hours, where release is sustained for 24 hours.

8.3.3 Endothelial cell recruitment and vessel formation

A modified murine Matrigel plug assay was utilized to measure angiogenesis in response to various delivery regimens *in vivo*. Specifically, a subcutaneous Matrigel plug serves as a cell-free matrix that is amenable to cellular invasion. A fiber is threaded through this plug to create a source for factor release to surrounding cells. The ends of the hollow fiber remain exposed, giving access to the contents of the lumen of the fiber (and consequently what is released into the cell-free matrix) over the course of experimentation. We explored delivery of: 1) VEGF alone (Figure 17b), 2) S1P alone (Figure 17d), 3) VEGF followed by S1P (Figure 17c), 4) S1P followed by VEGF (Figure 17e), and 5) dual delivery of VEGF and S1P (Figure 17f). Each experimental group contained an internal negative control where saline alone was administered through an implanted fiber (Figure 17a) over the course of experimentation (7 days). In the sequential delivery groups, factor exchange (when relevant) occurred at 3 days post-implantation (as endothelial cell recruitment and vessel formation has previously been observed as early as 2 days in murine Matrigel plugs²⁶⁰). Hemotoxylin and eosin stained sections (Figure 17a-Figure 17f) reveal detectible cellular infiltration in all groups (purple nuclear stain). However, cellular infiltration into the Matrigel is more prevalent in the plugs in which an angiogenic factor has been delivered (Figure 17b-Figure 17f). Importantly, in the plugs where VEGF delivery was followed by S1P delivery, H&E staining not only reveals denser cells, but the presence of red blood cells are indicative of functional angiogenesis within the Matrigel plug (Figure 17c and Figure 17g). This same result (the presence of red blood cells surrounded by mononuclear cells in a tubular formation) was sometimes seen in plugs in which VEGF or S1P were delivered alone

or together, but with much less frequency than in the group where VEGF delivery was followed by SIP delivery, as depicted in Figure 17.

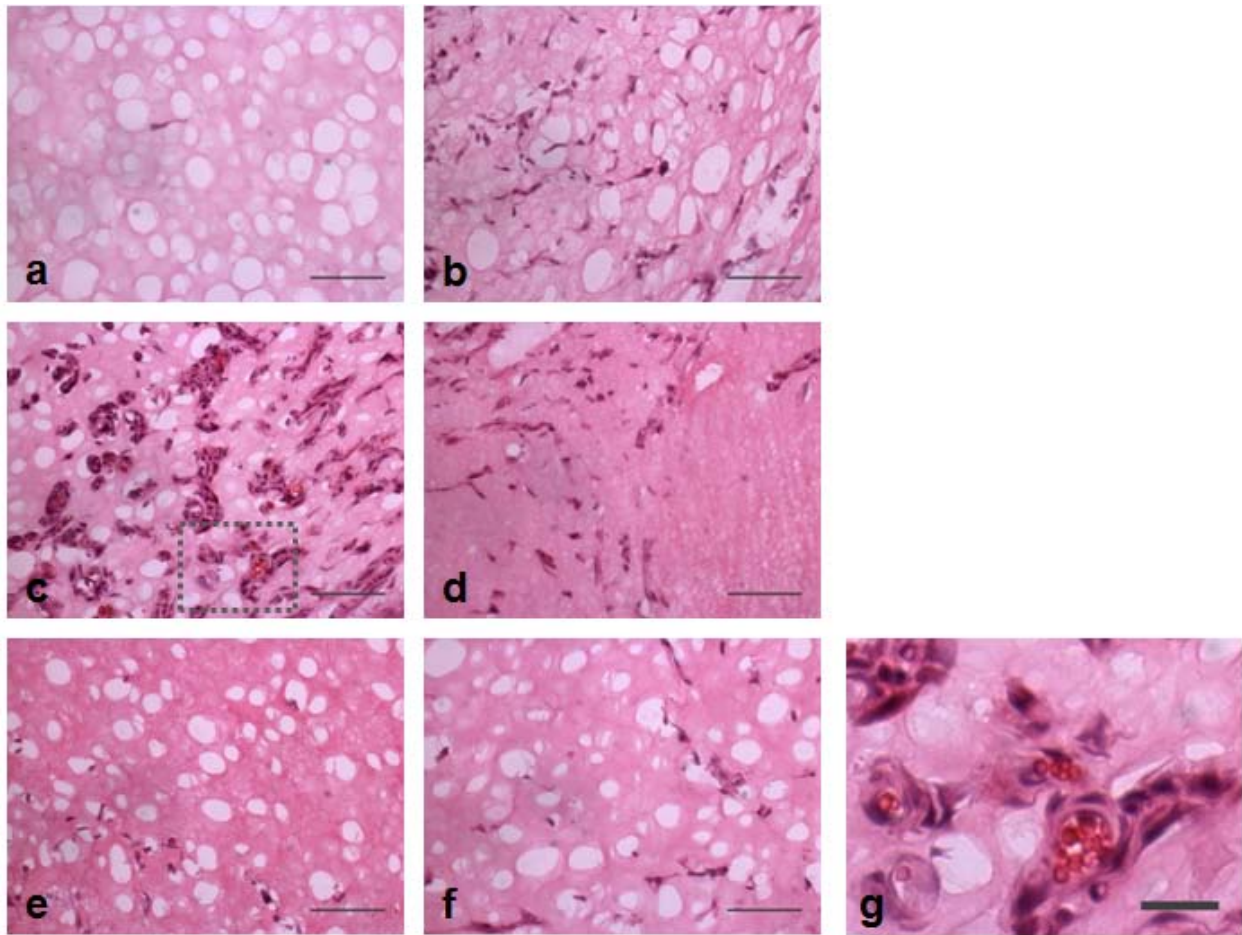


Figure 17. H&E images of murine Matrigel plugs where VEGF and/or S1P are delivered. Sequential delivery of VEGF and S1P results in cellular recruitment and functional angiogenesis in vivo. (a-f) H&E images of murine Matrigel plugs (scale bar=500µm). (a) Saline. (b) VEGF (100µg/mL). (c) VEGF (100µg/mL), followed by S1P (1800µM). (d) S1P (1800µM). (e) S1P (1800µM), followed by VEGF (100µg/mL). (f) VEGF (100µg/mL) and S1P together (1800µM). (d) Magnification of blood vessels observed when delivery of VEGF (100µg/mL) was followed by delivery S1P (1800µM), dotted line in (c) (scale bar=50µm).

Similar results were observed in the CD31 stained Matrigel plug sections (Figure 18a- Figure 18f). Generally, CD31+ staining was more prevalent in groups where angiogenesis promoting factors were delivered as compared to internal negative controls. However, greater amounts of CD31+ staining were observed in plugs where VEGF-then-S1P or VEGF alone was delivered as compared to all other groups (Figure 18b and Figure 18c). Additionally, we observed that in groups where VEGF delivery was followed by S1P delivery, endothelial cells had arranged into tubular structures that appear larger than that of a capillary, indicating that this delivery schedule is not only capable of promoting angiogenesis in the acellular matrix on the capillary level, but also a larger, more developed vascular network (Figure 18c).²⁶¹

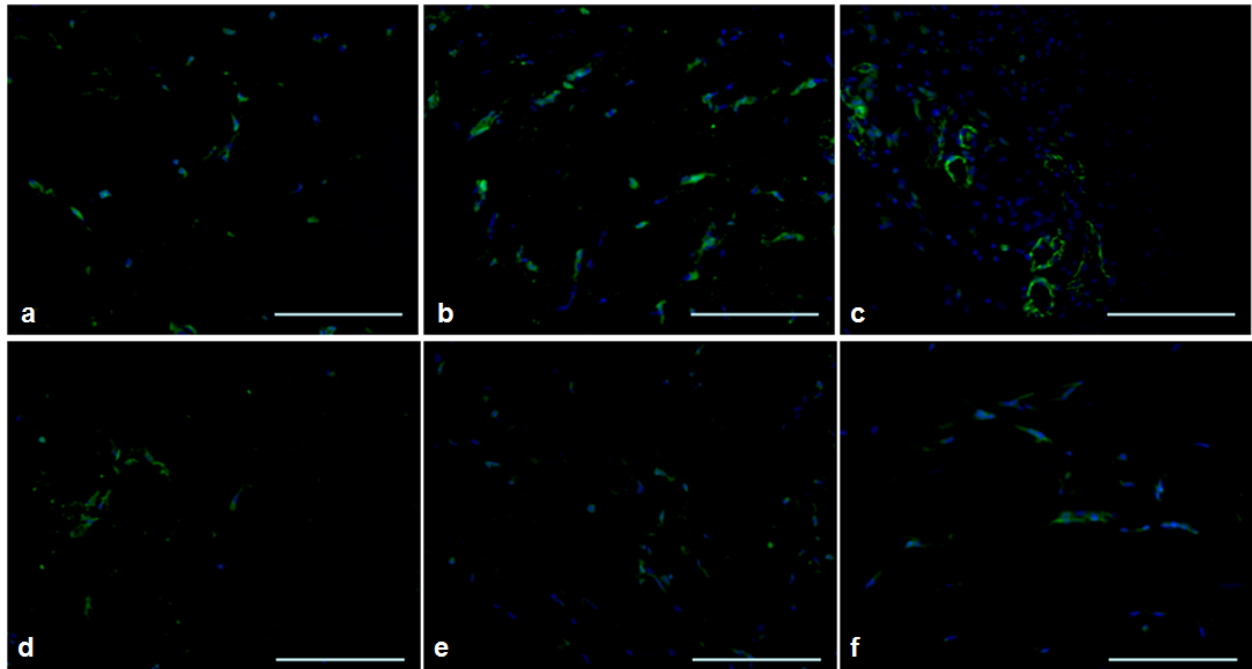


Figure 18. CD31 Matrigel plug staining where VEGF and/or S1P are delivered.

Delivery of VEGF followed by S1P results in a greater recruitment of CD31+ cells in vivo than other delivery schedules. (a-f). Immunofluorescent staining of CD31 (green) and nuclei (blue) in Matrigel plug cross-sections, scale bar=100µm. (a) Saline. (b) VEGF (100µg/mL). (c) VEGF (100µg/mL), followed by S1P (1800µM). (d) S1P (1800µM). (e) S1P (1800µM), followed by VEGF (100µg/mL). (f) VEGF (100µg/mL) and S1P (1800µM).

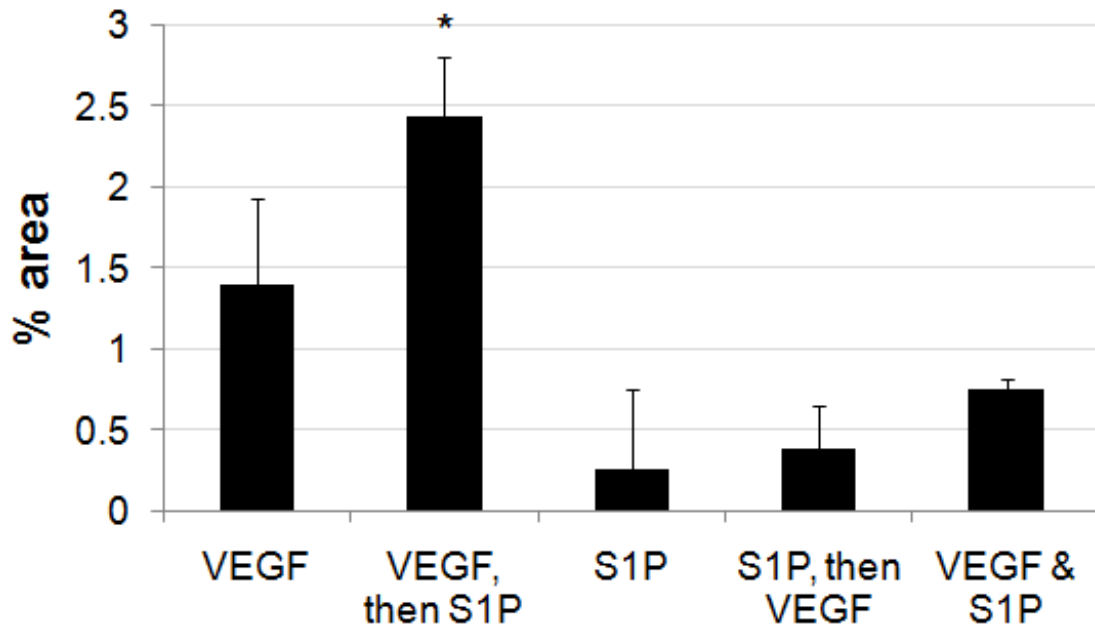


Figure 19. CD31 quantification where VEGF and/or S1P are delivered.

CD31 quantification based on Metamorph threshold imaging and normalization to a saline injected plug. Percent areas of images covered by CD31 staining are averaged across all plugs. Negative control plug percent areas (saline injection, left flank) for each mouse was subtracted from the Experimental Group percent areas (right flank) for a normalized percent area for each mouse. *significantly different when compared to all other groups (ANOVA, followed by Holm-Bonferroni correction for t-test of multiple comparisons, $k=4$, $\alpha=0.05$)

A semi-quantitative method for endothelial cell migration was also performed using CD31 staining of Matrigel plug sections. The percent area of images that were labeled with Alexa Fluor 488 (secondary antibody) was used to quantify CD31 expression in each sample. Images representing the entire periphery of the plug were recorded, and an average percent area was determined (Figure 19). It is evident that statistically more CD31+ cells are observed in sections of the Matrigel plug treated with the VEGF-then-S1P regimen than in any other experimental group.

8.3.4 Vascular maturation index

A quantitative method was used for determining the maturation level of a vessel using CD31 and alpha smooth muscle actin (α SMA) staining of Matrigel plug explants (CD31 is present on endothelial cells and α SMA is present on mural cells). The colocalization of these two cell types is indicative of mature vessels.²⁶² Five, 60x areas in which CD31+ cells have arranged in a capillary-like structure were examined, and the percent of α SMA+ colocalization was recorded as the maturation index.²⁶² In general, fluorescent images illustrate that α SMA colocalization with CD31 can be seen in Matrigel plugs in the following groups: VEGF-then-S1P (Figure 20b), S1P (Figure 20d) and S1P-then-VEGF (Figure 20e). A magnified image of α SMA+ vessels from the VEGF-then-S1P group (Figure 20f) shows α SMA staining surrounding the CD31+ vessels. In the plugs where only VEGF was delivered, we see only CD31 positive cells and no α SMA positive cells (Figure 20a). When VEGF and S1P are delivered together (dual delivery), both CD31 and α SMA positive cells have migrated into the Matrigel plug, but we did not observe substantial co-localization of these cells (representative image shown in Figure 20c). The

maturation index (percent of vessels co-localized with α SMA+ cells) is highest when sequential delivery is utilized, specifically when VEGF delivery is followed by S1P delivery (Figure 21).

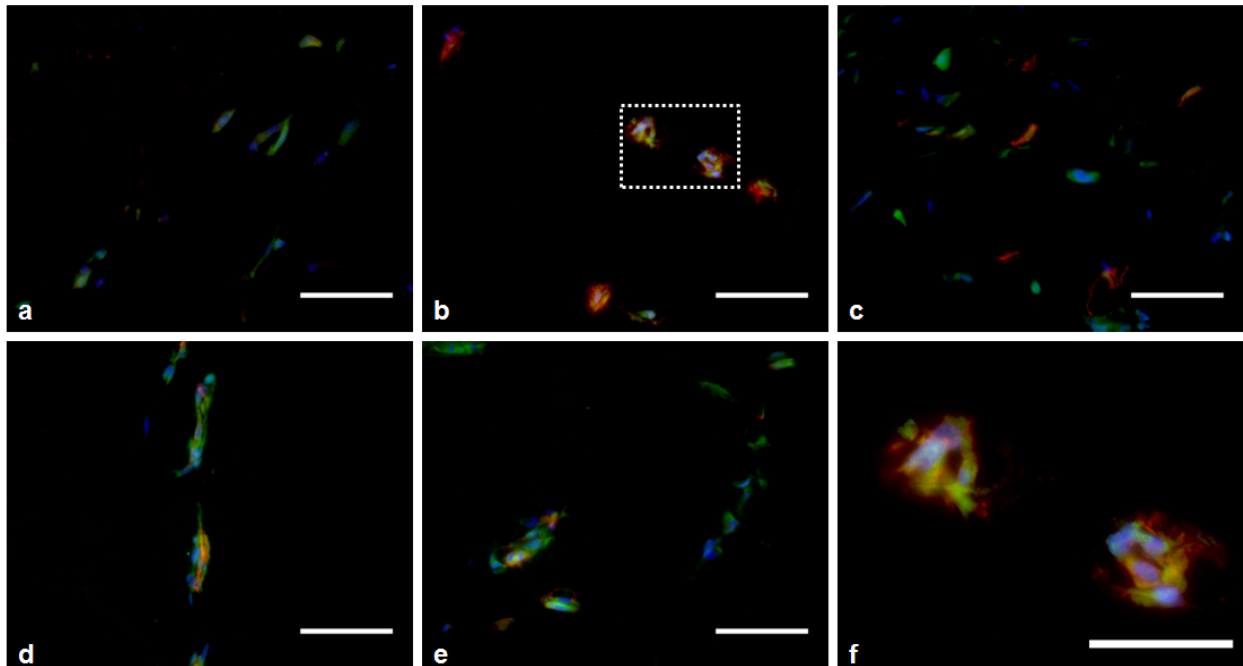


Figure 20. CD31 and α SMA Matrigel plug staining where VEGF and/or S1P are delivered. Delivery of VEGF followed by S1P results in greater colocalization of CD31 and α SMA in vivo than other delivery schedules. (a-e) Immunofluorescent staining of CD31 (green), α SMA (red) and nuclei (blue) in Matrigel plug cross-sections (scale bar=100 μ m). (a) VEGF (100 μ g/mL). (b) VEGF (100 μ g/mL), followed by S1P (1800 μ M). (c) VEGF (100 μ g/mL) and S1P (1800 μ M). (d) S1P (1800 μ M). (e) S1P (1800 μ M), followed by VEGF (100 μ g/mL). (f) Co-localization of CD31 and α SMA when delivery of VEGF (100 μ g/mL) was followed by delivery S1P (1800 μ M), dotted line in (b), scale bar=50 μ m.

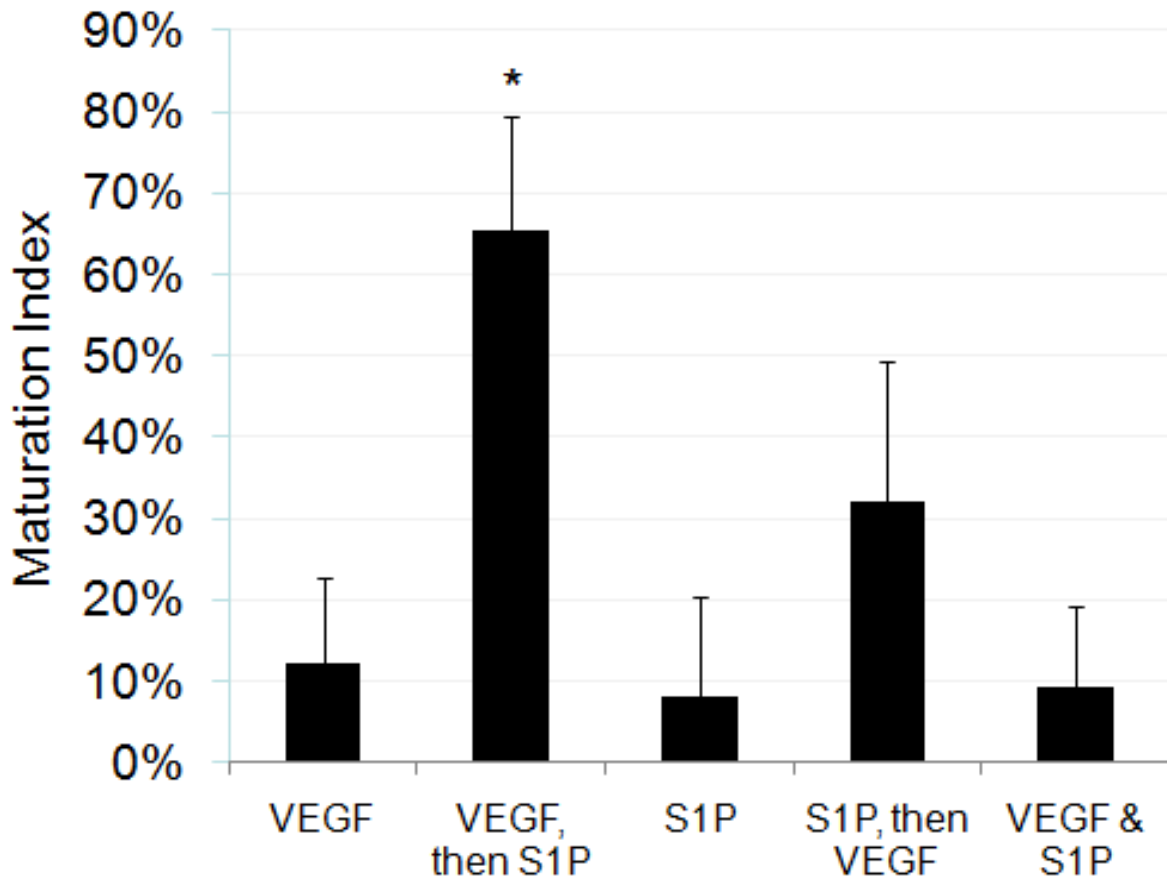


Figure 21. Maturation index where VEGF and/or S1P are delivered.

Maturation index calculated by the percent of CD31+ blood vessel that are co-localized with α SMA staining in areas where CD31+ blood vessels were observed. *significantly different when compared to all other groups (ANOVA, followed by Holm-Bonferroni correction for t-test of multiple comparisons, $k=4$, $\alpha=0.05$)

8.4 DISCUSSION

Controlled release systems capable of delivering single biological factors are common in medical therapies today²⁶³, while controlled release systems capable of delivering multiple factors either simultaneously or sequentially are under development as an active area of current research. Fine control over sequential delivery would yield a number of therapeutic advantages including the added efficiency resulting from more accurately mimicking natural schedules of angiogenic factor presentation *in situ*. To this end, studies have demonstrated dual protein release through fully implantable hollow fibers and/or scaffolds where the rate of release is controlled by the respective degradation rate of either the hollow fiber or the scaffold (or both).²⁶⁴⁻²⁶⁶ While these systems can effectively deliver a single factor or a combination of factors simultaneously at different rates, these systems are not capable of sequential delivery where the onset of delivery for one factor is accompanied by the simultaneous abrogation of release for the other factor. The goal of our study was to create and utilize a system that is capable of exploring sequential delivery of multiple angiogenic factors to an acellular site that is conducive to endothelial cell invasion.

Porous hollow fibers allow for sequential delivery of multiple factors to the surrounding environment as determined exclusively by the contents of the lumen at any time (as externally controlled by the user). Figure 16 demonstrates the capability of these hollow fibers to sequentially deliver molecules of relevant sizes and solubility. Further, the hollow fibers fabricated in this study have shown to be effective at delivering angiogenic factors over at least

1.25mm (radius of the Matrigel plug *in vivo*) at physiologically relevant concentrations in an externally controlled and sequential manner. Using the hollow fibers fabricated in this study, linear release is not achieved nor necessarily required. Instead, the majority of the release occurs over the first few hours following injection into the lumen of the fiber. Importantly, the consequent factor exposure (over a few hours) to the physiological environment is longer than if the factors were injected as a bolus injection, and the orientation of factor release produces several key advantages over bolus injection. Firstly, a concentrated solution of each factor has a high likelihood of toxicity if exposed to cells directly.²⁶⁷ Because the ends of the hollow fiber are exposed during this study, re-injection of each factor occurs each day in order to maintain release of each factor, achieving a predicted release similar to that depicted in Figure 22. Secondly, the hollow fiber sustains a gradient of growth factor originating from the surface of the fiber and extending out into the Matrigel plug, producing spatial based information that is required for the chemoattractive capacity of each factor.²⁶⁸ Indeed, in previous studies, when VEGF was incorporated directly into the Matrigel plug (100ng total), cellular infiltration was only observed at the perimeter of the plug (Figure 23), which is a great difference from what we see when a hollow fiber is used to deliver the growth factor from the center of the plug (Figure 17).

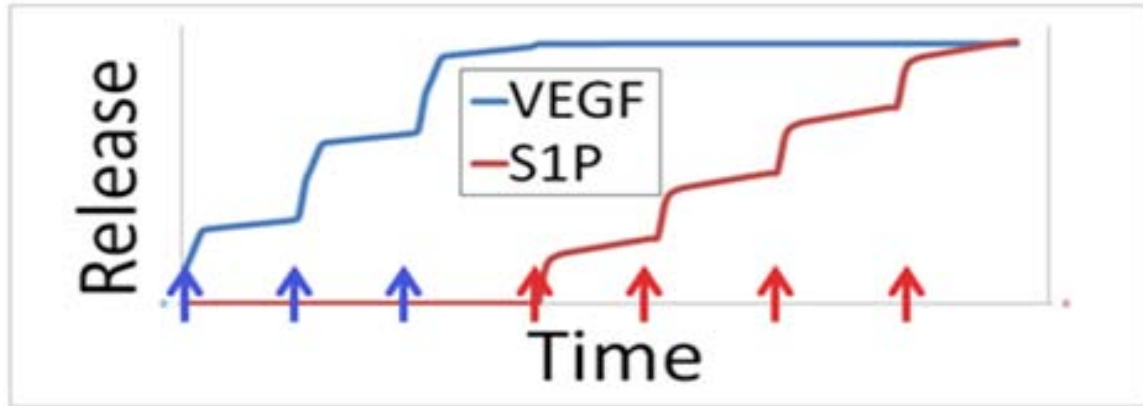


Figure 22. Projected *in vivo* release when injections occur daily.

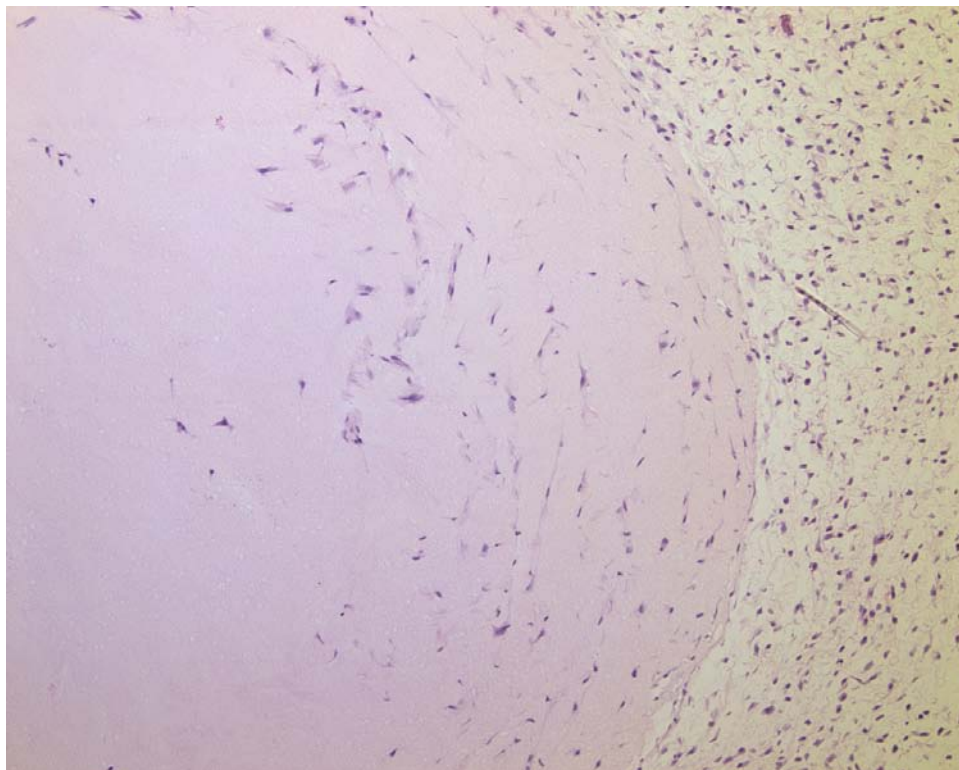


Figure 23. H&E of Matrigel plug loaded with 100ng VEGF, 10x.

In vivo, it is possible that these fibers may experience more advanced membrane fouling than observed in our *in vitro* studies either due to protein accumulation in the Matrigel plug or cell-mediated barrier formation at the surface of the fiber. The material used for the hollow fiber-based model, cellulose, was chosen to mitigate this risk as a biologically inert material.²⁶⁹ Indeed, at the experimental endpoint of our studies, no cellular infiltration into the membrane or cellular adhesion onto the membrane surface was observed. Furthermore, on the time-scale of our studies, we did not observe that potential hindrances to diffusion were extensive enough to impair the cellular infiltration and vessel formation induced by both single-factor and (to a greater extent) sequential delivery. Lastly, the point at which the fiber enters the skin may increase the risk for infection if administered clinically. Although infections have not been observed in this study, it should remain a concern for future studies, where an animal model that might be more prone to infection may be utilized. If therapeutic application for this technology is required, one potential solution would be to deliver antibiotics along with the growth factor.

An externally controlled delivery system (such as the one described here) is important to studying the effects of angiogenic factors *in vivo* given that the alternative (bolus injections of “naked” factors) would result in rapid diffusion and immediate exposure of released agents to enzymes and other proteins that can lead to a dramatic loss of bioactivity (e.g. the half-life of VEGF in serum is 33.7 minutes¹⁴²) and spatial gradients. Hollow fibers, conversely, would sustain the release of angiogenic factors (originating from the fiber and extending out through extracellular matrix) over an extended period of time. Our hollow fiber system (Figure 22h) allows for external control over delivery to an internal *in vivo* location. Following a rinsing step, delivery of one factor can be “turned off”, while delivery of another factor is simultaneously

“turned on” (Figure 16). This setup allows us to test the hypothesis (for the first time) that sequential delivery will improve angiogenic response.

Angiogenesis is an ideal regenerative process to explore the advantages of sequential delivery due to its well-studied, stage-wise nature.^{9, 270} Early stage angiogenic events include destabilization of existing vessels, as well as proliferation, migration and invasion, of activated endothelial cells.⁹ VEGF appears to be involved primarily in the initiation of angiogenesis⁶⁷, playing a major role in vascular permeability and endothelial cell recruitment⁹. This is consistent with our data indicating that VEGF efficiently recruits endothelial cells to a subcutaneous Matrigel plug (Figure 18b). However (as discussed in more detail below), the promising early angiogenic events observed when VEGF was exclusively delivered did not progress further as to produce detectable maturation events. Similarly, it has been shown elsewhere in long-term clinical trials that delivery of VEGF alone has led to unstable vessels.^{104, 271} Remarkably, these results are entirely consistent with studies that suggest that VEGF mediates cellular effects that are conducive to early-stage angiogenic events while being (by definition) inhibitory to later stage angiogenesis events. Specifically, VEGF inhibits pericyte coverage of vascular sprouts by suppressing receptors on vascular smooth muscle cells, leading to existing vessel *destabilization*.²⁵² Together, these data suggest that VEGF alone is likely insufficient to complete angiogenesis given its dual role as a promoter of endothelial cell function and a negative regulator of vessel maturation.^{102-103, 252}

In contrast, late stage angiogenesis events include inhibition of endothelial cell proliferation and migration, basement membrane secretion and pericyte recruitment.⁹ These events appear to be mediated (at least in part) through S1P and, as stated above, inhibited by VEGF. It has also been shown that elevated levels of S1P can lead to a reduction in endothelial

cell migration via rearrangement of their cytoskeleton.^{182, 272} These observations are consistent with our data, showing the S1P delivery is less effective at recruiting endothelial cells when compared to VEGF (Figure 19, p=0.023). Rather, S1P is released from activated platelets following injury and has been shown to promote vessel stabilization *in vivo*.^{74, 78} Indeed, the importance of S1P in vessel maturation is evident by the fact that knockout of the S1P receptor on endothelial cells S1P₁ is embryonic lethal in mice due to severe hemorrhaging.⁹² Upon closer inspection, it was observed that these embryos were deficient in mural cells and vascular pericytes, causing microvessels to dilate and rupture.⁹² Furthermore, VEGF has been shown to not only upregulate the S1P receptor (S1P₁) on endothelial cells¹⁸³ but also to increase sphingosine kinase activity²⁷³, leading to the conversion of sphingosine to S1P. For these reasons, it is logical to believe that late stage angiogenesis is characterized not only by the presence of S1P, but also the absence of VEGF.

In addition, productive angiogenesis requires both recruitment of endothelial cells into an acellular site and assembly of these cells into patent, stable vessels. A hallmark characteristic of stable (or mature) vessels is the presence of vascular pericytes supporting the endothelial cell structure.^{75, 252} Although microvascular pericytes are poorly understood²⁷⁴⁻²⁷⁵, their importance is demonstrated by the pathological phenotypes of mice with poor pericyte development.^{179, 276-277} It is known that pericyte function occurs in relatively late microvascular development events²⁷⁴⁻²⁷⁵, corresponding to our data that suggests S1P (a factor known for vessel stabilization via activated endothelial cell recruitment of vascular pericytes cells⁹³), is best delivered during late angiogenesis development. When examining endothelial cell/pericyte colocalization, it was observed that the highest amount of colocalization occurred when VEGF delivery was followed by S1P delivery (Figure 20 and Figure 21). This delivery schedule also resulted in the most

endothelial cell recruitment and tubular formation of these endothelial cells (Figure 18 and Figure 19). Pericyte coverage of newly forming vasculature provides support and stability for these recruited endothelial cells. As consistent with the literature cited above describing the cellular effects of VEGF and S1P, our results suggest that delivering S1P with VEGF diminishes the effects of both VEGF alone.

Because of the versatility of our experimental model, dosing of VEGF and S1P can be optimized to result in quicker, more stable vessel formation. Our sequential delivery regimen (Figure 17a) was based on reported evidence that endothelial cells can be recruited to a site and form vasculature is as little as three days²⁶⁰, as well as evidence for appropriate (physiologically relevant) concentrations of S1P and VEGF.^{78, 278} However, the cited literature references do not involve support of a growth factor gradient, which may affect the desired dosing. Simply changing the injection timing and concentration can be used to examine the effects of altering the quantities released and the schedule and timing of that release. Additionally, the hollow fiber porosity can be altered by changing key components in the fiber fabrication process, such as cellulose flow rate and cellulose concentration. Furthermore, changing the porosity of the fiber wall leads to a change the rate at which factors are delivered. For these reasons, our model can be used as a versatile tool to examine various delivery schedules for any given set of growth factors delivered sequentially. Information obtained from these studies could pave the way for programming fully injectable, sequential delivery systems, a feat made feasible through recently published mathematical models that can direct the design and fabrication of biodegradable matrices to produce complex controlled release behavior.¹⁹⁵⁻¹⁹⁶

Furthermore, this system can be used to explore sequential delivery of any number of different growth factors for therapeutic responses as well as for studying the biological events

leading to stage-wise regeneration of other tissues. To this end, we are currently exploring the delivery of basic fibroblast growth factor, or bFGF, followed by PDGF. These growth factors are also known to be involved with early and late stage angiogenesis events, respectively.^{67, 72-73,}
⁷⁶ It has also be observed that bFGF induced tubular structures will regress over time in the absence of other signals.¹⁰⁴ We believe that delivery of bFGF followed by PDGF will result in more mature, stable vessels than delivery of either factor alone as well as dual delivery of these factors. It is also expected that sequential delivery of growth factors will prove to be relevant in other wound healing mechanisms, such as bone healing, in which delivery of an angiogenesis promoting factor like PDGF (that can inhibit osteoblast differentiation) would be followed by delivery of a bone morphogenic protein.²⁷⁹

8.5 CONCLUSION

We have created a system capable of exploring true sequential delivery of angiogenic factors. When using this system to explore sequential delivery of VEGF and S1P for the purpose of promoting angiogenesis, we demonstrated that delivery of VEGF for 3 days followed by delivery of S1P for 4 days resulted in recruitment of more endothelial cells and a higher maturation index than the reverse sequential delivery schedule, single factor delivery or dual delivery. This system can be used to explore any number of delivery schedules, allowing for a facile way to explore different delivery schedules of growth factors *in vivo* for therapeutic responses as well as for studying the basic biological signals that accompany stage-wise regeneration of tissues.

8.6 SUPPLEMENTAL INFORMATION

8.6.1 Methods: Tubular formation assay

HUVECs (Human Umbilical Vein Endothelial Cells, Lonza) treated with 100 μ M Calphostin C (Calphostin C, Biomol International) for 30 minutes were cultured on Matrigel (Growth Factor Reduced Matrigel, BD Biosciences) in which a cellulose hollow fiber was embedded (200,000 cells/well). M199 containing 1%FBS and 600 μ M-1800 μ M S1P was injected into the hollow fibers. After 16 hours of humidified cell culture at 37°C and 5% CO₂, cells were fixed with 2% paraformaldehyde (Fisher) and stained with rhodamine phalloidin (rhodamine phalloidin, Invitrogen, Eugene, OR) with 0.1% triton (Sigma). Cultures were imaged using an Olympus Provis and quantification of tubular formation was performed by threshold analysis on fluorescent images (Metamorph).

8.6.2 Results: Endothelial cell tubular formation following angiogenic factor release from hollow fibers through Matrigel *in vitro*

An *in vitro* model was constructed to mimic several aspects of the three-dimensional release environment that would be encountered *in vivo*. This system (as schematically represented in Figure 22h) permits the administration of a factor through a hollow fiber so that it will diffuse through a layer of Matrigel to cells that are seeded on top (e.g. representing a surrounding cell source at a wound site). By observing Human Umbilical Vein Endothelial Cells, or HUVECs, on top of the Matrigel, we were able to demonstrate that S1P administered through the fiber is released and subsequently influences the behavior of surrounding cells. Specifically, we

observed a dose-dependent response with respect to tubular formation (as measured by rhodamine phalloidin staining and fluorescence microscopy) (Figure 22a-Figure 22f). These results suggest that delivery of a sparingly soluble agent is possible at relevant concentrations to cells at a distance (1.25mm) relevant to our *in vivo* model. Quantification of cellular surface area using threshold analysis on Metamorph software, reveals a significant difference in tubular formation between the groups where a fiber is injected with 1200 μ M and 1800 μ M S1P when compared to a fiber injected with media alone (Figure 22g).

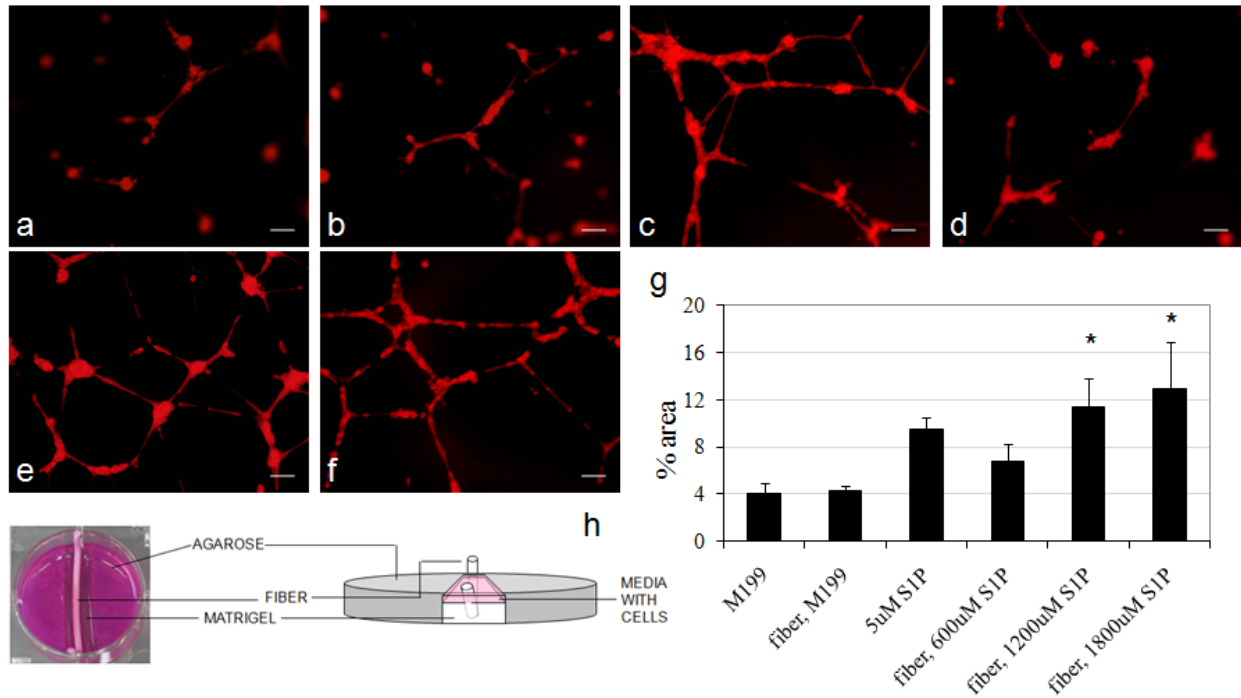


Figure 24. Tubular formation assay with HUVECs and S1P.

S1P released from hollow fibers affect HUVECs in a dose dependent manner in vitro. (a-f) Rhodamine phalloidin stained HUVECs on Matrigel, scale bar=15 μm. (a) HUVECs on Matrigel in media resulted in alignment of endothelial cells. (b) HUVECs seeded on Matrigel with media injected into fiber resulted in alignment of endothelial cells. (c) HUVECs on Matrigel with 5 μM S1P results in network formation of endothelial cells. (d) - (f) HUVEC exhibit a dose dependent response to S1P where an increase in the injected concentration of S1P increases the progression towards network formation of endothelial cells. (g) Percent area covered by endothelial cell tubes, identified by rhodamine phalloidin staining and quantified with Metamorph threshold analysis. *p<0.05 when compared to media injected into fiber (one-tailed t-test, n=3) (h) Schematic of the in vitro setup allowing for externally controlled delivery of an angiogenic factor to an endothelial cell population through Matrigel.

9.0 SEQUENTIAL DELIVERY OF BASIC-FGF AND PDGF

9.1 INTRODUCTION

Considering the temporal complexity of angiogenesis, it is not surprising that strategies focusing on delivery only a single angiogenic factor^{43, 104-106} or even two angiogenic factors simultaneously^{71, 280} have met limited success. In order to gain information regarding the most relevant time-frames, concentrations and growth factors, to be used in therapeutic sequential delivery strategies, we recently developed a simple and modular, externally-regulated delivery model (Chapter 8.0).²⁸¹ This model consists of a porous hollow fiber that extends into an acellular site *in vivo*, permitting external control over presence and absence of angiogenic growth factors at any time.²⁸¹ The fiber wall microstructure is controlled through the fiber fabrication process to ensure that large proteins could be effectively released to the surrounding matrix.²⁵⁵⁻²⁵⁸ The ends of the hollow fiber remain exposed, providing access to the contents of the lumen of the fiber (and consequently what is delivered) over the course of experimentation. Using this system, we were able to achieve sequential delivery of two different angiogenic “instructions”: 1) vascular endothelial growth factor (VEGF; involved in vasculature permeability/destabilization⁶⁷ and endothelial cell recruitment⁹) and 2) sphingosine-1-phosphate (S1P; promoting vessel stabilization *in vivo*^{74, 282} and involved in a reduction in endothelial cell migration^{182, 272}). In this prior study, when VEGF delivery was followed by delivery of S1P, we

observed significantly greater endothelial cell migration as well as substantial increases in vessel maturity, when compared to single or dual delivery of these factors.²⁸¹ This data suggests that attempting to sequentially stimulate various stages of angiogenesis via the presence and absence of angiogenic factors is a step towards the development of more complex and relevant angiogenic therapies.

Importantly, recent literature suggests that the concept of stage-wise delivery for angiogenesis has broader application than only VEGF and S1P. An ideal angiogenic therapy would involve stage-wise delivery of all growth factors known to support cellular action during the corresponding stage of angiogenesis. Examples of other growth factors involved in angiogenesis are bFGF and PDGF. Specifically, bFGF (17kDa) has been shown to play a major role in the initiation (sprouting) of new capillaries *in vivo*.²⁸³ PDGF (25kDa) released from activated platelets⁹, promotes the maturation of blood vessels through the recruitment and support of mural cells, the supporting structure for blood vessels^{67, 76}, among other actions.²⁸⁴⁻²⁸⁵ However, when bFGF and PDGF are presented simultaneously in a modified Boyden chamber assay, bFGF significantly inhibits PDGF-induced smooth muscle cell migration and proliferation via the PDGF and bFGF receptors.²⁸⁰ Conversely, in a chick chorioallantoic membrane assay, it has also been shown that PDGF inhibits bFGF-induced angiogenesis.⁷¹ Taken together, this data suggests that not only the presence, but the absence of bFGF and PDGF expression play a role in vascular remodeling.

For the reasons described above, a sequential delivery model was utilized to explore the delivery schedule of bFGF and PDGF, delivered alone, in sequence or together. Accordingly, we hypothesized that sequential delivery (bFGF followed by PDGF) would impact the significance and maturity of angiogenesis.

9.2 MATERIALS AND METHODS

9.2.1 Hollow fiber fabrication and characterization

Cellulose acetate hollow fibers were prepared using a double injection nozzle as described previously.²⁸¹ Briefly, twenty percent cellulose acetate (molecular weight=30kD, Aldrich) was pumped through the outer core of the nozzle and deionized water was pumped through the center core. The cellulose solution and deionized water were extruded into a deionized water bath where the cellulose solution precipitates in the form of a porous hollow fiber. Lyophilized hollow fiber cross sections were sputter coated with 3.5nm of gold-palladium and imaged at 5kV using a JEOL 9335 SEM.

9.2.2 *In vitro* release

In vitro release from cellulose hollow fibers was carried out as described previously.²⁸¹ Briefly, wells of a 6-well cell culture plate were filled with 5 mL Dulbecco's phosphate buffered saline, or PBS (Invitrogen). A cellulose hollow fiber was cut to fit the well and then injected with 10 μ L of rh-bFGF (R&D Systems) and rh-PDGF (R&D Systems) using a 28G $\frac{1}{2}$ insulin syringe (1/2 cc Lo-Dose U-100 insulin syringe, Becton Dickinson and Co.) and submerged in the PBS bath. Hollow fibers were injected first with bFGF (200 μ g/mL, 2ng bFGF total). Release of bFGF into a PBS bath was measured by sampling the supernatant and measuring using a bFGF ELISA kit (R&D Systems). After 24 hours, the fiber was rinsed five times with PBS and lumen contents were replaced with an aqueous solution of PDGF (300 μ g/mL, 3ng PDHG total). Again, release

was measured by sampling the supernatant and measuring using a PDGF ELISA kit (R&D Systems).

9.2.3 Murine Matrigel plug assay

A modified murine Matrigel plug assay was utilized as described previously.²⁸¹ Briefly, growth factor reduced Matrigel (500 μ L) was injected (approximately 1cm in diameter) into the subcutaneous space on the dorsal side of C57BL/6 mice (8-10 weeks old, Charles River) on both the left and right flank, following anesthesia with 2-3% inhaled isoflurane. A 14G catheter was used to thread cellulose hollow fibers through the skin and Matrigel plugs. Hollow fibers were fixed in place using tissue glue and an Elizabethan collar was used to prevent mice from extracting the hollow fiber. On the day of implantation, and every day for the next 6 days, hollow fibers on the left side were injected with sterile saline (as an internal negative control) and hollow fibers on the right side were injected with 10 μ L of an angiogenesis promoting factor: 200 μ g/mL bFGF (R&D) and/or 500 μ g/mL PDGF. The internal negative control (which includes the Matrigel plug, hollow fiber and saline injection) serves the purpose of controlling for variation between mice (e.g potentially any variable growth factor secretion due to inflammation caused by the Matrigel injection or hollow fiber implantation). For mice in the sequential delivery groups, factor switching occurred on the third day after implantation, following five rinses with saline. Seven days post-implantation, implants were extracted, fixed in 2% paraformaldehyde for 5 hours and 30% sucrose overnight and snap-frozen in liquid nitrogen. Frozen sections (8 μ m) were stained with Hemotoxylin and eosin (H&E) and analyzed for endothelial cell migration and vessel formation, and red blood cell presence in vessel-like structures where the lumen is greater than 100 μ m.

9.2.4 Immunofluorescence

Frozen Matrigel Plug sections (8 μ m) were incubated with primary antibodies rabbit anti-CD31 (Abcam) and Cy3-conjugated mouse anti- α -smooth muscle actin (Sigma) and secondary antibody goat anti rabbit Alexa Fluor 488[®] (Jackson Immuno). Sections were also counterstained with Hoechst (Sigma) to identify all mononuclear cells. CD31 labeled cross-section images were taken at 40x. These images were analyzed using threshold analysis on Metamorph to quantify the percent of each image occupied by CD31 staining. These values were averaged to obtain a representative percent for each cross-section and normalized to the internal positive control in which only saline was delivered. Negative control plug percent areas (saline injection, left flank) for each mouse was subtracted from the Experimental Group percent areas (right flank) for a normalized percent area for each mouse. CD31 and α SMA labeled cross-section images were taken at 60x. These images were analyzed by counting the number of CD31 positive areas (vessel equivalents) and the number of these areas that are colocalized with α SMA labeling.

9.2.5 Statistical analysis

ANOVA was performed when assays contained more than one experimental group, as in the tubular formation assay (n=3) and Murine Matrigel plug assay (n=3). A power analysis based on a previous, yet similar experiment was performed to determine N for *in vivo* experiments. Subsequently, a post hoc multiple comparison test was performed to compare means of different experimental groups (Holm-Bonferroni, $\alpha=0.05$, k=4).

9.3 RESULTS

9.3.1 Sequential bFGF and PDGF release from cellulose hollow fibers

Cellulose hollow fibers were fabricated with an inner diameter of $971 \pm 129 \mu\text{m}$ and wall thickness of $81 \pm 18 \mu\text{m}$ (Figure 23a). These fibers were used to sequentially release bFGF and PDGF *in vitro*, via manual injection of the growth factors at the desired timepoints. Porous fibers were loaded with bFGF for an initial period of release, rinsed and then subsequently loaded with PDGF. Egress of these molecules through the fibers and into a surrounding saline solution is represented in Figure 23b. Importantly, when growth factors are exchanged (corresponding with saline flushing prior to administration of a new factor, depicted by the dotted line), bFGF release is no longer detectable and PDGF is subsequently detectable in the supernatant. These results are in agreement with previous results²⁸¹, suggesting that our fibers are capable of detectable release of a growth factor sized protein over at least 24 hours as well as sequential delivery of two factors, as determined empirically.

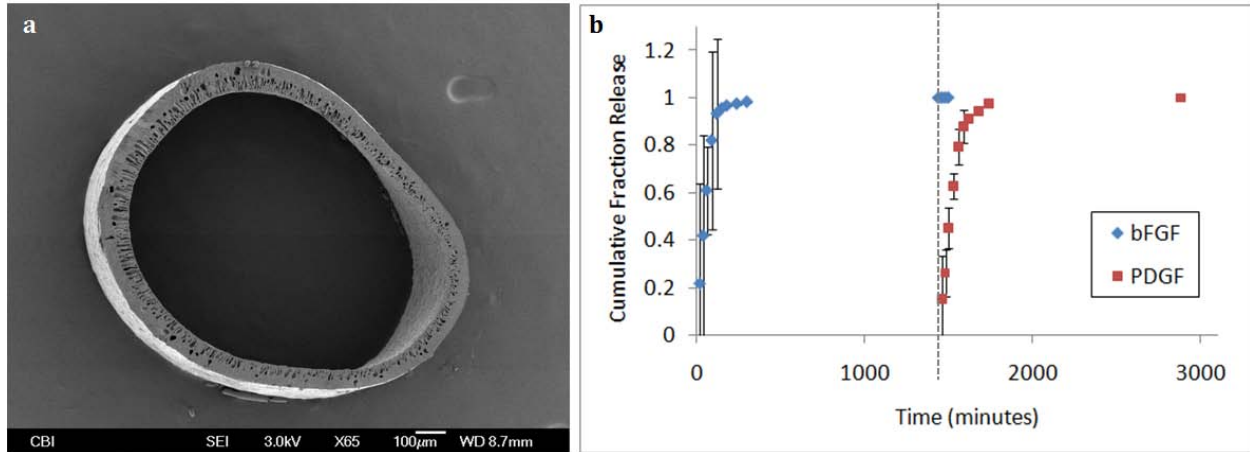


Figure 25. Cellulose hollow fiber image and sequential release of bFGF and PDGF.

Porous, cellulose hollow fibers are capable of sequential release. (a) Scanning electron micrographs of a cellulose hollow fiber fabricated using a double extrusion process. (b) Sample release profile representing sequentially deliver factors (dotted line represents the time at which fiber was rinsed). Injection of bFGF (200µg/mL), allows for detectable release for 24 hours. Fiber is rinsed five times with PBS at 24 hours, resulting in a drop in detectable bFGF. Injection of PDGF (300µg/mL) occurs at 24 hours, where release is detected for 24 hours.

9.3.2 Recruitment of endothelial cells to Matrigel plugs in response to various treatment schedules

A modified murine Matrigel plug assay was utilized to measure angiogenesis in response to various delivery regimens *in vivo*. Specifically, a subcutaneous Matrigel plug serves as a cell-free matrix that is amenable to cellular invasion. A fiber is threaded through this plug to create a source for factor release through the Matrigel to the surrounding environment. The ends of the hollow fiber remain exposed, giving access to the contents of the lumen of the fiber (and consequently what is released into the cell-free matrix) over the course of experimentation. We explored delivery of: 1) bFGF alone (Figure 24b), 2) bFGF followed by PDGF (Figure 24c), 3) PDGF alone (Figure 24d), 4) PDGF followed by bFGF (Figure 24e), and 5) dual delivery of

bFGF and PDGF (Figure 24f). Each experimental group contained an internal negative control where saline alone was administered through an implanted fiber (Figure 24a) over the course of experimentation (7 days). In the sequential delivery groups, factor exchange (when relevant) occurred at 3 days post-implantation. CD31 stained Matrigel plug sections (Figure 24a-Figure 24f) reveal endothelial cell infiltration in all plugs where growth factors (bFGF and/or PDGF) are delivered. However, greater amounts of CD31+ staining were observed in plugs where bFGF was followed by PDGF as compared to all other groups (Figure 24c). A semi-quantitative method for endothelial cell migration was also performed using CD31 staining of Matrigel plug sections. The percent area of images that were labeled with Alexa Fluor 488 (secondary antibody) was used to quantify CD31 expression in each sample. Images representing the entire periphery of the plug were recorded, normalized to the internal negative control and an average percent area was determined (Figure 25). Basic FGF was shown to be active when delivered, demonstrated by an increase in endothelial cell recruitment when compared to a saline injection (Figure 24b and Figure 25). It is evident that statistically more CD31+ cells are observed in sections of the Matrigel plug treated with the bFGF-then-PDGF regimen than in any other experimental group.

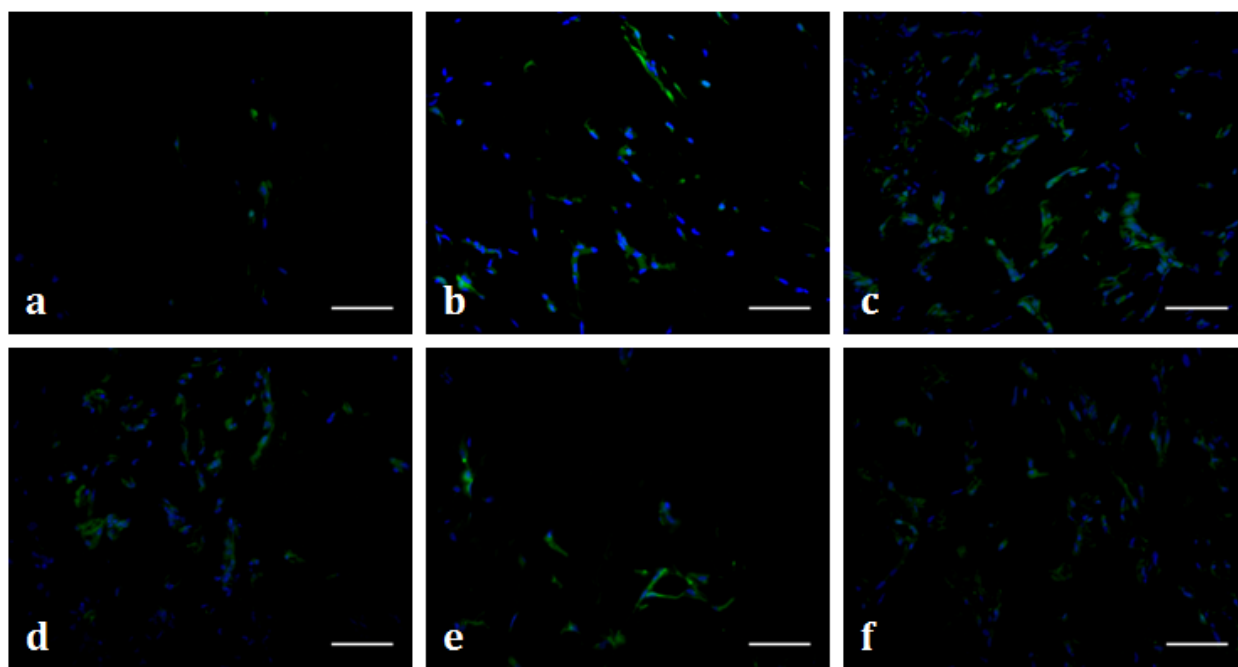


Figure 26. CD31 Matrigel plug staining where bFGF and/or PDGF are delivered.

Delivery of bFGF followed by PDGF results in greater recruitment of CD31+ cells in vivo than other delivery schedules. (a-f). Immunofluorescent staining of CD31 (green) and nuclei (blue) in Matrigel plug cross-sections (scale bar=100µm) treated with: (a) Saline. (b) bFGF (200µg/mL). (c) bFGF (200µg/mL), followed by PDGF (500µg/mL). (d) PDGF (500µg/mL). (e) PDGF (500µg/mL), followed by bFGF (200µg/mL). (f) bFGF (200µg/mL) and PDGF (500µg/mL).

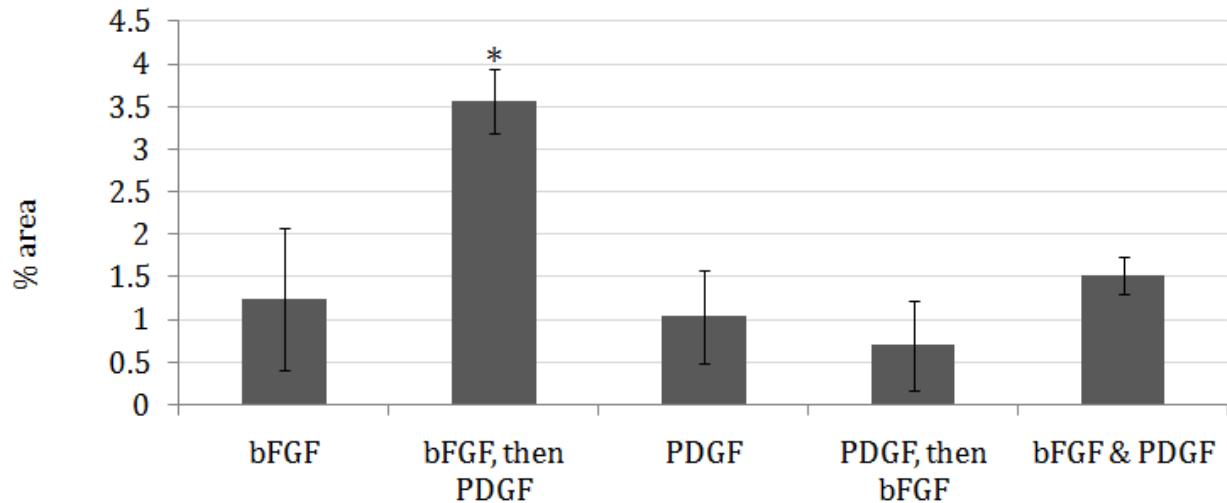


Figure 27. CD31 quantification where bFGF and/or PDGF are delivered.

CD31 quantification as normalized to an internal control (saline injected plug) using Metamorph threshold analysis. Percent areas of images covered by CD31 staining are averaged across all plugs. *indicates significant differences when compared to all other groups (ANOVA, followed by Holm-Bonferroni correction for t-test of multiple comparisons, $k=4$, $\alpha=0.05$)

9.3.3 Vessel maturation in response to various treatment schedules

A quantitative method was used for determining the maturation level of a vessel using CD31 and α SMA staining of Matrigel plug explants (CD31 is present on endothelial cells and α SMA is present on mural cells). The colocalization of these two cell types is indicative of mature vessels.²⁶² This method involves immunohistochemical analysis of CD31 and α SMA stained tissue sections and is a common and validated measure of vessel maturity^{144, 213, 281, 286}. Five, 60x areas in which CD31+ cells have arranged in a capillary-like structure were examined, and the percent of α SMA+ colocalization was recorded as the maturation index.²⁶² In general, fluorescent images illustrate that α SMA colocalization with CD31 can be observed in all plugs where PDGF was delivered (Figure 26b-Figure 26e). In the plugs where only bFGF was

delivered, we could detect only CD31 positive cells and no α SMA positive cells (Figure 26a). The maturation index (percent of vessels co-localized with α SMA+ cells) associated with the sequential delivery groups was statistically higher than all other groups in our study, specifically when bFGF delivery is followed by PDGF delivery (Figure 27).

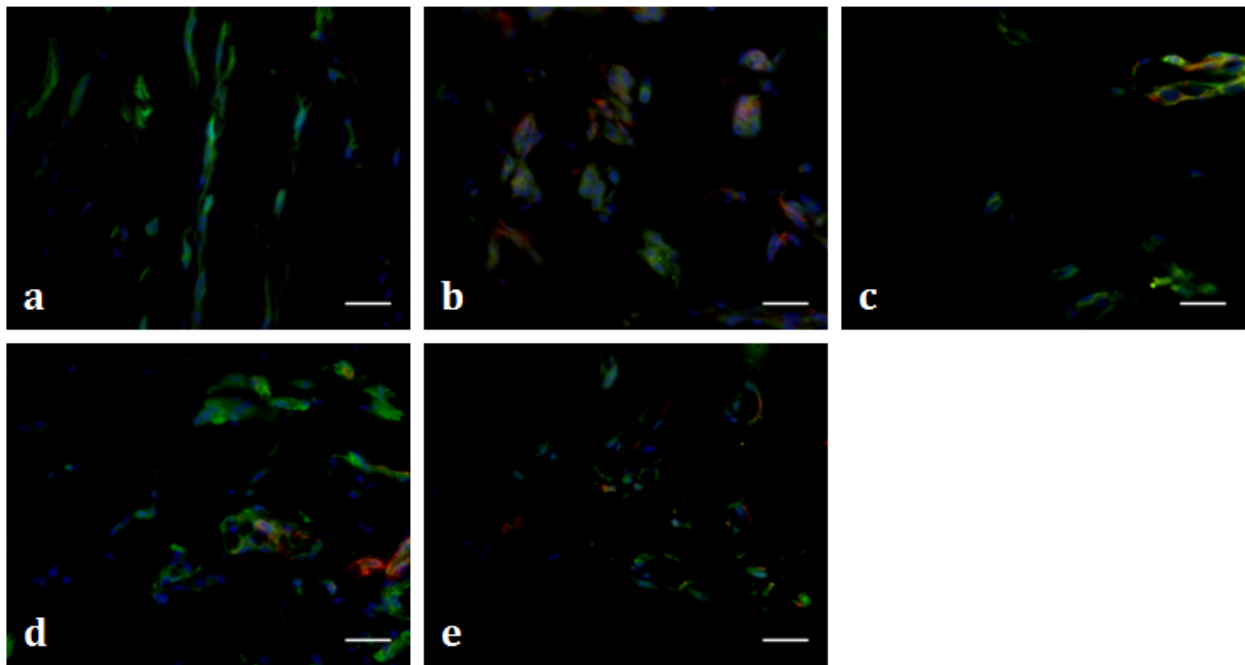


Figure 28. CD31 and α SMA Matrigel plug staining where bFGF and/or PDGF are delivered.

Delivery of VEGF followed by S1P results in greater colocalization of CD31 and α SMA *in vivo* than other delivery schedules. (a-e) Immunofluorescent staining of CD31 (green), α SMA (red) and nuclei (blue) in cross-sections of Matrigel plugs (scale bar=100 μ m) treated with: (a) bFGF (200 μ g/mL). (b) bFGF (500 μ g/mL), followed by PDGF (500 μ g/mL). (c) PDGF (500 μ g/mL). (d) PDGF (500 μ g/mL), followed by bFGF (200 μ g/mL). (e) bFGF (200 μ g/mL) and PDGF (500 μ g/mL).

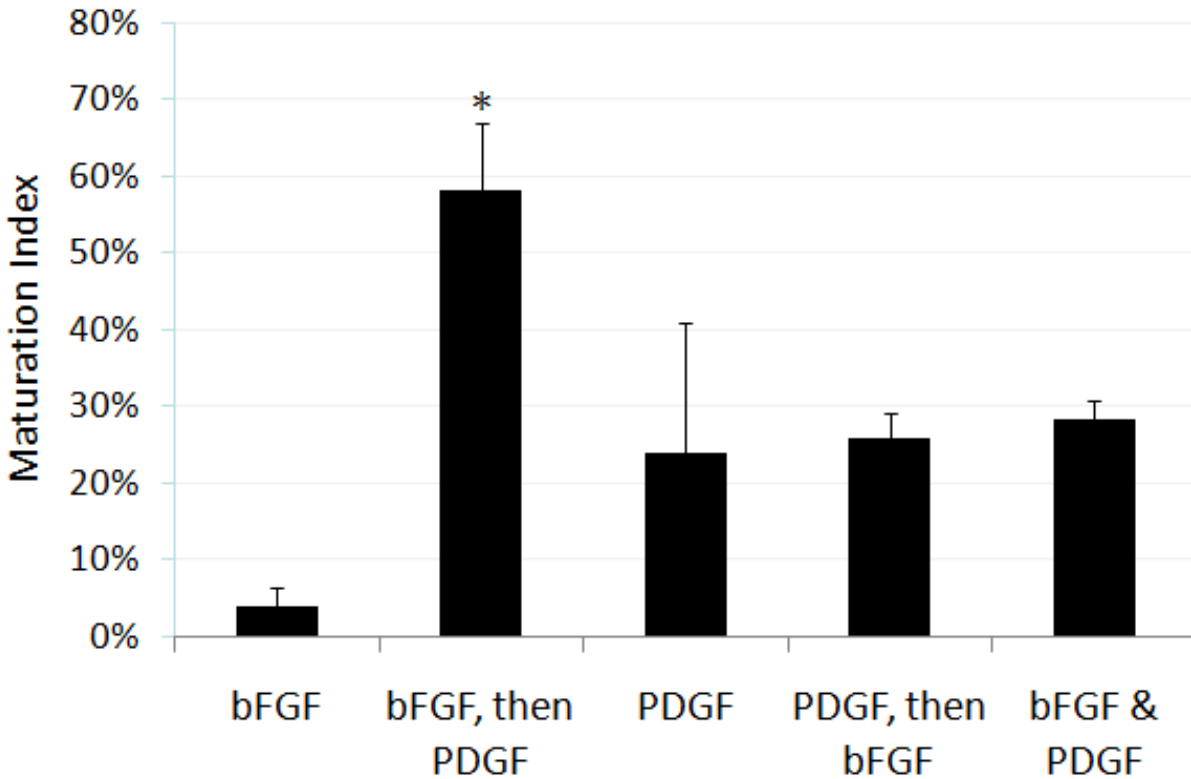


Figure 29. Maturation index where bFGF and/or PDGF are delivered.

Maturation index calculated by the percent of CD31+ cellular structures that are co-localized with α SMA staining. *indicates significant differences when compared to all other groups (ANOVA, followed by Holm-Bonferroni correction for t-test of multiple comparisons, $k=4$, $\alpha=0.05$)

9.3.4 Integration of neovasculature with native vasculature

Hematoxylin and eosin stained sections (Figure 28a-Figure 28f) reveal detectable cellular infiltration in all groups (purple nuclear stain). However, cellular infiltration into the Matrigel is more prevalent in the plugs in which an angiogenic factor has been delivered (Figure 28b-Figure 28f). Cells that have infiltrated into the Matrigel plug have arranged in tubular, vessel-like structures in plugs where PDGF is delivered alone (Figure 28d), following bFGF (Figure 28c) or

at the same time as bFGF (Figure 28f). However, when bFGF is delivered alone (Figure 28b) or following PDGF (Figure 28e), vessels are not observed. More importantly, tubular, vessel-like structures are filled with red blood cells only in groups where bFGF delivery is followed by PDGF (indicated by filled in arrow), suggesting integration with native vasculature (Figure 28c). The presence of red blood cells in the lumen of invading vessels was quantified by random selection of 10 vessel-like structures (lumen exceeding 100 μ m in diameter) using multiple wide-field 20x images from each experimental group. The number of these vessel-like structures filled with red blood cells in each group was identified and statistical analysis was performed in order to estimate the percent of invading vessels that are functionalized (i.e. Integrated with existing vasculature) (Figure 29). It was quite obvious from both visual inspection of numerous H&E images (Figure 28) as well as quantitative data (Figure 29) that when bFGF delivery is followed by PDGF delivery, there are dramatically higher numbers of red blood cell filled lumens than in any other schedules in which vessel-like structures (lumen >100 μ m) were observed.

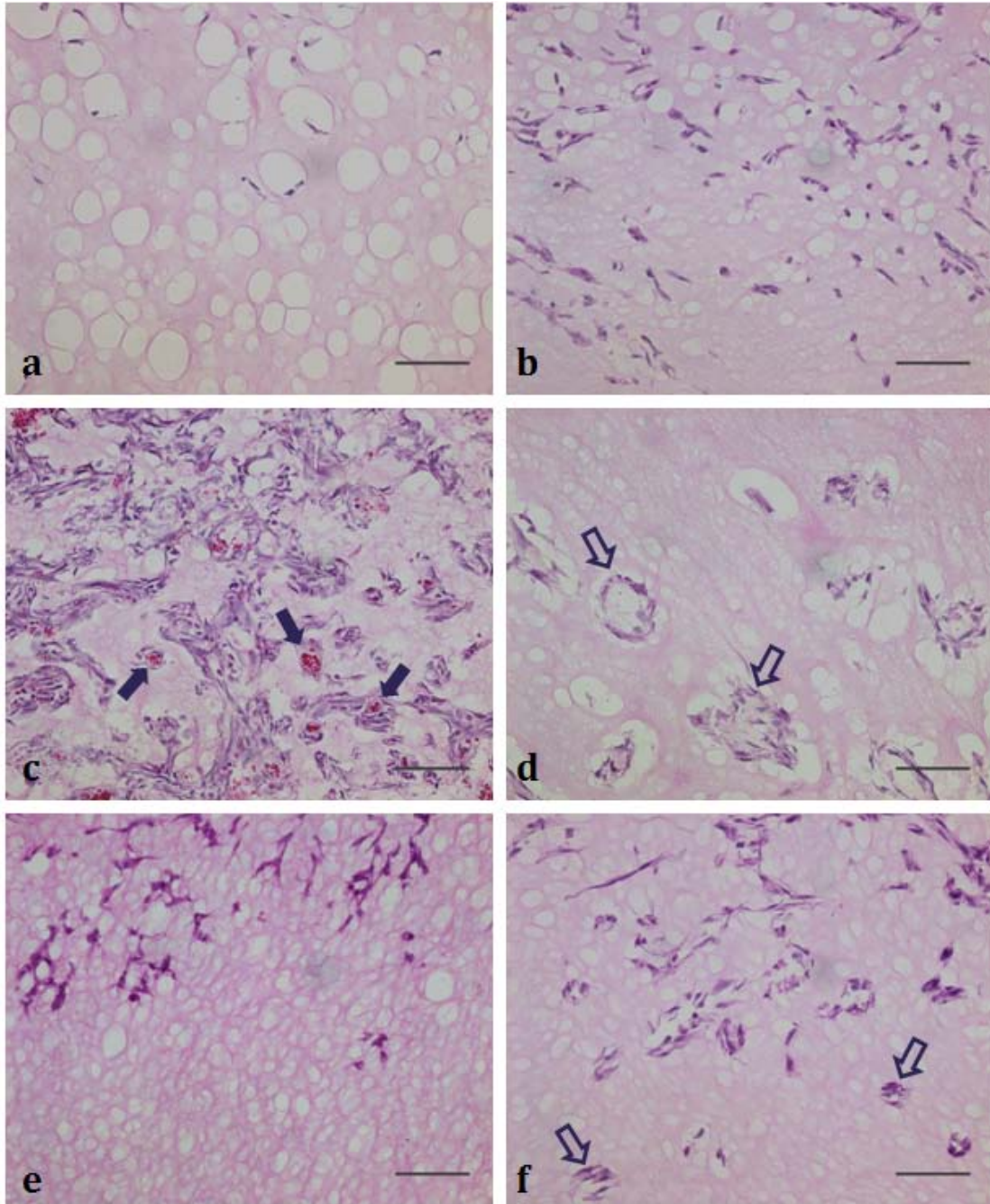


Figure 30. H&E images of murine Matrigel plugs where bFGF and/or PDGF are delivered.

Sequential delivery of VEGF and S1P results in cellular recruitment and functional angiogenesis *in vivo*. (a-f) H&E images of murine Matrigel plugs (scale bar=500µm). (a) Saline. (b) bFGF (200µg/mL). (c) bFGF (200µg/mL), followed by PDGF (500µg/mL). (d) PDGF (500µg/mL). (e) PDGF (500µg/mL), followed by bFGF (200µg/mL). (f) bFGF (200µg/mL) and PDGF (500µg/mL). ➔ indicates red blood cell filled vessels. ⇨ indicates empty vessels.

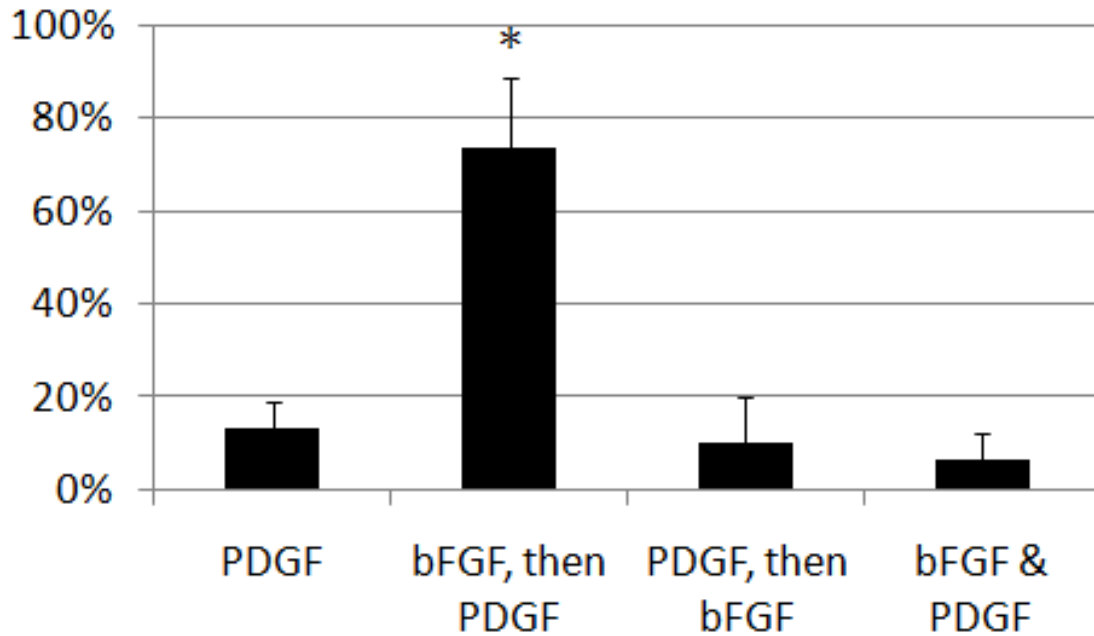


Figure 31. Vessel integration quantification when bFGF and/or PDGF are delivered.

Percent of vessel-like structures (lumen>100 μ m) filled with red blood cells. *indicates significant differences when compared to all other groups (ANOVA, followed by Holm-Bonferroni correction for t-test of multiple comparisons, $k=3$, $\alpha=0.05$)

9.4 DISCUSSION

While the physiological effects of many growth factors are generally known, in some specific tissues, the combination and interactions of the growth factors are only recently being explored. In recent literature, the most cited of these tissues is bone, where researchers are exploring delivery of angiogenesis inducing factors as well as bone morphogenic proteins.²⁸⁷⁻²⁸⁸ In the context of angiogenesis, it has recently been shown that delivery of an early-stage, endothelial cell recruitment factor, VEGF, before delivery of a late-stage, mural cell recruitment factor, S1P,

results in more overall endothelial cell recruitment as well as a higher vessel maturity, than when these factors are delivered together.²⁸¹ Accordingly, VEGF and S1P may act as a series of “instructions” to sequentially promote separate stages of the process. Yet, it is likely that other known angiogenic growth factors are involved in this series of sequential “instructions” as well. The goal of this study was to extend our sequential delivery model to study two other factors that have been implicated in stage-wise stimulus of blood vessel growth, namely bFGF and PDGF. Consequently, the knowledge gained from this research could serve as valuable additions to our understanding of the stage-wise process of angiogenesis as well as advancing therapeutic approaches to promoting angiogenesis.

Although the externally-regulated delivery model used in this study is not autonomously capable of sequential delivery itself, it provides a flexible format for temporal separation of various growth factors over any desired timeframe. Thus, a primary benefit of the model system discussed here is to inform the design of future systems that are capable of autonomously delivering these growth factors over a successful delivery schedule. Furthermore, the system allows for the introduction of a growth factor in a more gradual method than via bolus injection (a method previously proven to be effective²⁸¹), where uniform distribution of a growth factor at non-toxic levels would be extremely difficult. A second feature of this model system is the internal negative control. Specifically, a matching Matrigel plug with implanted hollow fiber is present on the left flank of each animal enrolled in this study. This Matrigel plug was analyzed for angiogenesis in the same fashion as the Matrigel plugs in the experimental groups so that the level of angiogenesis cause by the Matrigel injection as well as the hollow fiber implantation can be monitored. Although endothelial cell migration levels in the internal controls are consistently

very low and often negligible (Figure 24a), the level of endothelial migration observed in each mouse was used to normalized all reported results (Figure 25).

Basic FGF has been implicated in endothelial cell migration and has also been known to induce a proangiogenic phenotype in endothelial cells.⁷¹ This paradigm is consistent with our data suggesting that endothelial cell migration occurs to a greater extent when bFGF is delivered for 7 days as compared to saline controls (Figure 24a and Figure 24b) despite the fact that bFGF is found to be unstable in the presence of many proteases expected to be present under inflammatory conditions.²⁸⁹⁻²⁹¹ However, it has been shown that bFGF can inhibit PDGF-induced smooth muscle cell migration and proliferation via the PDGF and bFGF receptors²⁸⁰, events that correspond with late-stage angiogenesis. In agreement with these prior findings, our results suggest that exclusive, persistent delivery of bFGF results in endothelial cell migration (marked by CD31+ cells, Figure 24b) without colocalization with vascular pericytes (marked by α SMA+ cells, Figure 26a). These data suggest that delivery of bFGF alone is not sufficient to sustain (and may even inhibit the progress) of growing neovasculature, a theory supported by a recent study in mice.²⁹² It is possible that the role of bFGF may be primarily limited to promotion of early stage-angiogenic events.

PDGF, in contrast, is known to promote the maturation of blood vessels through the recruitment and support of mural cells.^{67, 71} Likewise, we observe that in all groups where PDGF is delivered, there is an increased presence of α SMA+ and CD31+ cell colocalization, regardless of the time-frame of delivery (Figure 26). These data are important given that the process of pericyte coverage is imperative to the stability, and in turn the fate, of newly forming vessels.²⁹² Importantly, although newly forming vessels can be transient, and often regress²⁹²⁻²⁹³, such blood vessels are known to not contain α SMA positive cells which (when present) interact with, and

stabilize endothelial cells and inhibit regression.²⁹⁴ This process begins only once endothelial cells have been recruited and new basement membrane is secreted.⁹ It is not surprising then that the presence of PDGF, through its binding to PDGF-R α on endothelial cells, negatively affects the action of bFGF – mediated recruitment.⁷¹

For the reasons described above, we hypothesized that the delivery of bFGF should precede delivery of PDGF to best promote the growth of stable and mature neovasculature. Using our simple and flexible hollow fiber model for sequential delivery, this delivery schedule (bFGF, followed by PDGF) could be compared to delivery of each factor alone, dual delivery of both factors, as well as the reverse schedule (PDGF, followed by bFGF). A sequential delivery schedule (in contrast to dual delivery) would support bFGF induced endothelial cell migration and proliferation without inhibition by PDGF, followed by PDGF induced vessel maturation, without inhibition by bFGF. Accordingly, this delivery schedule resulted in both greater overall endothelial cell presence in a Matrigel plug after 7 days (Figure 24) as well as a higher maturation index of vessels formed by these endothelial cells (Figure 26).

It was observed that delivery of bFGF and PDGF alone, as well as together induced similar levels of endothelial cell recruitment (Figure 24g). It is important to note that while bFGF and PDGF may have conflicting effects on the recruitment and organization of both endothelial cells and vascular pericytes, complete inhibition of angiogenesis is not observed when both factors are added together (Figure 24f and Figure 26f). This can possibly be explained by the pluripotency of PDGF.²⁹⁵⁻²⁹⁶ Although PDGF has been shown to be involved in mural cell recruitment and other late stage angiogenesis events¹⁷⁸, it is also the only growth factor involved in FDA-approved treatment for non-healing wounds, suggesting that its effects may not be limited to one stage of angiogenesis.¹² Regardless, this treatment is only 30%

effective¹⁰ and likely not capable of optimally directing a multi-stage process without the direction of other biomolecules.

The need for additional biomolecular input for functional angiogenesis is evident our data. Endothelial cells are recruited to the Matrigel plug when PDGF is delivered during early angiogenesis (first 3 days, Figure 24d and Figure 24f), but these vessels are not interconnected with existing vessels (as indicated by their lack of red blood cells in the vessels) (Figure 28d, Figure 28f and Figure 29). While endothelial cell migration and vessel maturation are important in angiogenesis, vessels do not become functional until they are integrated with the native vasculature. One way of determining whether or not a new vessel has integrated with the host's existing vessels is by looking for the presence of red blood cells. Only in plugs where PDGF delivery follows bFGF delivery (Figure 28c and Figure 29) did we consistently observe red blood cells in the lumen of these structures. This suggests that this growth factor delivery schedule allows for more proper formation of vessels that are integrated with the native vasculature, allowing oxygen and nutrient delivery to newly forming tissue. It is possible that constitutive delivery of PDGF does not allow for destabilization of native vessels to the extent necessary to allow juncture with newly forming vessels. Although PDGF may not be capable of inhibition of endothelial cell migration and proliferation (as seen in Figure 24d), PDGF might block the act of basement membrane destabilization.⁷¹

Though not discussed, there are additional methods for determining interconnectivity of newly forming vessels. One method is through dextran-FITC injection into the tail vein of the mouse, followed by Matrigel plug recovery, as described previously.^{260, 297} This method allows for visualization of vessels (via FITC illumination) and quantification of vessel volume. Visualization of the new blood vessels may also allow for examination of “leaky” or

hemorrhagic vessels, which would be an indication of an integrated, but immature vessel. Vessel volume can be determined through FITC concentration measurements following digestion of the Matrigel plug. Due to the nature of our system, cellular infiltration as well as angiogenesis occurred rapidly, resulting in quick degradation of the Matrigel plug and incorporation of the implant with the surrounding tissue. When attempting to isolate the Matrigel plug for FITC quantification following Dextran-FITC tail vein injection, it was difficult to determine where the Matrigel plug ended and where the native tissue began. For this reason, only red blood cell filled lumen counts (Figure 31) were analyzed.

Because our model is modular and easily tuned, sequential delivery of a wide variety of factors is possible. To date, bFGF and PDGF is now the second set of growth factors that have been shown to be temporally relevant in mature angiogenesis using our sequential delivery model. Additional growth factors can be explored in other wound healing models, as temporal relevance of growth factors is likely not unique to angiogenesis. For example, platelet derived growth factor (PDGF) and bone morphogenetic protein 2 (BMP-2) have been implicated as playing a major role in the osteogenic processes; however, each protein appears to accomplish different tasks during different stages in the regeneration of bone.²⁹⁸⁻³⁰⁰ For instance, PDGF appears to aid in cellular recruitment, differentiation and proliferation, as well as angiogenesis, while BMPs seem to play a key role in the development of mature osteoblasts and bone tissue formation.³⁰¹ Furthermore, PDGF has been shown to actually inhibit mature osteoblast activity in the later stages of bone formation.²⁸⁷ Hence, an ideal delivery strategy would first present early stage factors to induce angiogenesis and recruit osteoprogenitors and then present later stage factors to differentiate cells and induce mineralized tissue formation.

9.5 CONCLUSION

We have created a flexible model for the study of sequentially delivered angiogenic factors. When using this system to explore sequential delivery of bFGF and PDGF, we observed that delivery of bFGF for 3 days followed by delivery of PDGF for 4 days resulted in recruitment of more endothelial cells and a higher maturation index than the reverse sequential delivery schedule, single factor delivery or dual delivery. Additionally, sequential delivery of bFGF followed by PDGF resulted in vasculature that has integrated with the native vasculature, allowing for oxygen delivery to a previously cell-free environment. This approach could be likewise utilized to explore any number of delivery schedules and the resulting therapeutic responses as well as for studying the basic biological signals that accompany stage-wise regeneration of tissues.

10.0 MODELING RELEASE FROM POROUS HOLLOW FIBERS

10.1 INTRODUCTION

Hollow fiber membranes have widespread use in industries such as food, juice, pharmaceutical, metal working, dairy, wine and most recently municipal drinking water.³⁰²⁻³¹² Depending on the application, hollow fiber membranes can be highly practical and cost effective alternatives to conventional chemical and physical separation processes due to their high surface area to volume ratio. In the separation technology field, large volumes can be filtered, while utilizing minimal space, with low power consumption.³¹³⁻³¹⁴

Recently, in the field of drug delivery, hollow fibers have been shown to be capable of growth factor delivery both *in vitro*^{74, 265-266} and *in vivo*^{106, 264, 315}. This concept was recently extended by using hollow fibers as a platform for sequential delivery of growth factors that are specific for angiogenesis.²⁸¹ First, factors involved in early stages of angiogenesis were delivered to facilitate blood vessel destabilization and endothelial cell recruitment and proliferation. Subsequently, factors involved in late stages of angiogenesis were delivered to facilitate mural cell recruitment and blood vessel stabilization. The hollow fibers can extend into an acellular site or a wound, permitting a fine level of control over release as a function of time by externally manipulating the contents of the fiber lumen. Such a platform could also be readily applied to delivery of growth factors associated with other physiological processes, such as bone,

where an angiogenic growth factor's presence prior to a bone morphogenic growth factor can enhance bone healing.^{246, 248, 316}

Externally-regulated delivery (such as with hollow fibers) provides a flexible template that is well-suited to facilitate a better understanding of which growth factors are necessary at various stages of a physiological process, without the time and cost associated with more complex delivery strategies. One of the primary reasons for this flexibility is that the rate of delivery is determined solely by the characteristics of the hollow fiber (pore size, wall thickness, etc.) and the composition and concentrations of agents in the fiber lumen. This rate can be determined experimentally, in a similar fashion to other growth factor delivery systems, tracking *in vitro* release into a saline solution. Modeling release of biologics from these hollow fibers would facilitate the design of delivery regimes with even less cost of time and money as well as allowing the exploration of the feasibility of any number of complex release profiles.

In order to model release of biomolecules from hollow fibers, a basic understanding of associated release mechanisms is in order. Protein transport through polymer matrices can often be rudimentally described by Fick's law of diffusion, under the assumption that the diffusivity of each protein does not change over time, where a protein will travel from an area of high concentration to low concentration with a rate dictated by its constitutive diffusion coefficient (D) and the extent of concentration driving force. However, when recombinant proteins are loaded at a very high concentration (in conjunction with processing excipients) into a hollow fiber, other phenomena may also arise. For instance, proteins, such as the ones delivered for angiogenesis,²⁸¹ have isoelectric points between 9 and 10. For this reason, at high concentrations, the negatively charged proteins increase the osmolality of the solution. An even greater impact on the osmolality of the protein solution lies within the processing method, where

the excipients used to process and isolate the recombinant protein varies. With a high osmolality, an osmotic pressure difference is created between the lumen of the protein loaded fiber, and the surrounding physiologic environment. The osmotic pressure difference that develops between the hollow fiber and its surrounding environment causes an influx of water to the fiber, decreasing the lumen concentration and increasing the lumen volume. The increase in volume, in turn, creates a hydrostatic pressure difference that causes a net flux of water, and thus, protein, out of the fiber.³¹⁷ Therefore, both diffusion as well as osmosis-driven convection must be considered with modeling release from porous hollow fibers.

Accordingly, this work describes the development of a mathematical model that can predict the release of VEGF, bFGF or PDGF, from cellulose hollow fibers fabricated under varying conditions. This model takes into consideration, not only the flow of proteins due to diffusion, but also convection caused by bulk flow of water.³¹⁸ Model predictions were compared to *in vitro* release data, where protein release into a saline bath was measured.

10.2 THEORY AND MODEL DEVELOPMENT

10.2.1 Diffusion

Hollow fibers fabricated using a double injection nozzle often have both large macropores (Mp) as well as small micropores (μp), as a result of solvent extraction and spinodal decomposition²⁵⁶ (Figure 30, left). Diffusion of a large molecule such as a protein through a polymer matrix can rudimentarily described by Fick's law of diffusion, where transport of a molecule is governed by the concentration difference and the individual diffusivity for a given molecule/solvent

combination. When using Fick's law to predict protein release from a hollow fiber membrane, the overall cross-sectional area for diffusion can be approximated by two separate "paths" that the molecule can take (Figure 30, right). In the first path, the protein would travel through only the microporous section of the hollow fibers, where the micropore porosity would contribute to the transport rate. Alternately, in the second path, the protein would travel through a combination of microporous and macroporous regions, where the micropore porosity as well as the size and geometry of the macropores would both contribute to the transport rate. The number of molecules that travel through path 1 versus the amount of molecules that travel through path 2 can be predicted by the height of the macropores compared to the distance between them, where j_1 is the fraction of path 1 (Equation 1), but also with consideration of available surface area and the molecule's preference for a path of least resistance (path 2).

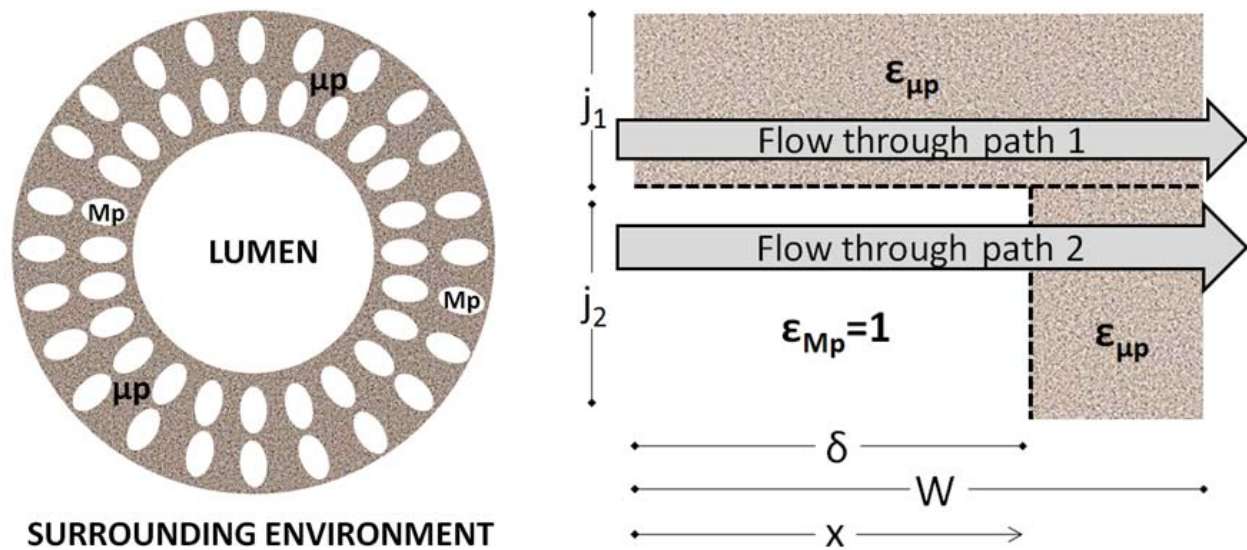


Figure 32. Hollow fiber schematic and model theory.

$$j_1 = \frac{(\text{distance between macropores})}{(\text{distance between macropores}) + (\text{height of macropores})}$$

Equation 1

The transport resistance through path 1 and path 2 (individual porous matrices) can be determined by the porosity of each of these paths, where transport through a single macropore would have a porosity of 1. The ratio of macropore distance of diffusion to micropore distance of diffusion can be determined by the width of the macropores. Based on diffusion by Fick's law, the concentration in the lumen of the hollow fiber can be calculated according to Equation 2, where C_0 =concentration in the hollow fiber lumen ($\mu\text{g/mL}$), V_{hf} =equals the volume of solution in the hollow fiber lumen (mL), β =diffusivity determined by specific hollow fiber characteristics and molecule diffusion coefficient (cm/s) and t =time (s).

$$C_0 = C_0^{\text{initial}} * e^{\frac{-\beta}{V_{hf}} * t}$$

Equation 2

10.2.2 Osmotic and hydrostatic pressure

When predicting transport across a membrane, it is necessary to also consider the osmolality of the solutions on both side of the membrane. A difference in osmolality, and thus osmotic pressure difference, will cause transport of water across the membrane in the direction of high

osmolality. This process is known as osmosis, defined as the solvent diffusion through a semi-permeable membrane.³¹⁹⁻³²⁰

Mass transport can be driven by osmotic pressure, hydrostatic pressure or in some cases both.³²¹⁻³²² Volume flux due to osmosis can be described as derived by Kedem and Katchalsky (Equation 3), where this relationship can be represented as linear relationship between force and flow (J_v =solvent volume flux (m/s), L_p =filtration coefficient (m³/N•s), P =hydrostatic pressure (Pa), σ =reflection coefficient, π =osmotic pressure (Pa)).³¹⁹

$$J_v = L_p \Delta P - L_p \sigma \Delta \pi$$

Equation 3

10.2.3 Model

The goal of this model is to calculate transport across a porous membrane through modeling of the processes of diffusion and convection based on solvent flux. The diffusivity of each protein can be estimated from the diffusivity of the protein in water (D , as reported in previous studies) and the porosity (ϵ) of each hollow fiber (Equation 4). If the porosity is 1 (such as in a macropore), the diffusivity of an agent will be equal to the diffusivity of that agent in water (Equation 5).

$$D_{\mu p} = \epsilon D$$

Equation 4

$$D_{Mp} = D$$

Equation 5

The geometry of the hollow fiber wall is used to determine transport across the membrane.³¹⁴ This calculation is based on Fick's law, under the assumption of the following boundary conditions:

$$1: @x = 0, C_{Mp} = C_0(t)$$

$$2: @x = W, C_{\mu p} = 0$$

$$3: @x = \delta, C_{Mp} = C_{\mu p}$$

$$4: @x = \delta, D_{Mp} \frac{dC_{Mp}}{dx} = D_{\mu p} \frac{dC_{\mu p}}{dx}$$

and the following flux equations:

$$1: J^1 = -D_{\mu p} \left. \frac{dC^1}{dx} \right|_{x=0}$$

$$2: J^2 = -D_{Mp} \left. \frac{dC^2}{dx} \right|_{x=0}$$

$$3: J^2 = -D_{\mu p} \left. \frac{dC^2}{dx} \right|_{x=W}$$

Using the above boundary conditions, β in Equation 2 can be calculated (Equation 6), where $D_{\mu p}$ =diffusivity of the molecule through the micropores (cm^2/s), D_{Mp} =diffusivity of the molecule through the macropores (cm^2/s), j_1 =fraction of molecules traveling through micropores (path 1), j_2 =fraction of molecules traveling through macropores (path 2), W =thickness of hollow fiber wall (cm) and δ =macropore width (cm). Equation 6 can be applied to Equation 2, leading

to a final equation for the concentration within the hollow fiber, with respect to time (Equation 7), when considering transport by diffusion only.

$$\beta = \left[\frac{j_1 D_{\mu p}}{W} + \frac{j_2 D_{\mu p}}{\delta \left(\frac{D_{\mu p}}{D_{M p}} - 1 \right) + W} \right]$$

Equation 6

$$C_0 = C_0^{\text{initial}} * e^{-\frac{\left[\frac{j_1 D_{\mu p}}{W} + \frac{j_2 D_{\mu p}}{\delta \left(\frac{D_{\mu p}}{D_{M p}} - 1 \right) + W} \right] * t}{V_{hf}}}$$

Equation 7

Volume flux of water into and out of the fiber can be calculated according to Equation 3. The osmolality of each solution can be measured experimentally in order to determine a linear relationship between osmolality and concentration. The hydrostatic pressure can be calculated according to Equation 8, where ρ is the density of the solution (kg/m^3), $g=9.81\text{m/s}^2$ and h =height of the solution (m). The density of the solution can be estimated as the density of water (any weight that can be attributed to the weight of the protein is considered negligible).

$$P = \rho g h$$

Equation 8

The filtration coefficient (L_p) is a measure of a membrane's permeability to water, with a higher permeability correlating to a higher porosity and a thinner membrane.³²³ Theoretically,

the filtration coefficient value represents the membrane surface area as well as hydraulic conductance and can be calculated according to Equation 9, where ϵ =porosity, r =pore radius, μ =viscosity and τ =tortuosity. In this equation, it is assumed that the porosity of the membrane is uniform.

$$L_p = \frac{\epsilon \cdot r^2}{8 \cdot \mu \tau}$$

Equation 9

In the case of hollow fiber membranes with both micropores and macropores (as depicted in Figure 30), the water permeability through the macropores will be substantially greater than the micropores (macropore radius~10-50 μ m versus micropore radius~0.25-0.5 μ m). For this reason, the filtration coefficient can be estimated as a function of the macropore size alone.

The reflection coefficient relates to how a semipermeable membrane can reflect solute particles that could otherwise pass through and is sometimes viewed as a “correction factor”. A value of zero results in all particles passing through, while a value of one is such that no particle can pass.^{319, 324} For this reason, the reflection coefficient can be estimated as a function of the porosity of the membrane.

Taken together, the solvent flux can be calculated from Equation 3, where the osmotic pressure is a function of the concentration in the hollow fiber lumen and the hydrostatic pressure is a function of the volume in the hollow fiber lumen. If the hydrostatic pressure is great enough that the solvent flux is positive (resulting in bulk flow out of the fiber), the bulk flow will contain solute and thus contribute to overall transport. The overall transport will amount to the sum of the amount released via diffusion and the amount released via solvent flux.

10.3 METHODS AND MATERIALS

10.3.1 Hollow fiber fabrication

Cellulose acetate hollow fibers were prepared using a double injection nozzle (inner tube=20G, outer tube=14G). Cellulose acetate (30kD, Aldrich) was dissolved at a final concentration of 49.67% DMSO, 14.67% acetone, 14.67% isopropyl alcohol, 1% water and 20% cellulose acetate, and was pumped with syringe pumps (Braintree Scientific) through the outer tube of the nozzle (14G), and deionized water was pumped through the center core (20G). The cellulose solution and deionized water were extruded into a deionized water bath where the cellulose solution precipitates in the form of a porous hollow fiber (Figure 31). Cellulose and water flow rate were varied according to Table 1 for the purpose of fabricating fibers with varying pore morphology. Lyophilized hollow fiber cross sections were sputter coated with 3.5nm of gold-palladium and imaged at 5kV using a JEOL 9335 SEM.

10.3.2 Hollow fiber image analysis and characterization

Scanning electron microscopy images were taken of three representative cross-sections of each fiber. Using Metamorph software, measurements of wall thickness, macro-pore dimensions, micro-pore dimensions and porosity, were taken of each cross-section. These measurements were used to characterize each fiber fabrication condition described in Table 1, and used to calculate model parameters described in Section 10.2.³¹³

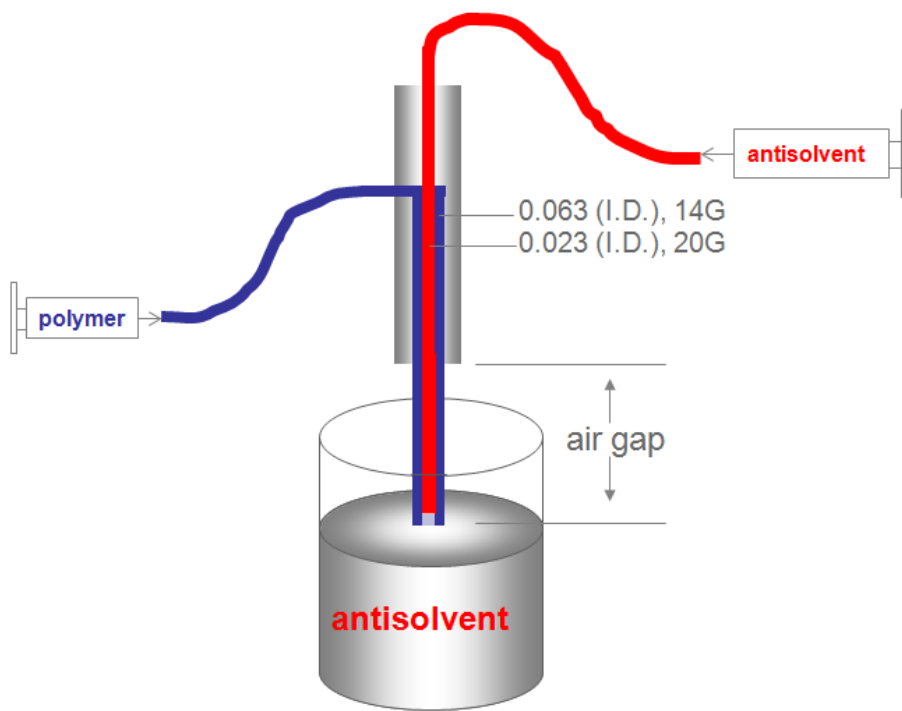


Figure 33. Hollow fiber fabrication schematic.
 Polymer solution is 20% cellulose acetate solution and antisolvent is deionized water.

Table 1. Hollow fiber fabrication conditions.

	Water flow rate (mL/min)	Cellulose flow rate (mL/min)
Fiber I (8/1.5)	8	1.5
Fiber II (13/2.5)	13	2.5
Fiber III (10/1.5)	10	1.5

10.3.3 Release studies

Wells of a 6-well cell culture plate were filled with 5 mL Dulbecco's phosphate buffered saline, or PBS (Invitrogen), supplemented with 1% bovine serum albumin (BSA). Recombinant human VEGF, rh-bFGF and rm-PDGF (R&D Systems) was reconstituted using 1% BSA in PBS at various concentrations ranging from 0-200 μ g/mL. Cellulose hollow fibers cut at 10cm were injected with 30 μ L of growth factor solution and submerged in the 5mL PBS (1% BSA) and place on a shaker. At 10 time points over a 24 hour period, a sample of the PBS bath was taken, and the fiber was removed from the PBS bath and placed in a fresh PBS bath. This process was repeated for each fiber/growth factor/concentration combination. Growth factor concentration of each sample taken was measured using an ELISA kit (R&D Systems).

10.3.4 Osmolality determination

Osmolality measurements were recorded for varying concentrations of bFGF (31.25 μ g/mL, 62.5 μ g/mL, 125 μ g/mL, 250 μ g/mL), VEGF (41.67 μ g/mL, 83.33 μ g/mL, 250 μ g/mL) and PDGF (12.5 μ g/mL, 25 μ g/mL, 50 μ g/mL, 100 μ g/mL) using an osmometer (Precision Systems Osmometer, Model 5004). These values were used to calculate osmotic pressure differences across the hollow fiber wall when a concentrated solution of protein is injected into the lumen of the hollow fiber that is placed in a saline bath (see Section 10.3.3).

10.4 RESULTS

10.4.1 Hollow fiber characteristics

Hollow fibers fabricated according to conditions described in Table 2 reveal distinct differences in macro- and micro-pore morphology. Measurements of fiber and macropore geometry were taken from SEM images similar to those shown in Figure 32. Table 2 shows the measurements from the SEM image analysis, with calculated j_1 based on measured macro-pore area (macro-pore area is estimated as length times width). The effective diffusion coefficient is calculated from individual parameters (j_1 , j_2 , W , δ , ε) and represents the effective diffusivity, without accounting for the individual diffusivity of each molecule (See **Equation 10**). These results reveal that release based on diffusion is linearly related to the microporosity of the fiber.

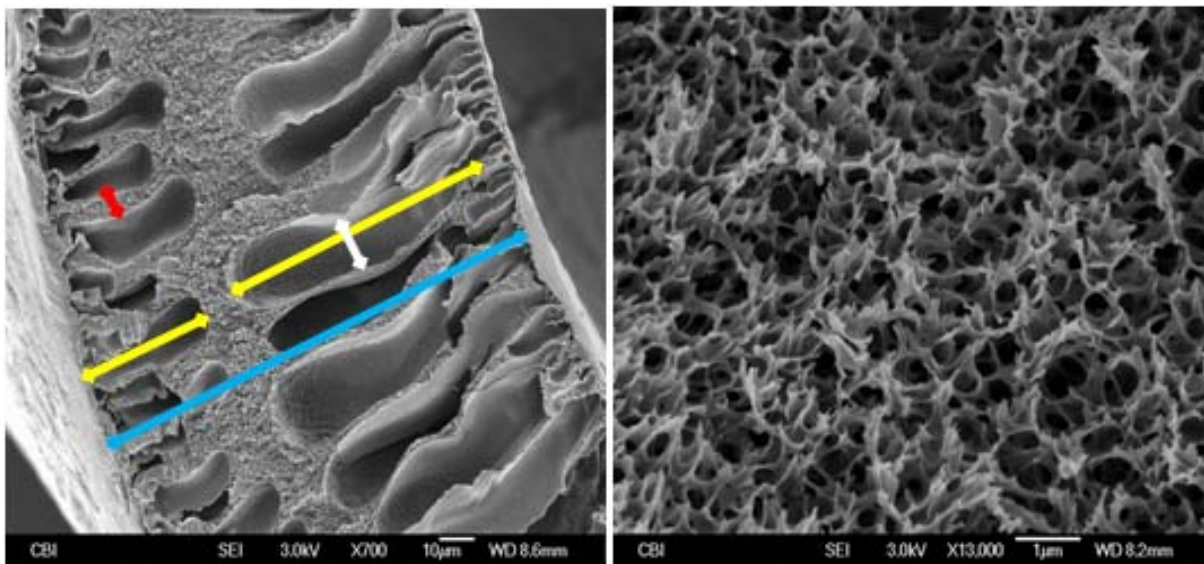


Figure 34. Representative fiber characterization images.

$$\text{Effective Diffusion Coefficient} = \frac{D_{eff}}{D_{\text{protein in water}}}$$

Equation 10

Table 2. Hollow fiber model parameters.

	j_1	j_2	W (μm)	δ (μm)	ϵ	Effective Diffusion Coefficient
Fiber I	0.311	0.689	99.68	84.08	0.0442	0.0217
Fiber II	0.262	0.738	76.84	45.26	0.2077	0.0867
Fiber III	0.374	0.626	87.14	67.33	0.0884	0.0469

10.4.2 Osmolality

Measurements taken with an osmometer demonstrate that osmolality is a linear function of the protein concentration, in the concentration range that is utilized in this study (Figure 33). The osmolality of bFGF is most dependent upon the concentration, whereas the osmolality of PDGF is least dependent upon the concentration, with little change at all.

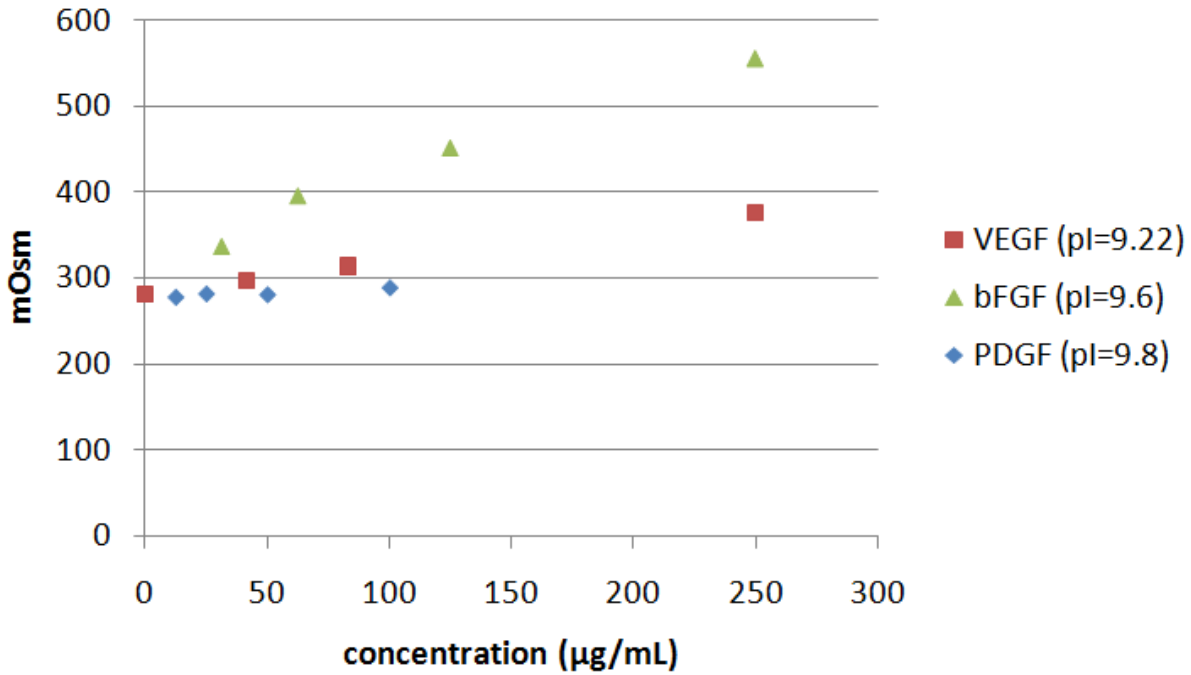


Figure 35. Osmolality of VEGF, bFGF and PDGF, as a function of concentration.

10.4.3 Model predictions and release data

Model predictions were made with 10% variation in microporosity, injection volume, macropore geometry and fiber wall thickness, in order to observe the effect that changes in these variables would have on predicted release. Changes up to $\pm 10\%$ in the microporosity did not produce a noticeable change in the release rate of an example protein VEGF. Changes up to $\pm 10\%$ in the injection volume has a noticeable effect on the rate of release and thus time until complete release (Figure 34), with about a 0.27 hour change in complete release of protein, when $\epsilon_{sp}=0.1$,

$W=99.67\mu\text{m}$, $\delta=84.08\mu\text{m}$, $j_1=0.311$ and injection concentration of VEGF= $100\mu\text{g/mL}$. Changes up to $\pm 10\%$ in the fraction of j_1 (the fraction of particles that travel through the microporous area only) also has a noticeable effect on the rate of release (Figure 35). The theoretical change in j_1 predicts about a 0.33 hour change in complete release of protein, when $\epsilon_{sp}=0.1$, $W=99.67\mu\text{m}$, $\delta=84.08\mu\text{m}$, $V_{hf}=0.01$ and injection concentration of VEGF= $100\mu\text{g/mL}$. Lastly, changes up to $\pm 10\%$ in the fiber wall thickness have a noticeable effect on the rate of release (Figure 36). The theoretical change in W predicts about a 0.6 hour change in complete release of protein, when $\epsilon_{sp}=0.1$, $j_1=0.311$, $\delta=84.08\mu\text{m}$, $V_{hf}=0.01$ and injection concentration of VEGF= $100\mu\text{g/mL}$.

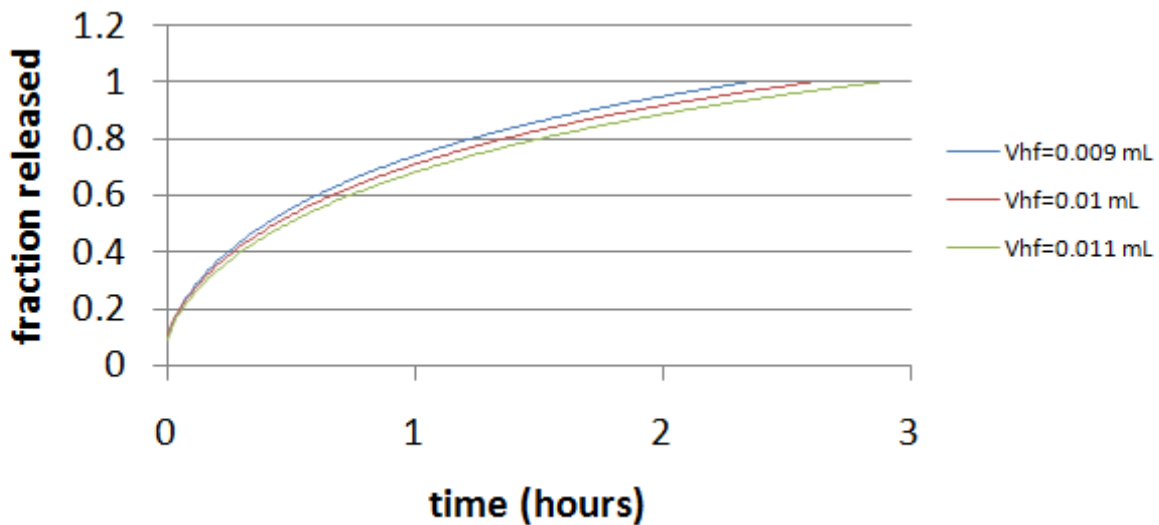


Figure 36. Effect of injection volume on release.

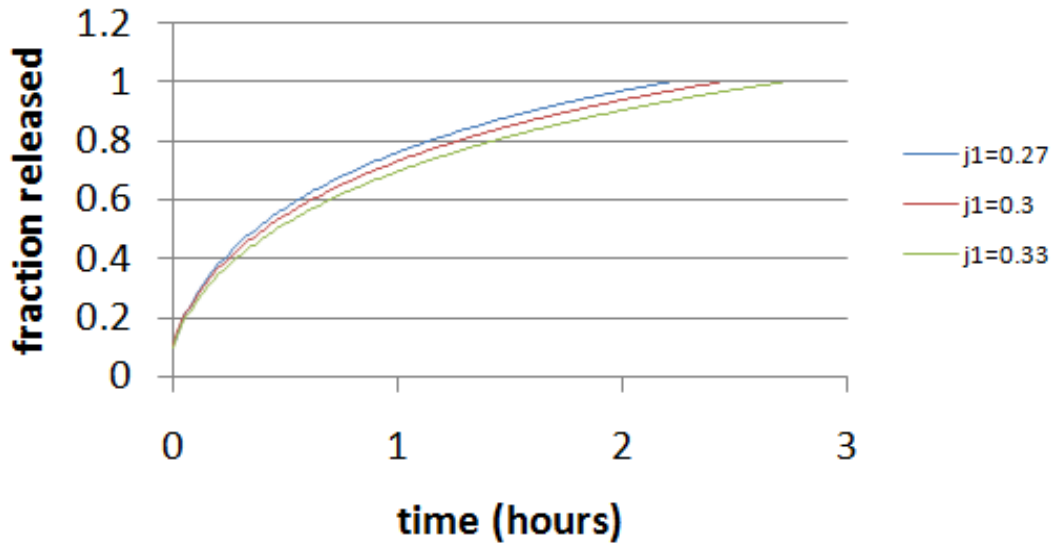


Figure 37. Effect of micropore/macropore fractions on release.

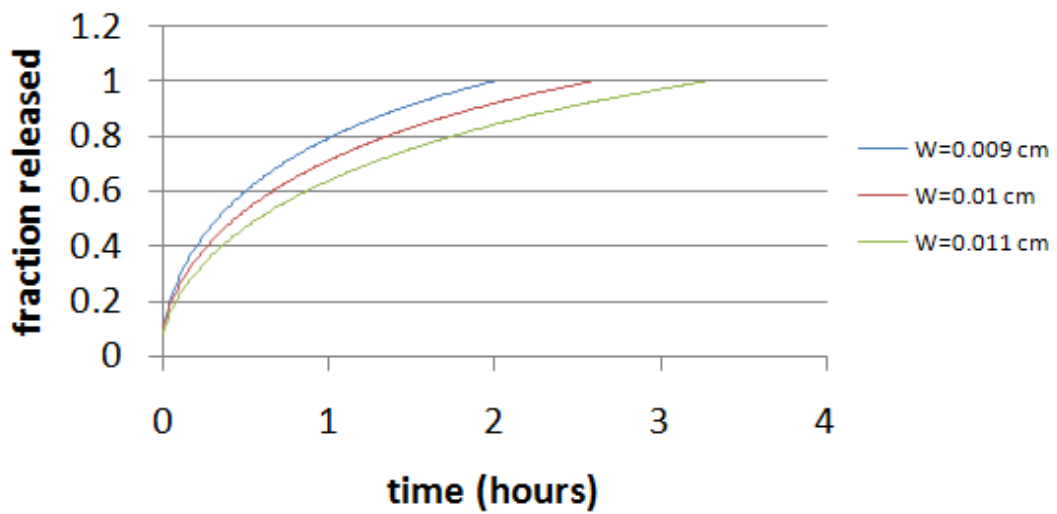


Figure 38. Effect of wall thickness on release.

First, *in vitro* release data was compared to model predictions on an individual basis (Figure 39). When an injection of 100 μ g/mL PDGF was injected into Fiber II (Figure 39, left) and when an injection of 100 μ g/mL VEGF was injected into Fiber I (Figure 39, right), the model matches the empirical release data well.

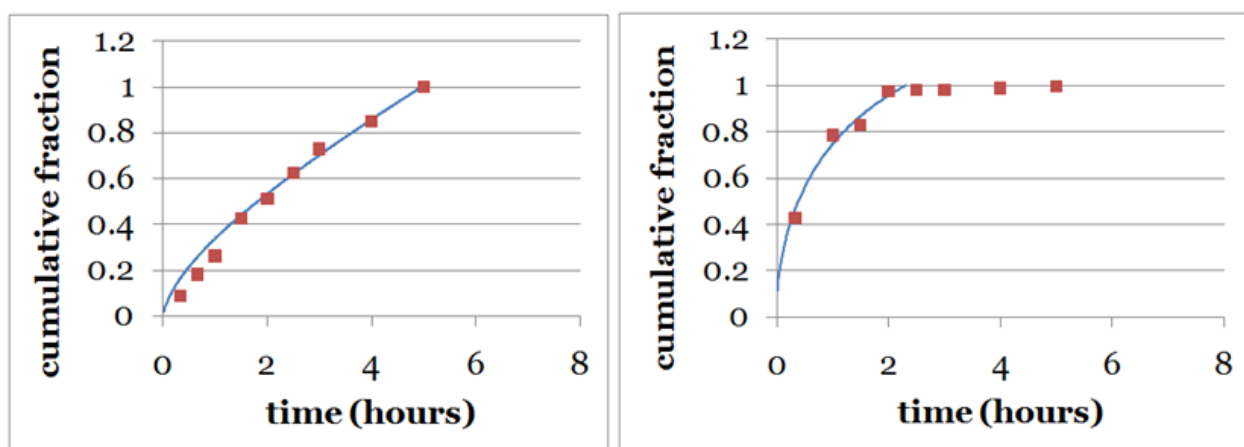


Figure 39. Model prediction and *in vitro* data.

Fraction released versus time for protein from cellulose hollow fibers. Blue line represents model prediction and red squares represents *in vitro* data for an injection of 100 μ g/mL PDGF in Fiber II (left) and 100 μ g/mL VEGF in Fiber I (right).

Next, release of bFGF was compared, keeping the injection concentration the same (200 μ g/mL), but varying the physical properties of the fiber (Table 2). Results of both model predictions and *in vitro* release can be seen in Figure 37. Fiber III predicts (as well as *in vitro* data) the fastest rate of release (showing the shortest time until depletion of the lumen reservoir),

while Fiber II (as well as *in vitro* data) predicts the slowest rate of release (showing the longest time until depletion of the lumen reservoir).

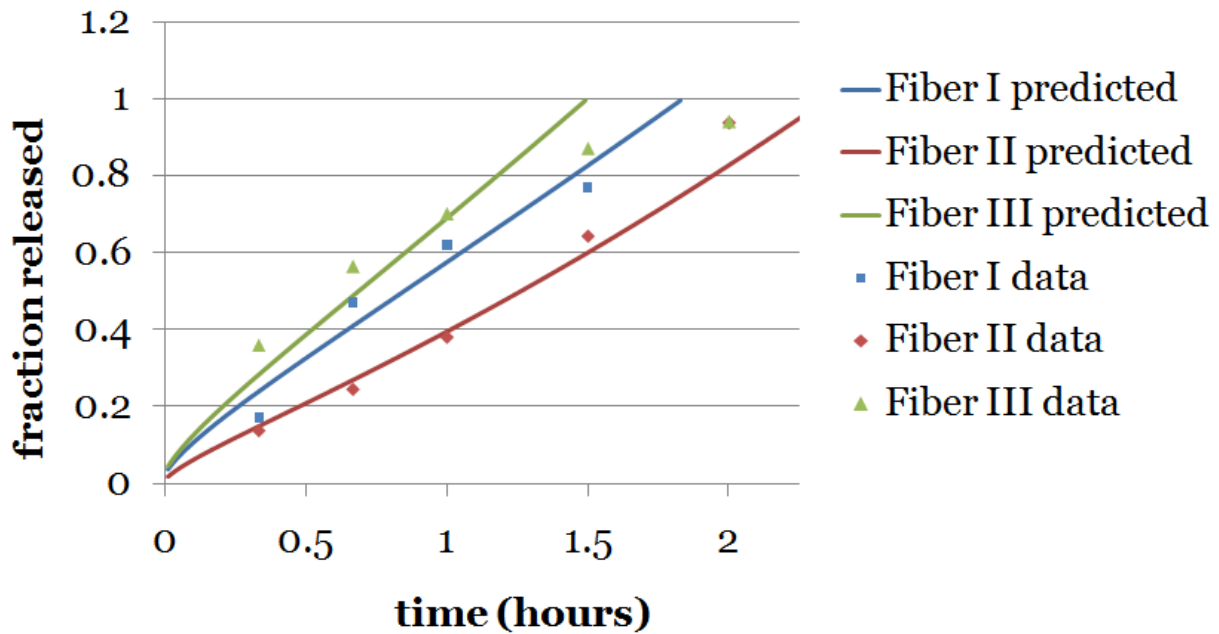


Figure 40. Model prediction and *in vitro* data for bFGF release from Fiber I, Fiber II and Fiber III.

Fraction released versus time for bFGF from cellulose hollow fibers fabricated under varying conditions. Blue line represents model prediction for Fiber I (fabricated with water flowing at 8mL/min and cellulose at 1.5mL/min). Blue squares represent release data for Fiber I. Red line represents model prediction for Fiber II (fabricated with water flowing at 13mL/min and cellulose at 2.5mL/min). Red diamonds represent release data for Fiber II. Green line represents model prediction for Fiber III (fabricated with water flowing at 10mL/min and cellulose at 1.5mL/min). Green triangles represent release data for Fiber III.

Release was also compared by varying the growth factor used, but consistently using Fiber III (fabricated with water flowing at 8.5mL/min and cellulose flowing at 1.5mL/min). Results of both model predictions and *in vitro* release can be seen in Figure 38. In the first hour, release of VEGF reaches about 75%, while release of PDGF only reaches about 50%, but over the next 0.5 hours, VEGF release is only about 5%, while PDGF continues to release another 25%. Additionally, at 1.5 hours the fraction of bFGF released exceeds the fraction of VEGF released.

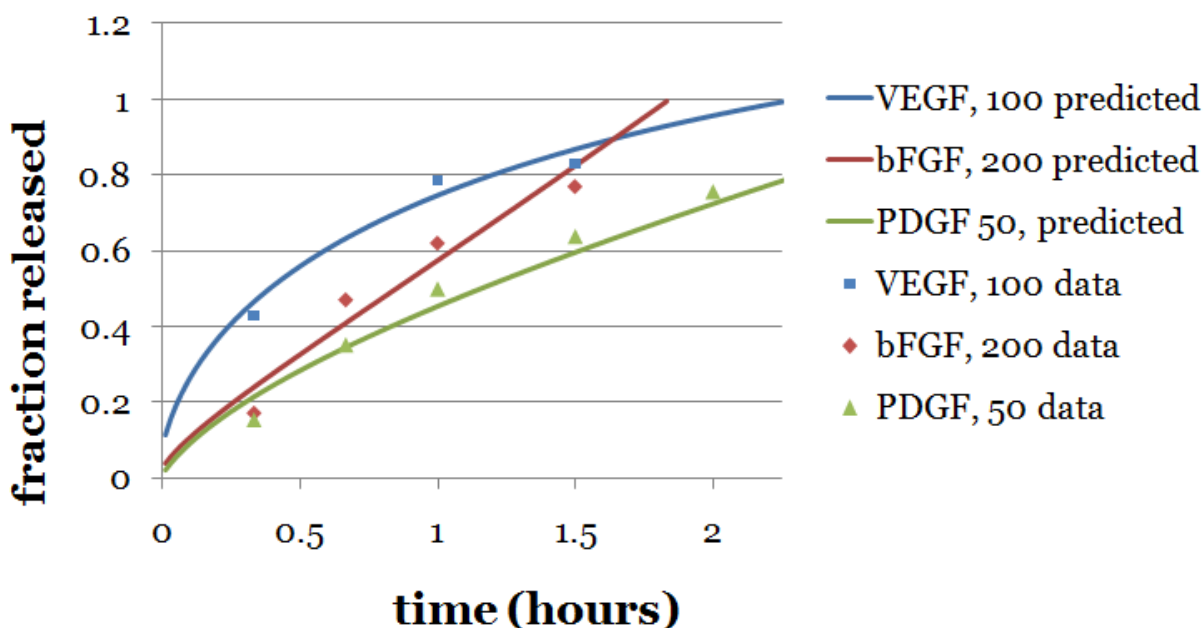


Figure 41. Model prediction and *in vitro* data for VEGF, bFGF and PDGF, release from Fiber III.

Fraction released versus time for VEGF, bFGF and PDGF, from cellulose hollow Fiber III (fabricated with water flowing at 8mL/min and cellulose at 1.5mL/min). Blue line represents model prediction for release of VEGF injected at 100µg/mL. Blue squares represent release data for release of VEGF injected at 100µg/mL. Red line represents model prediction for release of bFGF injected at 200 µg/mL. Red diamonds represent release data for release of bFGF injected at 200 µg/mL. Green line represents model prediction for release of PDGF injected at 50 µg/mL. Green triangles represent release data for release of PDGF injected at 50 µg/mL.

10.4.4 Model prediction for long term release

The advantage of this model is that release profiles can be predicted without carrying out a bench-top study. Injection concentration and volume can be readily changed, while the fiber wall geometry is a result of the hollow fiber fabrication process. Figure 34 - Figure 36 reveals that injection volume, macropore geometry and fiber wall thickness, all have an effect on the release profile of an example protein VEGF, with as little as a 10% change. In order for the model developed in this study to be used in a way that would allow for a greater impact on physiological processes, fibers with micropore and macropore geometry other than those represented in Table 2 would need to be developed. If a hollow fiber could be fabricated so that $j_1=0.75$, $W=0.01\text{cm}$, $\delta=0.008\text{cm}$ and $\varepsilon_{sp}=0.1$, and $100\mu\text{g/mL}$ of VEGF is injected, the model can predict release for varying injection volumes (0.01mL, 0.03mL and 0.05mL). Figure 39 represents model predictions for the aforementioned fiber parameters and injection characteristics, demonstrating that injection volume can play a large role in the release profile of VEGF. For instance, increasing the injection concentration by 0.02mL can increase the time before termination of release by approximately 50 hours, which is a physiologically relevant time frame.

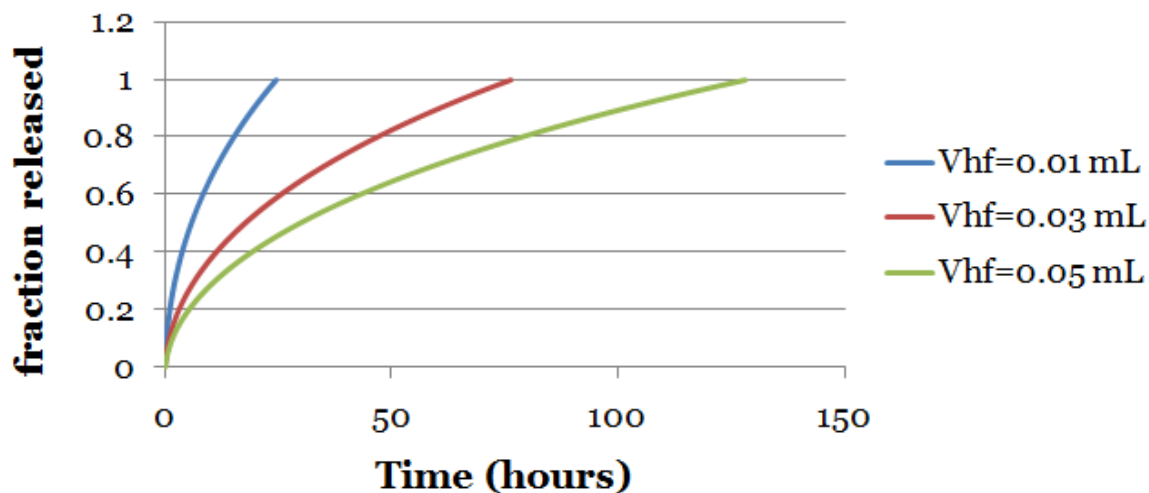


Figure 42. Long term release predictions for VEGF, with varying injection volume (V_{hf}).

10.5 DISCUSSION

Although traditionally used for filtration purposes, hollow fibers have recently emerged in the drug delivery field, where proteins involved in bone growth²⁶⁵, aneurysm healing²⁶⁶ and neovascularization²⁶⁴ have been delivered. Additionally, the need for fine control over growth factor delivery timing is becoming more important, as the scientific community learns more about the timing and sequence of growth factor involvement in biological processes.^{1, 189-192} The methods described in Sections 8.2.3 and 9.2.3 is intended to make steps toward analyzing release of angiogenesis promoting factors from cellulose hollow fibers.

An externally-regulated hollow fiber delivery model can aid in the development of future therapies where growth factor timing is important, as this method can test a variety of release

schedules without complex changes to the release formulation. The model described in this study is a step towards more accurate predictions of release from a porous hollow fiber, given the concentration and diffusivity of the injected protein in addition to hollow fiber geometry measurements. This information allows for the calculation of the effective diffusivity, osmotic pressure difference across the fiber wall and solvent flux, which all contribute to the transport of proteins from the lumen of the hollow fiber to the surrounding environment.

Through *in vitro* studies, it was determined that protein transport through a hollow fiber wall is not based on diffusion alone. Equation 7 predicts that diffusive mass transport flux alone would set the time required to reach complete release (0.01mL injection of 200 μ g/mL, fiber 8/1.5) on the order of weeks. For this reason, other likely means of mass transport of protein across the hollow fiber wall were explored. Although the charge and resulting isoelectric point can have an effect on the osmolality of a highly concentrated protein solution, it was discovered that the excipient with which the protein was lyophilized during the manufacturer's isolation process had the greatest effect on protein contribution to osmolality. For instance, an excipient with a low contribution to osmolality resulted in a small relationship between osmolality and concentration (ex: PDGF), and an excipient with a high contribution to osmolality resulted in a large relationship between osmolality and concentration (ex: bFGF). Specifically, PDGF was lyophilized with 40% (v/v) acetonitrile and 0.1% (v/v) trifluoroacetic acid, contributing slightly to the osmolality (Figure 33, blue diamonds). VEGF was lyophilized from PBS, contributing moderately to the osmolality (Figure 33, red squares). Basic FGF was lyophilized with 20mM Tris and 1000mM NaCl, contributing greatly to the osmolality (Figure 33, green triangles). The contribution that each of these excipients make to the osmolality of the solution injected into the hollow fiber results in the osmotic pressure difference between the lumen and surrounding

environment and consequent osmosis into the fiber. Osmotic-driven solvent flux plays a role in the inevitable hydrostatic pressure increase within the fiber and ultimate protein transport.

In Figure 38, it is observed that the predicted release rate (as well as measured *in vitro* release) of VEGF (blue) decreases after about an hour. Based on the model described in this study, this decrease is likely due to a decrease in osmotic pressure difference (due to protein release), causing a decrease in overall solvent flux out of the fiber. In contrast, the predicted release rate (as well as measured *in vitro* release) of bFGF (red) does not decrease in the time that it takes for all of the lumen contents to be released. In agreement with this data, our model predicts that the greater osmolality dependence on bFGF concentration (versus VEGF concentration) as well as the higher injection concentration does not predict a osmotic pressure drop great enough to slow down the release rate within the time it takes for all of the contents of the fiber to be released (Figure 38). Similarly, and in accordance with our experimental data, our model does not predict a noticeable decrease in the PDGF release rate over the time period observed *in vitro* (red) due to the relatively insignificant osmotic pressure dependence on PDGF concentration.

Fiber characteristics such as microporosity, macropore geometry and wall thickness, all factor into the rate of protein transport across the hollow fiber membrane wall. In terms of diffusion, it was found that the microporosity played the largest role in transport, where a linear relationship could be determined between the effective diffusivity coefficient and microporosity (Table 2). A linear relationship could not be determined for any other measured hollow fiber characteristic. In terms of solvent flux, macropore geometry and wall thickness, both of which play a role in osmotic and hydrostatic pressure based flow, were found to play a significant role in protein transport (Figure 35 and Figure 36). However, microporosity, which only plays a role

in osmotic pressure based flow, did not have a significant effect on release. In addition, there was also a correlation between the volume of injected protein solution and overall release during our experimental timeframes (Figure 34).

Although macropore geometry, injection volume and wall thickness, each have a greater affect than microporosity on the overall release, a greater change than predicted in those cases (less than the one hour, Section 10.4.3) would make a bigger impact on a physiologic process. For example, using the process of angiogenesis as an example, our prior studies (Chapter 8.0 and Chapter 9.0) suggest that delivery of an early stage factor would ideally be delivered for three days prior to a switch to delivery of a late stage factor for four days.²⁸¹ In order for changes in release to make an greater impact on a physiological process, a significant decrease in release rate would need to occur. As mentioned above, one way that this could occur would be to completely remove release due to convection by creating a high concentration protein solution with the same osmolality of saline (ex: a protein purified without excipients), where release based on diffusion can be on the order of weeks. Another way for this to occur would be to decrease the size of the macropores, thus increasing the overall area that is only microporous (j_1). Our model suggests that such a change would have a significant effect on release, due to the strong relationship between solvent flux (via the filtration coefficient) and macropore area. If solvent flux is reduced by a decrease in macropore size, a significant decrease in the rate of release is observed (as seen in Figure 39). This model can be used to determine the ideal fiber parameters and injection characteristics for the release of proteins according to a specific schedule.

Future work has the potential to improve the accuracy of this model. Currently, this model takes into consideration the protein diffusivity, injected concentration and many geometric

measurements of the hollow fiber. However, it does not take into consideration other factors such as protein/fiber interactions and exact determination of reflection and filtration coefficients. It is possible that the lacking of these details is why the model can only predict release trends (Figure 38, green) in some cases. For this specific example, the predicted time for complete release is underestimated by about 0.5 hours. The data presented here is also limited to the specific proteins and release conditions explored in this study. In order predict release of any protein under any release condition, it would be necessary to observe release under varying conditions and how these variations affect the transport of proteins across the hollow fiber wall. For example, because it would be extremely difficult to determine the exact concentration of these excipients in each solution, it would be necessary to isolate the protein completely from its excipients, through dialysis, before drawing any further conclusions of the transport of proteins across the hollow fiber membrane. Lastly, it would be necessary to explore hollow fiber fabrication techniques so that hollow fibers with smaller macropores can be fabricated.

10.6 CONCLUSION

A new model for predicted release from hollow fiber membranes has been developed. This model attributes transport from the lumen of the hollow fiber to the surrounding environment to not only diffusion but convection caused by solvent flux, as well. Using the equations described here, it is possible to predict release of VEGF, bFGF and PDGF, from a cellulose hollow fiber, after determination of specific characteristics of the hollow fiber. The conclusions drawn here are the result of the specific experiments performed in this study. Following further experimentation, the findings in this study support future use of this model as a design tool,

allowing researchers to rapidly acquire the hollow fiber design specifications necessary for a desired release profile.

11.0 SUMMARY AND CONCLUSIONS

Sequential delivery strategies hold tremendous potential in the fields of tissue engineering and regenerative medicine where stage-wise processes are ubiquitous. The hollow fiber-based delivery system described here can be used to explore the delivery of a wide variety of proteins as well as a wide variety of specific applications. In this specific example, sequential delivery of angiogenesis promoting factors was explored in a murine Matrigel plug model, where endothelial cell migration, vasculature integration and vessel maturation, were explored. When VEGF was delivered before S1P, we observed a statistically significant increase in both endothelial cell migration as well as vessel maturation, when compared to all other delivery schedules. We also observed the most integration between newly formed vasculature and existing vasculature when VEGF was delivered before S1P. When bFGF was delivered before PDGF, we also saw a statistically significant increase in both endothelial cell migration as well as vessel maturation, when compared to all other delivery schedules. When examining vessel integration, it was discovered that the delivery of PDGF may aid in the formation of tubule structures, but only when bFGF was delivered before PDGF did we consistently see integration between newly forming vasculature and existing vasculature.

In addition to investigating an *in vivo* response to sequentially delivered angiogenesis promoting factors, growth factor release from the hollow fiber membrane was explored. It was determined that transport from the lumen of the hollow fiber to the surrounding environment can

be described not only by diffusion but by osmosis-driven convection as well. Because the excipient used in the protein purification process increases the osmolality of a highly concentrated recombinant growth factor solution, an osmotic pressure difference exists between the lumen of the hollow fiber and the surrounding environment. This results in an influx of water into the fiber, decreasing lumen concentration while increasing the hydrostatic pressure of the fiber. Ultimately, the bulk solute flux out of the fiber due to solvent flow led to protein transport at a faster rate than diffusion alone.

A model accounting for both diffusion and convection of recombinant protein was developed, allowing not only for prediction of release from cellulose hollow fiber membranes, but design of alternative hollow fiber membranes that can achieve release for a longer period of time. This model can now be used as a tool for the development of fibers for delivery schedules for a broad range of applications. The hollow fiber system as a whole can be used to explore any number of delivery schedules, allowing for a facile way to explore different delivery schedules of growth factors *in vivo* for therapeutic responses as well as for studying the basic biological signals that accompany stage-wise regeneration of tissues.

12.0 FUTURE WORK

The work described here is a stepping stone toward the development of therapeutics in the medical field by demonstrating the importance of growth factor delivery timing. At the very least, the hollow fiber delivery system can be used to explore various delivery schedules in order to probe an ideal delivery regime for a specific application. This delivery schedule can then be applied to emerging temporal controlled release systems, such as the ones described in Chapter 7.0 (combined release systems, layer-by-layer films, microchips and tunable microparticles). One example of an additional physiological system in which sequential delivery of growth factors can advance medical treatment is bone healing and *de novo* bone formation.³²⁵⁻³²⁶ Bone morphogenetic protein-2 has been identified as playing an important role in the development of bone and cartilage and has even been approved by the Food and Drug Administration for the treatment of bone healing in combination with a collagen scaffold (Infuse®). However, PDGF has also been shown to play an important role in the early stages of bone healing, initiating both angiogenesis and proliferation of pre-osteoblasts at a wound site. Externally controlled hollow fiber drug delivery can be used to explore various delivery schedules in a bone healing model, such as the rabbit cranial defect model, where a critical size defect is created in the skull of a rabbit. In this model, due to the size of the defect and the area to which an individual hollow fiber can deliver proteins, it might be necessary to explore the use of multiple hollow fibers in series to achieve a clinically significant therapeutic outcome.

Externally controlled hollow fiber drug delivery can also be explored as a potential therapeutically relevant delivery system if hollow fibers with similar mechanical properties and pore geometry can be formed from triggerably degradable materials. For example, incorporation of n-isopropylacrylamide into the backbone of a biocompatible polymer can cause a polymer to be water soluble at cold temperatures, but insoluble in water at body temperature. Using this property, hollow fibers created from such a material can be used *in vivo* until the therapy is complete, at which point cold saline can be used to “wash away” the hollow fiber. Such could possibly leave only newly formed tissue and obviate the need to surgically remove the delivery system.

BIBLIOGRAPHY

1. Fischbach, C. and Mooney, D. J. Polymeric systems for bioinspired delivery of angiogenic molecules. *Polymers for Regenerative Medicine* **191**, 2006.
2. Calhoun, C. C., Cardenes, O., Ducksworth, J. and Le, A. D. Off-label use of becaplermin gel (recombinant platelet-derived growth factor-BB) for treatment of mucosal defects after corticocancellous bone graft: report of 2 cases with review of the literature. *J Oral Maxillofac Surg* **67**, 2516, 2009.
3. Langer, R. and Vacanti JP. Tissue engineering. *Science* **260**, 920, 1993.
4. Cronin KJ, Messina A, Knight KR, Cooper-White JJ, Stevens GW, Penington AJ and Morrison WA. New murine model of spontaneous autologous tissue engineering, combining an arteriovenous pedicle with matrix materials. *Plastic and Reconstructive Surgery* **113**, 260, 2004.
5. Kaihara S, Borenstein J, Koka R, Lalan S, Ochoa ER, Ravens M, Pien H, Cunningham B and Vacanti JP. Silicon micromachining to tissue engineer branched vascular channels for liver fabrication. *Tissue Engineering* **6**, 105, 2000.
6. Bates DO and Jones RO. The role of vascular endothelial growth factor in wound healing. *The International Journal of Lower Extremity Wounds* **2**, 107, 2003.
7. Krishnamoorthy, L., Morris, H. L. and Harding, K. G. A dynamic regulator: the role of growth factors in tissue repair. *J Wound Care* **10**, 99, 2001.
8. Przybylski, M. A review of the current research on the role of bFGF and VEGF in angiogenesis. *J Wound Care* **18**, 516, 2009.
9. Bouïs D, Kusumanto Y, Meijer C, Mulder NH and Hospers GA. A review on pro- and anti-angiogenic factors as targets of clinical intervention. *Pharmacol Res* **53**, 89, 2006.
10. Bauer SM, Bauer RJ and Velazquez OC. Angiogenesis, vasculogenesis, and induction of healing in chronic wounds. *Vascular and Endovascular Surgery* **39**, 293, 2005.

11. Singer, A. J. and Clark, R. A. Cutaneous wound healing. *N Engl J Med* **341**, 738, 1999.
12. Papanas, N. and Maltezos, E. Becaplermin gel in the treatment of diabetic neuropathic foot ulcers. *Clin Interv Aging* **3**, 233, 2008.
13. Gillitzer, R. and Goebeler, M. Chemokines in cutaneous wound healing. *J Leukoc Biol* **69**, 513, 2001.
14. Levenson, S. M., Geever, E. F., Crowley, L. V., Oates, J. F., 3rd, Berard, C. W. and Rosen, H. The Healing of Rat Skin Wounds. *Ann Surg* **161**, 293, 1965.
15. Yager, D. R., Kulina, R. A. and Gilman, L. A. Wound fluids: a window into the wound environment? *Int J Low Extrem Wounds* **6**, 262, 2007.
16. Mendicino M, Liu M, Ghanekar A, He W, Kosciak C, Shalev I, Javadi M, Turnbull J, Chen W, Fung L, Sakamoto S, Marsden P, Waddell TK, Phillips MJ, Gorczynski R, Levy GA and Grant D. Targeted deletion of Fgl-2/fibroleukin in the donor modulates immunologic response and acute vascular rejection in cardiac xenografts. *Circulation* **112**, 248, 2005.
17. Connolly, C. U.S. Combat Fatality Rate Lowest Ever. *Washington Post* 2004.
18. Vlahos, K. B. Soldiers' Lives Saved But Injuries Persist Long After Battle. *Foxnews.com* **2007**, 2006.
19. Doxey, D. L., Ng, M. C., Dill, R. E. and Iacopino, A. M. Platelet-derived growth factor levels in wounds of diabetic rats. *Life Sci* **57**, 1111, 1995.
20. Doxey, D. L., Nares, S., Park, B., Trieu, C., Cutler, C. W. and Iacopino, A. M. Diabetes-induced impairment of macrophage cytokine release in a rat model: potential role of serum lipids. *Life Sci* **63**, 1127, 1998.
21. Teixeira, A. S. and Andrade, S. P. Glucose-induced inhibition of angiogenesis in the rat sponge granuloma is prevented by aminoguanidine. *Life Sci* **64**, 655, 1999.
22. Cha, J. and Falanga, V. Stem cells in cutaneous wound healing. *Clin Dermatol* **25**, 73, 2007.
23. Stosich, M. S., Moioli, E. K., Wu, J. K., Lee, C. H., Rohde, C., Yoursef, A. M., Ascherman, J., Diraddo, R., Marion, N. W. and Mao, J. J. Bioengineering strategies to generate vascularized soft tissue grafts with sustained shape. *Methods* **47**, 116, 2009.
24. Yoshitomi, Y., Kojima, S., Umemoto, T., Kubo, K., Matsumoto, Y., Yano, M., Sugi, T. and Kuramochi, M. Serum hepatocyte growth factor in patients with peripheral arterial occlusive disease. *J Clin Endocrinol Metab* **84**, 2425, 1999.

25. Chen, F. M., Zhang, M. and Wu, Z. F. Toward delivery of multiple growth factors in tissue engineering. *Biomaterials* **31**, 6279, 2010.
26. Wu, S. C., Marston, W. and Armstrong, D. G. Wound care: the role of advanced wound healing technologies. *J Vasc Surg* **52**, 59S, 2010.
27. Veves, A., Sheehan, P. and Pham, H. T. A randomized, controlled trial of Promogran (a collagen/oxidized regenerated cellulose dressing) vs standard treatment in the management of diabetic foot ulcers. *Arch Surg* **137**, 822, 2002.
28. Veves, A., Falanga, V., Armstrong, D. G. and Sabolinski, M. L. Graftskin, a human skin equivalent, is effective in the management of noninfected neuropathic diabetic foot ulcers: a prospective randomized multicenter clinical trial. *Diabetes Care* **24**, 290, 2001.
29. Steed DL. Clinical evaluation of recombinant human platelet-derived growth factor for the treatment of lower extremity ulcers. *Plastic and Reconstructive Surgery* **117**, 143S, 2006.
30. Williams, D. To engineer is to create: the link between engineering and regeneration. *Trends Biotechnol* **24**, 4, 2006.
31. Morrison, W. A. Progress in tissue engineering of soft tissue and organs. *Surgery* **145**, 127, 2009.
32. Chrobak, K. M., Potter, D. R. and Tien, J. Formation of perfused, functional microvascular tubes in vitro. *Microvasc Res* **71**, 185, 2006.
33. Ko IK and Iwata H. An approach to constructing three-dimensional tissue. *Annals of the New York Academy of Sciences* **944**, 443, 2001.
34. Rivron, N. C., Liu, J. J., Rouwkema, J., de Boer, J. and van Blitterswijk, C. A. Engineering vascularised tissues in vitro. *Eur Cell Mater* **15**, 27, 2008.
35. Black, A. F., Hudon, V., Damour, O., Germain, L. and Auger, F. A. A novel approach for studying angiogenesis: a human skin equivalent with a capillary-like network. *Cell Biol Toxicol* **15**, 81, 1999.
36. Tremblay, P. L., Hudon, V., Berthod, F., Germain, L. and Auger, F. A. Inosculation of tissue-engineered capillaries with the host's vasculature in a reconstructed skin transplanted on mice. *Am J Transplant* **5**, 1002, 2005.
37. Rouwkema, J., de Boer, J. and Van Blitterswijk, C. A. Endothelial cells assemble into a 3-dimensional prevascular network in a bone tissue engineering construct. *Tissue Eng* **12**, 2685, 2006.

38. Koike, N., Fukumura, D., Gralla, O., Au, P., Schechner, J. S. and Jain, R. K. Tissue engineering: creation of long-lasting blood vessels. *Nature* **428**, 138, 2004.
39. Jain, R. K. Molecular regulation of vessel maturation. *Nat Med* **9**, 685, 2003.
40. Fidkowski, C., Kaazempur-Mofrad, M. R., Borenstein, J., Vacanti, J. P., Langer, R. and Wang, Y. Endothelialized microvasculature based on a biodegradable elastomer. *Tissue Eng* **11**, 302, 2005.
41. Stosich, M. S. and Mao, J. J. Adipose tissue engineering from human adult stem cells: clinical implications in plastic and reconstructive surgery. *Plast Reconstr Surg* **119**, 71, 2007.
42. Bauer SM, Bauer RJ, Liu ZJ, Chen H, Goldstein L and Velazquez OC. Vascular endothelial growth factor-C promotes vasculogenesis, angiogenesis, and collagen constriction in three-dimensional collagen gels. *J Vasc Surg* **41**, 699, 2005.
43. Kawanabe T, Kawakami T, Yatomi Y, Shimada S and Soma Y. Sphingosine 1-phosphate accelerates wound healing in diabetic mice. *J Dermatol Sci* **48**, 53, 2007.
44. Pandya NM, Dhalla NS and Santani DD. Angiogenesis--a new target for future therapy. *Vasc Pharmacol* **44**, 265, 2006.
45. Wu Y, Chen L, Scott PG and Tredget EE. Mesenchymal stem cells enhance wound healing through differentiation and angiogenesis. *Stem Cells* **25**, 2648, 2007.
46. Li, J., Zhang, Y. P. and Kirsner, R. S. Angiogenesis in wound repair: angiogenic growth factors and the extracellular matrix. *Microsc Res Tech* **60**, 107, 2003.
47. Abo-Auda, W. and Benza, R. L. Therapeutic angiogenesis: review of current concepts and future directions. *J Heart Lung Transplant* **22**, 370, 2003.
48. Scherer, S. S., Pietramaggiori, G., Matthews, J., Perry, S., Assmann, A., Carothers, A., Demcheva, M., Muise-Helmericks, R. C., Seth, A., Vournakis, J. N., Valeri, R. C., Fischer, T. H., Hechtman, H. B. and Orgill, D. P. Poly-N-acetyl glucosamine nanofibers: a new bioactive material to enhance diabetic wound healing by cell migration and angiogenesis. *Ann Surg* **250**, 322, 2009.
49. Polverini, P. J. Angiogenesis in health and disease: insights into basic mechanisms and therapeutic opportunities. *J Dent Educ* **66**, 962, 2002.
50. Greenblatt, M. and Shubi, P. Tumor angiogenesis: transfilter diffusion studies in the hamster by the transparent chamber technique. *J Natl Cancer Inst* **41**, 111, 1968.

51. Tonnesen, M. G., Feng, X. and Clark, R. A. Angiogenesis in wound healing. *J Investig Dermatol Symp Proc* **5**, 40, 2000.
52. Pettet, G., Chaplain, M. A., McElwain, D. L. and Byrne, H. M. On the role of angiogenesis in wound healing. *Proc Biol Sci* **263**, 1487, 1996.
53. Antonio, N., Fernandes, R., Rodriguez-Losada, N., Jimenez-Navarro, M. F., Paiva, A., de Teresa Galvan, E., Goncalves, L., Ribeiro, C. F. and Providencia, L. A. Stimulation of endothelial progenitor cells: a new putative effect of several cardiovascular drugs. *Eur J Clin Pharmacol* **66**, 219, 2010.
54. Critser, P. J. and Yoder, M. C. Endothelial colony-forming cell role in neoangiogenesis and tissue repair. *Curr Opin Organ Transplant* **15**, 68, 2010.
55. Kumar, A. H. and Caplice, N. M. Clinical potential of adult vascular progenitor cells. *Arterioscler Thromb Vasc Biol* **30**, 1080, 2010.
56. Asahara, T. Cell therapy and gene therapy using endothelial progenitor cells for vascular regeneration. *Handb Exp Pharmacol* 181, 2007.
57. Yamahara, K. and Itoh, H. Potential use of endothelial progenitor cells for regeneration of the vasculature. *Ther Adv Cardiovasc Dis* **3**, 17, 2009.
58. Mund, J. A., Ingram, D. A., Yoder, M. C. and Case, J. Endothelial progenitor cells and cardiovascular cell-based therapies. *Cytotherapy* **11**, 103, 2009.
59. Tateishi-Yuyama, E., Matsubara, H., Murohara, T., Ikeda, U., Shintani, S., Masaki, H., Amano, K., Kishimoto, Y., Yoshimoto, K., Akashi, H., Shimada, K., Iwasaka, T. and Imaizumi, T. Therapeutic angiogenesis for patients with limb ischaemia by autologous transplantation of bone-marrow cells: a pilot study and a randomised controlled trial. *Lancet* **360**, 427, 2002.
60. Tateno, K., Minamino, T., Toko, H., Akazawa, H., Shimizu, N., Takeda, S., Kunieda, T., Miyauchi, H., Oyama, T., Matsuura, K., Nishi, J., Kobayashi, Y., Nagai, T., Kuwabara, Y., Iwakura, Y., Nomura, F., Saito, Y. and Komuro, I. Critical roles of muscle-secreted angiogenic factors in therapeutic neovascularization. *Circ Res* **98**, 1194, 2006.
61. Kawamoto, A., Katayama, M., Handa, N., Kinoshita, M., Takano, H., Horii, M., Sadamoto, K., Yokoyama, A., Yamanaka, T., Onodera, R., Kuroda, A., Baba, R., Kaneko, Y., Tsukie, T., Kurimoto, Y., Okada, Y., Kihara, Y., Morioka, S., Fukushima, M. and Asahara, T. Intramuscular transplantation of G-CSF-mobilized CD34(+) cells in patients with critical limb ischemia: a phase I/IIa, multicenter, single-blinded, dose-escalation clinical trial. *Stem Cells* **27**, 2857, 2009.

62. Lenk, K., Adams, V., Lurz, P., Erbs, S., Linke, A., Gielen, S., Schmidt, A., Scheinert, D., Biamino, G., Emmrich, F., Schuler, G. and Hambrecht, R. Therapeutical potential of blood-derived progenitor cells in patients with peripheral arterial occlusive disease and critical limb ischaemia. *Eur Heart J* **26**, 1903, 2005.
63. Buschmann, I., Heil, M., Jost, M. and Schaper, W. Influence of inflammatory cytokines on arteriogenesis. *Microcirculation* **10**, 371, 2003.
64. Weiss, S., Zimmermann, G., Pufe, T., Varoga, D. and Henle, P. The systemic angiogenic response during bone healing. *Arch Orthop Trauma Surg* **129**, 989, 2009.
65. Raza, A., Franklin, M. J. and Dudek, A. Z. Pericytes and vessel maturation during tumor angiogenesis and metastasis. *Am J Hematol* **85**, 593, 2010.
66. O'Connor, D. S., Schechner, J. S., Adida, C., Mesri, M., Rothermel, A. L., Li, F., Nath, A. K., Pober, J. S. and Altieri, D. C. Control of apoptosis during angiogenesis by survivin expression in endothelial cells. *Am J Pathol* **156**, 393, 2000.
67. Richardson TP, Peters MC, Ennett AB and Mooney DJ. Polymeric system for dual growth factor delivery. *Nat Biotechnol* **19**, 1029, 2001.
68. Senger, D. R., Galli, S. J., Dvorak, A. M., Perruzzi, C. A., Harvey, V. S. and Dvorak, H. F. Tumor cells secrete a vascular permeability factor that promotes accumulation of ascites fluid. *Science* **219**, 983, 1983.
69. Ferrara, N. and Alitalo, K. Clinical applications of angiogenic growth factors and their inhibitors. *Nat Med* **5**, 1359, 1999.
70. Ferrara, N., Carver-Moore, K., Chen, H., Dowd, M., Lu, L., O'Shea, K. S., Powell-Braxton, L., Hillan, K. J. and Moore, M. W. Heterozygous embryonic lethality induced by targeted inactivation of the VEGF gene. *Nature* **380**, 439, 1996.
71. De Marchis F, Ribatti D, Giampietri C, Lentini A, Faraone D, Scoccianti M, Capogrossi MC and Facchiano A. Platelet-derived growth factor inhibits basic fibroblast growth factor angiogenic properties in vitro and in vivo through its alpha receptor. *Blood* **99**, 2045, 2002.
72. Unger EF, Banai S, Shou M, Lazarous DF, Jaklitsch MT, Scheinowitz M, Correa R, Klingbeil C and Epstein SE. Basic fibroblast growth factor enhances myocardial collateral flow in a canine model.

Am J Physiol **266**, H1588, 1994.

73. Nakajima H, Sakakibara Y, Tambara K, Iwakura A, Doi K, Marui A, Ueyama K, Ikeda T, Tabata Y and Komeda M. Therapeutic angiogenesis by the controlled release of basic fibroblast growth factor for ischemic limb and heart injury: toward safety and minimal invasiveness. *J Artif Organs* **7**, 58, 2004.
74. Wacker BK, Scott EA, Kaneda MM, Alford SK and Elbert DL. Delivery of sphingosine 1-phosphate from poly(ethylene glycol) hydrogels. *Biomacromolecules* **7**, 1335, 2006.
75. Cao, R., Brakenhielm, E., Pawliuk, R., Wariaro, D., Post, M. J., Wahlberg, E., Leboulch, P. and Cao, Y. Angiogenic synergism, vascular stability and improvement of hind-limb ischemia by a combination of PDGF-BB and FGF-2. *Nat Med* **9**, 604, 2003.
76. Magnusson PU, Looman C, Ahgren A, Wu Y, Claesson-Welsh L and Heuchel RL. Platelet-Derived Growth Factor Receptor- β Constitutive Activity Promotes Angiogenesis In Vivo and In Vitro. *Arterioscler Thromb Vasc Biol* **27**, 2142, 2007.
77. Rosen, H. and Goetzl, E. J. Sphingosine 1-phosphate and its receptors: an autocrine and paracrine network. *Nat Rev Immunol* **5**, 560, 2005.
78. Lee OH, Kim YM, Lee YM, Moon EJ, Lee DJ, Kim JH, Kim KW and Kwon YG. Sphingosine 1-phosphate induces angiogenesis: its angiogenic action and signaling mechanism in human umbilical vein endothelial cells. *Biochem Biophys Res Commun* **264**, 743, 1999.
79. Le Stunff, H., Milstien, S. and Spiegel, S. Generation and metabolism of bioactive sphingosine-1-phosphate. *J Cell Biochem* **92**, 882, 2004.
80. Fourcade, O., Simon, M. F., Viode, C., Rugani, N., Leballe, F., Ragab, A., Fournie, B., Sarda, L. and Chap, H. Secretory phospholipase A2 generates the novel lipid mediator lysophosphatidic acid in membrane microvesicles shed from activated cells. *Cell* **80**, 919, 1995.
81. Takuwa, Y. Subtype-specific differential regulation of Rho family G proteins and cell migration by the Edg family sphingosine-1-phosphate receptors. *Biochim Biophys Acta* **1582**, 112, 2002.
82. Kluk, M. J. and Hla, T. Signaling of sphingosine-1-phosphate via the S1P/EDG-family of G-protein-coupled receptors. *Biochim Biophys Acta* **1582**, 72, 2002.
83. Lee, M. J., Thangada, S., Claffey, K. P., Ancellin, N., Liu, C. H., Kluk, M., Volpi, M., Sha'afi, R. I. and Hla, T. Vascular endothelial cell adherens junction assembly and morphogenesis induced by sphingosine-1-phosphate. *Cell* **99**, 301, 1999.

84. Kimura, T., Watanabe, T., Sato, K., Kon, J., Tomura, H., Tamama, K., Kuwabara, A., Kanda, T., Kobayashi, I., Ohta, H., Ui, M. and Okajima, F. Sphingosine 1-phosphate stimulates proliferation and migration of human endothelial cells possibly through the lipid receptors, Edg-1 and Edg-3. *Biochemical Journal* **348 Pt 1**, 71, 2000.
85. Lucke, S. and Levkau, B. Endothelial functions of sphingosine-1-phosphate. *Cell Physiol Biochem* **26**, 87, 2010.
86. Hla, T. Physiological and pathological actions of sphingosine 1-phosphate. *Semin Cell Dev Biol* **15**, 513, 2004.
87. Rosen, H., Gonzalez-Cabrera, P. J., Sanna, M. G. and Brown, S. Sphingosine 1-phosphate receptor signaling. *Annu Rev Biochem* **78**, 743, 2009.
88. Hla, T., Lee, M. J., Ancellin, N., Paik, J. H. and Kluk, M. J. Lysophospholipids--receptor revelations. *Science* **294**, 1875, 2001.
89. Brunham, L. R., Kruit, J. K., Iqbal, J., Fievet, C., Timmins, J. M., Pape, T. D., Coburn, B. A., Bissada, N., Staels, B., Groen, A. K., Hussain, M. M., Parks, J. S., Kuipers, F. and Hayden, M. R. Intestinal ABCA1 directly contributes to HDL biogenesis in vivo. *J Clin Invest* **116**, 1052, 2006.
90. Parini, P., Johansson, L., Broijersen, A., Angelin, B. and Rudling, M. Lipoprotein profiles in plasma and interstitial fluid analyzed with an automated gel-filtration system. *Eur J Clin Invest* **36**, 98, 2006.
91. Sloop, C. H., Dory, L. and Roheim, P. S. Interstitial fluid lipoproteins. *J Lipid Res* **28**, 225, 1987.
92. Liu, Y., Wada, R., Yamashita, T., Mi, Y., Deng, C. X., Hobson, J. P., Rosenfeldt, H. M., Nava, V. E., Chae, S. S., Lee, M. J., Liu, C. H., Hla, T., Spiegel, S. and Proia, R. L. Edg-1, the G protein-coupled receptor for sphingosine-1-phosphate, is essential for vascular maturation. *J Clin Invest* **106**, 951, 2000.
93. Allende, M. L. and Proia, R. L. Sphingosine-1-phosphate receptors and the development of the vascular system. *Biochim Biophys Acta* **1582**, 222, 2002.
94. Theilmeyer, G., Schmidt, C., Herrmann, J., Keul, P., Schafers, M., Herrgott, I., Mersmann, J., Larmann, J., Hermann, S., Stypmann, J., Schober, O., Hildebrand, R., Schulz, R., Heusch, G., Haude, M., von Wnuck Lipinski, K., Herzog, C., Schmitz, M., Erbel, R., Chun, J. and Levkau, B. High-density lipoproteins and their constituent, sphingosine-1-phosphate, directly protect the heart against ischemia/reperfusion injury in vivo via the S1P3 lysophospholipid receptor. *Circulation* **114**, 1403, 2006.

95. Li, W. W. Tumor angiogenesis: molecular pathology, therapeutic targeting, and imaging. *Acad Radiol* **7**, 800, 2000.
96. Hanahan, D. and Folkman, J. Patterns and emerging mechanisms of the angiogenic switch during tumorigenesis. *Cell* **86**, 353, 1996.
97. Chen, F. M. and Jin, Y. Periodontal tissue engineering and regeneration: current approaches and expanding opportunities. *Tissue Eng Part B Rev* **16**, 219, 2010.
98. Lee, K., Silva, E. A. and Mooney, D. J. Growth factor delivery-based tissue engineering: general approaches and a review of recent developments. *J R Soc Interface* 2010.
99. Andreadis, S. T. and Geer, D. J. Biomimetic approaches to protein and gene delivery for tissue regeneration. *Trends in Biotechnology* **24**, 331, 2006.
100. Barrientos, S., Stojadinovic, O., Golinko, M. S., Brem, H. and Tomic-Canic, M. Growth factors and cytokines in wound healing. *Wound Repair Regen* **16**, 585, 2008.
101. Tayalia, P. and Mooney, D. J. Controlled Growth Factor Delivery for Tissue Engineering. *Advanced Materials* **21**, 3269, 2009.
102. Hendel RC, Henry TD, Rocha-Singh K, Isner JM, Kereiakes DJ, Giordano FJ, Simons M and Bonow RO. Effect of intracoronary recombinant human vascular endothelial growth factor on myocardial perfusion: evidence for a dose-dependent effect. *Circulation* **101**, 118, 2000.
103. Yancopoulos GD, Davis S, Gale NW, Rudge JS, Wiegand SJ and Holash J. Vascular-specific growth factors and blood vessel formation. *Nature* **407**, 242, 2000.
104. Simons M, Bonow RO, Chronos NA, Cohen DJ, Giordano FJ, Hammond HK, Laham RJ, Li W, Pike M, Sellke FW, Stegmann TJ, Udelson JE and Rosengart TK. Clinical trials in coronary angiogenesis: issues, problems, consensus: An expert panel summary. *Circulation* **102**, E73, 2000.
105. Schweigerer, L., Neufeld, G., Friedman, J., Abraham, J. A., Fiddes, J. C. and Gospodarowicz, D. Basic fibroblast growth factor: production and growth stimulation in cultured adrenal cortex cells. *Endocrinology* **120**, 796, 1987.
106. Tabata Y, Miyao M, Ozeki M and Y., I. Controlled release of vascular endothelial growth factor by use of collagen hydrogels. *Journal of Biomaterials Science. Polymer edition* **11**, 915, 2000.

107. Hammond, H. K. and McKirnan, M. D. Angiogenic gene therapy for heart disease: a review of animal studies and clinical trials. *Cardiovasc Res* **49**, 561, 2001.
108. Laham, R. J., Simons, M. and Sellke, F. Gene transfer for angiogenesis in coronary artery disease. *Annu Rev Med* **52**, 485, 2001.
109. Baumgartner, I., Pieczek, A., Manor, O., Blair, R., Kearney, M., Walsh, K. and Isner, J. M. Constitutive expression of phVEGF165 after intramuscular gene transfer promotes collateral vessel development in patients with critical limb ischemia. *Circulation* **97**, 1114, 1998.
110. Lederman, R. J., Tenaglia, A. N., Anderson, R. D., Hermiller, J. B., Rocha-Singh, K., Mendelsohn, F. O., Hiatt, W. R., Moon, T., Whitehouse, M. J. and Annex, B. H. Design of the therapeutic angiogenesis with recombinant fibroblast growth factor-2 for intermittent claudication (TRAFFIC) trial. *Am J Cardiol* **88**, 192, 2001.
111. Robson, M. C., Phillips, T. J., Falanga, V., Odenheimer, D. J., Parish, L. C., Jensen, J. L. and Steed, D. L. Randomized trial of topically applied repifermin (recombinant human keratinocyte growth factor-2) to accelerate wound healing in venous ulcers. *Wound Repair Regen* **9**, 347, 2001.
112. Pierce, G. F., Tarpley, J. E., Allman, R. M., Goode, P. S., Serdar, C. M., Morris, B., Mustoe, T. A. and Vande Berg, J. Tissue repair processes in healing chronic pressure ulcers treated with recombinant platelet-derived growth factor BB. *Am J Pathol* **145**, 1399, 1994.
113. Mitragotri, S. and Lahann, J. Physical approaches to biomaterial design. *Nat Mater* **8**, 15, 2009.
114. Fischbach, C. and Mooney, D. J. Polymers for pro- and anti-angiogenic therapy. *Biomaterials* **28**, 2069, 2007.
115. Boonthekul, T., Hill, E. E., Kong, H. J. and Mooney, D. J. Regulating myoblast phenotype through controlled gel stiffness and degradation. *Tissue Eng* **13**, 1431, 2007.
116. Datta, N., Pham, Q. P., Sharma, U., Sikavitsas, V. I., Jansen, J. A. and Mikos, A. G. In vitro generated extracellular matrix and fluid shear stress synergistically enhance 3D osteoblastic differentiation. *Proc Natl Acad Sci U S A* **103**, 2488, 2006.
117. Krenning, G., van Luyn, M. J. and Harmsen, M. C. Endothelial progenitor cell-based neovascularization: implications for therapy. *Trends Mol Med* **15**, 180, 2009.
118. Cho, S. W., Moon, S. H., Lee, S. H., Kang, S. W., Kim, J., Lim, J. M., Kim, H. S., Kim, B. S. and Chung, H. M. Improvement of postnatal neovascularization by human embryonic

stem cell derived endothelial-like cell transplantation in a mouse model of hindlimb ischemia. *Circulation* **116**, 2409, 2007.

119. Kong, D., Melo, L. G., Gnecci, M., Zhang, L., Mostoslavsky, G., Liew, C. C., Pratt, R. E. and Dzau, V. J. Cytokine-induced mobilization of circulating endothelial progenitor cells enhances repair of injured arteries. *Circulation* **110**, 2039, 2004.
120. Sheikh, A. Y., Lin, S. A., Cao, F., Cao, Y., van der Bogt, K. E., Chu, P., Chang, C. P., Contag, C. H., Robbins, R. C. and Wu, J. C. Molecular imaging of bone marrow mononuclear cell homing and engraftment in ischemic myocardium. *Stem Cells* **25**, 2677, 2007.
121. Li, Z., Wu, J. C., Sheikh, A. Y., Kraft, D., Cao, F., Xie, X., Patel, M., Gambhir, S. S., Robbins, R. C. and Cooke, J. P. Differentiation, survival, and function of embryonic stem cell derived endothelial cells for ischemic heart disease. *Circulation* **116**, I46, 2007.
122. Pittenger, M. F. and Martin, B. J. Mesenchymal stem cells and their potential as cardiac therapeutics. *Circ Res* **95**, 9, 2004.
123. Silva, E. A., Kim, E. S., Kong, H. J. and Mooney, D. J. Material-based deployment enhances efficacy of endothelial progenitor cells. *Proc Natl Acad Sci U S A* **105**, 14347, 2008.
124. Tang, Z. C., Liao, W. Y., Tang, A. C., Tsai, S. J. and Hsieh, P. C. The enhancement of endothelial cell therapy for angiogenesis in hindlimb ischemia using hyaluronan. *Biomaterials* 2010.
125. Callegari, A., Bollini, S., Iop, L., Chiavegato, A., Torregrossa, G., Pozzobon, M., Gerosa, G., De Coppi, P., Elvassore, N. and Sartore, S. Neovascularization induced by porous collagen scaffold implanted on intact and cryoinjured rat hearts. *Biomaterials* **28**, 5449, 2007.
126. Lei, P., Padmashali, R. M. and Andreadis, S. T. Cell-controlled and spatially arrayed gene delivery from fibrin hydrogels. *Biomaterials* **30**, 3790, 2009.
127. Landa, N., Miller, L., Feinberg, M. S., Holbova, R., Shachar, M., Freeman, I., Cohen, S. and Leor, J. Effect of injectable alginate implant on cardiac remodeling and function after recent and old infarcts in rat. *Circulation* **117**, 1388, 2008.
128. Kimura, Y. and Tabata, Y. Controlled release of stromal-cell-derived factor-1 from gelatin hydrogels enhances angiogenesis. *J Biomater Sci Polym Ed* **21**, 37, 2010.

129. Brunner, G., Nguyen, H., Gabrilove, J., Rifkin, D. B. and Wilson, E. L. Basic fibroblast growth factor expression in human bone marrow and peripheral blood cells. *Blood* **81**, 631, 1993.
130. Hamano, K., Li, T. S., Kobayashi, T., Kobayashi, S., Matsuzaki, M. and Esato, K. Angiogenesis induced by the implantation of self-bone marrow cells: a new material for therapeutic angiogenesis. *Cell Transplant* **9**, 439, 2000.
131. Noishiki, Y., Tomizawa, Y., Yamane, Y. and Matsumoto, A. Autocrine angiogenic vascular prosthesis with bone marrow transplantation. *Nat Med* **2**, 90, 1996.
132. Kamihata, H., Matsubara, H., Nishiue, T., Fujiyama, S., Tsutsumi, Y., Ozono, R., Masaki, H., Mori, Y., Iba, O., Tateishi, E., Kosaki, A., Shintani, S., Murohara, T., Imaizumi, T. and Iwasaka, T. Implantation of bone marrow mononuclear cells into ischemic myocardium enhances collateral perfusion and regional function via side supply of angioblasts, angiogenic ligands, and cytokines. *Circulation* **104**, 1046, 2001.
133. Bel, A., Planat-Bernard, V., Saito, A., Bonnevie, L., Bellamy, V., Sabbah, L., Bellabas, L., Brinon, B., Vanneaux, V., Pradeau, P., Peyrard, S., Larghero, J., Pouly, J., Binder, P., Garcia, S., Shimizu, T., Sawa, Y., Okano, T., Bruneval, P., Desnos, M., Hagege, A. A., Casteilla, L., Puceat, M. and Menasche, P. Composite cell sheets: a further step toward safe and effective myocardial regeneration by cardiac progenitors derived from embryonic stem cells. *Circulation* **122**, S118, 2010.
134. Amann, B., Luedemann, C., Ratei, R. and Schmidt-Lucke, J. A. Autologous bone marrow cell transplantation increases leg perfusion and reduces amputations in patients with advanced critical limb ischemia due to peripheral artery disease. *Cell Transplant* **18**, 371, 2009.
135. Franz, R. W., Parks, A., Shah, K. J., Hankins, T., Hartman, J. F. and Wright, M. L. Use of autologous bone marrow mononuclear cell implantation therapy as a limb salvage procedure in patients with severe peripheral arterial disease. *J Vasc Surg* **50**, 1378, 2009.
136. Lara-Hernandez, R., Lozano-Vilardell, P., Blanes, P., Torreguitart-Mirada, N., Galmes, A. and Besalduch, J. Safety and efficacy of therapeutic angiogenesis as a novel treatment in patients with critical limb ischemia. *Ann Vasc Surg* **24**, 287, 2010.
137. Ozawa, C. R., Banfi, A., Glazer, N. L., Thurston, G., Springer, M. L., Kraft, P. E., McDonald, D. M. and Blau, H. M. Microenvironmental VEGF concentration, not total dose, determines a threshold between normal and aberrant angiogenesis. *J Clin Invest* **113**, 516, 2004.
138. Segers, V. F. and Lee, R. T. Stem-cell therapy for cardiac disease. *Nature* **451**, 937, 2008.

139. Peattie RA, Nayate AP, Firpo MA, Shelby J, Fisher RJ and Prestwich GD. Stimulation of in vivo angiogenesis by cytokine-loaded hyaluronic acid hydrogel implants. *Biomaterials* **25**, 2789, 2004.
140. Simmons CA, Alsberg E, Hsiong S, Kim WJ and Mooney DJ. Dual growth factor delivery and controlled scaffold degradation enhance in vivo bone formation by transplanted bone marrow stromal cells. *Bone* **35**, 562, 2004.
141. Li, S. H., Cai, S. X., Liu, B., Ma, K. W., Wang, Z. P. and Li, X. K. In vitro characteristics of poly(lactic-co-glycolic acid) microspheres incorporating gelatin particles loading basic fibroblast growth factor. *Acta Pharmacol Sin* **27**, 754, 2006.
142. Eppler, S. M., Combs, D. L., Henry, T. D., Lopez, J. J., Ellis, S. G., Yi, J. H., Annex, B. H., McCluskey, E. R. and Zioncheck, T. F. A target-mediated model to describe the pharmacokinetics and hemodynamic effects of recombinant human vascular endothelial growth factor in humans. *Clin Pharmacol Ther* **72**, 20, 2002.
143. Silva, E. A. and Mooney, D. J. Spatiotemporal control of vascular endothelial growth factor delivery from injectable hydrogels enhances angiogenesis. *J Thromb Haemost* **5**, 590, 2007.
144. Sun, Q., Chen, R. R., Shen, Y., Mooney, D. J., Rajagopalan, S. and Grossman, P. M. Sustained vascular endothelial growth factor delivery enhances angiogenesis and perfusion in ischemic hind limb. *Pharm Res* **22**, 1110, 2005.
145. Sellke, F. W., Tofukuji, M., Laham, R. J., Li, J., Hariawala, M. D., Bunting, S. and Simons, M. Comparison of VEGF delivery techniques on collateral-dependent microvascular reactivity. *Microvasc Res* **55**, 175, 1998.
146. Lopez, J. J., Laham, R. J., Carrozza, J. P., Tofukuji, M., Sellke, F. W., Bunting, S. and Simons, M. Hemodynamic effects of intracoronary VEGF delivery: evidence of tachyphylaxis and NO dependence of response. *Am J Physiol* **273**, H1317, 1997.
147. Takeshita, S., Zheng, L. P., Brogi, E., Kearney, M., Pu, L. Q., Bunting, S., Ferrara, N., Symes, J. F. and Isner, J. M. Therapeutic angiogenesis. A single intraarterial bolus of vascular endothelial growth factor augments revascularization in a rabbit ischemic hind limb model. *J Clin Invest* **93**, 662, 1994.
148. Henry, T. D., Rocha-Singh, K., Isner, J. M., Kereiakes, D. J., Giordano, F. J., Simons, M., Losordo, D. W., Hendel, R. C., Bonow, R. O., Eppler, S. M., Zioncheck, T. F., Holmgren, E. B. and McCluskey, E. R. Intracoronary administration of recombinant human vascular endothelial growth factor to patients with coronary artery disease. *Am Heart J* **142**, 872, 2001.

149. Henry, T. D., Annex, B. H., McKendall, G. R., Azrin, M. A., Lopez, J. J., Giordano, F. J., Shah, P. K., Willerson, J. T., Benza, R. L., Berman, D. S., Gibson, C. M., Bajamonde, A., Rundle, A. C., Fine, J. and McCluskey, E. R. The VIVA trial: Vascular endothelial growth factor in Ischemia for Vascular Angiogenesis. *Circulation* **107**, 1359, 2003.
150. Langer, R. Controlled release of a therapeutic protein. *Nat Med* **2**, 742, 1996.
151. Fu, K., Klivanov, A. M. and Langer, R. Protein stability in controlled-release systems. *Nat Biotechnol* **18**, 24, 2000.
152. Sheridan, M. H., Shea, L. D., Peters, M. C. and Mooney, D. J. Bioabsorbable polymer scaffolds for tissue engineering capable of sustained growth factor delivery. *J Control Release* **64**, 91, 2000.
153. Arras, M., Mollnau, H., Strasser, R., Wenz, R., Ito, W. D., Schaper, J. and Schaper, W. The delivery of angiogenic factors to the heart by microsphere therapy. *Nat Biotechnol* **16**, 159, 1998.
154. Chung, H. J., Kim, H. K., Yoon, J. J. and Park, T. G. Heparin immobilized porous PLGA microspheres for angiogenic growth factor delivery. *Pharm Res* **23**, 1835, 2006.
155. Cleland, J. L., Duenas, E. T., Park, A., Daugherty, A., Kahn, J., Kowalski, J. and Cuthbertson, A. Development of poly-(D,L-lactide-coglycolide) microsphere formulations containing recombinant human vascular endothelial growth factor to promote local angiogenesis. *Journal of Controlled Release* **72**, 13, 2001.
156. Golub, J. S., Kim, Y. T., Duvall, C. L., Bellamkonda, R. V., Gupta, D., Lin, A. S., Weiss, D., Robert Taylor, W. and Guldberg, R. E. Sustained VEGF delivery via PLGA nanoparticles promotes vascular growth. *Am J Physiol Heart Circ Physiol* **298**, H1959, 2010.
157. Layman H, Spiga MG, Brooks T, Pham S, Webster KA and Andreopoulos FM. The effect of the controlled release of basic fibroblast growth factor from ionic gelatin-based hydrogels on angiogenesis in a murine critical limb ischemic model. *Biomaterials* **28**, 2646, 2007.
158. Losi, P., Briganti, E., Magera, A., Spiller, D., Ristori, C., Battolla, B., Balderi, M., Kull, S., Balbarini, A., Di Stefano, R. and Soldani, G. Tissue response to poly(ether)urethane-polydimethylsiloxane-fibrin composite scaffolds for controlled delivery of pro-angiogenic growth factors. *Biomaterials* **31**, 5336, 2010.
159. Lee, K. Y. and Mooney, D. J. Hydrogels for tissue engineering. *Chem Rev* **101**, 1869, 2001.

160. Lee, K. Y., Peters, M. C., Anderson, K. W. and Mooney, D. J. Controlled growth factor release from synthetic extracellular matrices. *Nature* **408**, 998, 2000.
161. Peters, M. C., Isenberg, B. C., Rowley, J. A. and Mooney, D. J. Release from alginate enhances the biological activity of vascular endothelial growth factor. *J Biomater Sci Polym Ed* **9**, 1267, 1998.
162. Fujita, M., Ishihara, M., Morimoto, Y., Simizu, M., Saito, Y., Yura, H., Matsui, T., Takase, B., Hattori, H., Kanatani, Y., Kikuchi, M. and Maehara, T. Efficacy of photocrosslinkable chitosan hydrogel containing fibroblast growth factor-2 in a rabbit model of chronic myocardial infarction. *J Surg Res* **126**, 27, 2005.
163. Iwakura, A., Fujita, M., Kataoka, K., Tambara, K., Sakakibara, Y., Komeda, M. and Tabata, Y. Intramyocardial sustained delivery of basic fibroblast growth factor improves angiogenesis and ventricular function in a rat infarct model. *Heart Vessels* **18**, 93, 2003.
164. Liu, Y., Sun, L., Huan, Y., Zhao, H. and Deng, J. Effects of basic fibroblast growth factor microspheres on angiogenesis in ischemic myocardium and cardiac function: analysis with dobutamine cardiovascular magnetic resonance tagging. *Eur J Cardiothorac Surg* **30**, 103, 2006.
165. Bao, P., Kodra, A., Tomic-Canic, M., Golinko, M. S., Ehrlich, H. P. and Brem, H. The role of vascular endothelial growth factor in wound healing. *J Surg Res* **153**, 347, 2009.
166. Seo, M. S., Kwak, N., Ozaki, H., Yamada, H., Okamoto, N., Yamada, E., Fabbro, D., Hofmann, F., Wood, J. M. and Campochiaro, P. A. Dramatic inhibition of retinal and choroidal neovascularization by oral administration of a kinase inhibitor. *Am J Pathol* **154**, 1743, 1999.
167. Carpizo, D. and Iruela-Arispe, M. L. Endogenous regulators of angiogenesis--emphasis on proteins with thrombospondin--type I motifs. *Cancer Metastasis Rev* **19**, 159, 2000.
168. Kondo, S., Kubota, S., Shimo, T., Nishida, T., Yosimichi, G., Eguchi, T., Sugahara, T. and Takigawa, M. Connective tissue growth factor increased by hypoxia may initiate angiogenesis in collaboration with matrix metalloproteinases. *Carcinogenesis* **23**, 769, 2002.
169. Hashiya, N., Jo, N., Aoki, M., Matsumoto, K., Nakamura, T., Sato, Y., Ogata, N., Ogihara, T., Kaneda, Y. and Morishita, R. In vivo evidence of angiogenesis induced by transcription factor Ets-1: Ets-1 is located upstream of angiogenesis cascade. *Circulation* **109**, 3035, 2004.

170. Milkiewicz, M., Ispanovic, E., Doyle, J. L. and Haas, T. L. Regulators of angiogenesis and strategies for their therapeutic manipulation. *Int J Biochem Cell Biol* **38**, 333, 2006.
171. Brown, N. J., Smyth, E. A., Cross, S. S. and Reed, M. W. Angiogenesis induction and regression in human surgical wounds. *Wound Repair Regen* **10**, 245, 2002.
172. Kumar, I., Staton, C. A., Cross, S. S., Reed, M. W. and Brown, N. J. Angiogenesis, vascular endothelial growth factor and its receptors in human surgical wounds. *Br J Surg* **96**, 1484, 2009.
173. Brown, L. F., Yeo, K. T., Berse, B., Yeo, T. K., Senger, D. R., Dvorak, H. F. and van de Water, L. Expression of vascular permeability factor (vascular endothelial growth factor) by epidermal keratinocytes during wound healing. *J Exp Med* **176**, 1375, 1992.
174. Vlodavsky, I., Fuks, Z., Ishai-Michaeli, R., Bashkin, P., Levi, E., Korner, G., Bar-Shavit, R. and Klagsbrun, M. Extracellular matrix-resident basic fibroblast growth factor: implication for the control of angiogenesis. *J Cell Biochem* **45**, 167, 1991.
175. Di Vita, G., Patti, R., D'Agostino, P., Caruso, G., Arcara, M., Buscemi, S., Bonventre, S., Ferlazzo, V., Arcoleo, F. and Cillari, E. Cytokines and growth factors in wound drainage fluid from patients undergoing incisional hernia repair. *Wound Repair Regen* **14**, 259, 2006.
176. Tsopanoglou, N. E. and Maragoudakis, M. E. On the mechanism of thrombin-induced angiogenesis. Potentiation of vascular endothelial growth factor activity on endothelial cells by up-regulation of its receptors. *J Biol Chem* **274**, 23969, 1999.
177. Hirschi, K. K., Rohovsky, S. A., Beck, L. H., Smith, S. R. and D'Amore, P. A. Endothelial cells modulate the proliferation of mural cell precursors via platelet-derived growth factor-BB and heterotypic cell contact. *Circ Res* **84**, 298, 1999.
178. Darland, D. C. and D'Amore, P. A. Blood vessel maturation: vascular development comes of age. *J Clin Invest* **103**, 157, 1999.
179. Lindahl, P., Johansson, B. R., Leveen, P. and Betsholtz, C. Pericyte loss and microaneurysm formation in PDGF-B-deficient mice. *Science* **277**, 242, 1997.
180. Shoab, S. S., Scurr, J. H. and Coleridge-Smith, P. D. Plasma VEGF as a marker of therapy in patients with chronic venous disease treated with oral micronised flavonoid fraction - a pilot study. *Eur J Vasc Endovasc Surg* **18**, 334, 1999.

181. Antonelli-Orlidge, A., Saunders, K. B., Smith, S. R. and D'Amore, P. A. An activated form of transforming growth factor beta is produced by cocultures of endothelial cells and pericytes. *Proc Natl Acad Sci U S A* **86**, 4544, 1989.
182. Wendler CC and Rivkees SA. Sphingosine-1-phosphate inhibits cell migration and endothelial to mesenchymal cell transformation during cardiac development. *Dev Biol* **291**, 264, 2006.
183. Igarashi J, Erwin PA, Dantas AP, Chen H and Michel T. VEGF induces S1P1 receptors in endothelial cells: Implications for cross-talk between sphingolipid and growth factor receptors. *Proc Natl Acad Sci U S A* **100**, 10664, 2003.
184. Grakoui, A., Bromley, S. K., Sumen, C., Davis, M. M., Shaw, A. S., Allen, P. M. and Dustin, M. L. The immunological synapse: a molecular machine controlling T cell activation. *Science* **285**, 221, 1999.
185. Steinman, R. M., Hawiger, D. and Nussenzweig, M. C. Tolerogenic dendritic cells. *Annu Rev Immunol* **21**, 685, 2003.
186. Hamaguchi, K., Utsunomiya, N., Takaki, R., Yoshimatsu, H. and Sakata, T. Cellular interaction between mouse pancreatic alpha-cell and beta-cell lines: possible contact-dependent inhibition of insulin secretion. *Exp Biol Med (Maywood)* **228**, 1227, 2003.
187. Bartness, T. J., Shrestha, Y. B., Vaughan, C. H., Schwartz, G. J. and Song, C. K. Sensory and sympathetic nervous system control of white adipose tissue lipolysis. *Mol Cell Endocrinol* 2009.
188. Martin, T. J. and Sims, N. A. Osteoclast-derived activity in the coupling of bone formation to resorption. *Trends Mol Med* **11**, 76, 2005.
189. Risau, W. Mechanisms of angiogenesis. *Nature* **386**, 671, 1997.
190. Carmeliet, P. Angiogenesis in life, disease and medicine. *Nature* **438**, 932, 2005.
191. Carmeliet, P. Angiogenesis in health and disease. *Nat Med* **9**, 653, 2003.
192. Reid, R. L., Fretts, R. and Van Vugt, D. A. The theory and practice of ovulation induction with gonadotropin-releasing hormone. *Am J Obstet Gynecol* **158**, 176, 1988.
193. Kim, B. S., Smith, R. C., Poon, Z. and Hammond, P. T. MAD (multiagent delivery) nanolayer: delivering multiple therapeutics from hierarchically assembled surface coatings. *Langmuir* **25**, 14086, 2009.

194. Hammond, P. T. Form and function in multilayer assembly: New applications at the nanoscale. *Advanced Materials* **16**, 1271, 2004.
195. Rothstein, S. N., Federspiel, W. J. and Little, S. R. A simple model framework for the prediction of controlled release from bulk eroding polymer matrices. *J Mater Chem* **18**, 1873, 2008.
196. Rothstein, S. N., Federspiel, W. J. and Little, S. R. A unified mathematical model for the prediction of controlled release from surface and bulk eroding polymer matrices. *Biomaterials* **30**, 1657, 2009.
197. Cohen, S., Yoshioka, T., Lucarelli, M., Hwang, L. H. and Langer, R. Controlled delivery systems for proteins based on poly(lactic/glycolic acid) microspheres. *Pharm Res* **8**, 713, 1991.
198. Mikos, A. G., Thorsen, A. J., Czerwonka, L. A., Bao, Y., Langer, R., Winslow, D. N. and Vacanti, J. P. Preparation and Characterization of Poly(L-Lactic Acid) Foams. *Polymer* **35**, 1068, 1994.
199. Sachlos, E. and Czernuszka, J. T. Making tissue engineering scaffolds work. Review: the application of solid freeform fabrication technology to the production of tissue engineering scaffolds. *Eur Cell Mater* **5**, 29, 2003.
200. Mooney, D. J., Baldwin, D. F., Suh, N. P., Vacanti, J. P. and Langer, R. Novel approach to fabricate porous sponges of poly(D,L-lactic-co-glycolic acid) without the use of organic solvents. *Biomaterials* **17**, 1417, 1996.
201. Cima, L. G., Vacanti, J. P., Vacanti, C., Ingber, D., Mooney, D. and Langer, R. Tissue Engineering by Cell Transplantation Using Degradable Polymer Substrates. *Journal of Biomechanical Engineering-Transactions of the Asme* **113**, 143, 1991.
202. Mikos, A. G., Bao, Y., Cima, L. G., Ingber, D. E., Vacanti, J. P. and Langer, R. Preparation of poly(glycolic acid) bonded fiber structures for cell attachment and transplantation. *J Biomed Mater Res* **27**, 183, 1993.
203. Lo, W., Stevens, R., Doyle, R., Campbell, A. M. and Liang, W. Y. Fabrication and Characterization of Highly Textured (Bi,Pb)(2)Sr2ca2cu3ox Superconducting Ceramics Using High Magnetic-Field and Cold Isostatic Pressing. *Journal of Materials Research* **10**, 2433, 1995.
204. Thomson, R. C., Yaszemski, M. J., Powers, J. M. and Mikos, A. G. Fabrication of Biodegradable Polymer Scaffolds to Engineer Trabecular Bone. *Journal of Biomaterials Science-Polymer Edition* **7**, 23, 1995.

205. Hsu, Y. Y., Gresser, J. D., Trantolo, D. J., Lyons, C. M., Gangadharam, P. R. and Wise, D. L. Effect of polymer foam morphology and density on kinetics of in vitro controlled release of isoniazid from compressed foam matrices. *J Biomed Mater Res* **35**, 107, 1997.
206. Yannas, I. V., Burke, J. F., Gordon, P. L., Huang, C. and Rubenstein, R. H. Design of an artificial skin. II. Control of chemical composition. *J Biomed Mater Res* **14**, 107, 1980.
207. Dagalakakis, N., Flink, J., Stasikelis, P., Burke, J. F. and Yannas, I. V. Design of an artificial skin. Part III. Control of pore structure. *J Biomed Mater Res* **14**, 511, 1980.
208. Doillon, C. J., Whyne, C. F., Brandwein, S. and Silver, F. H. Collagen-based wound dressings: control of the pore structure and morphology. *J Biomed Mater Res* **20**, 1219, 1986.
209. Sachlos, E., Reis, N., Ainsley, C., Derby, B. and Czernuszka, J. T. Novel collagen scaffolds with predefined internal morphology made by solid freeform fabrication. *Biomaterials* **24**, 1487, 2003.
210. Madihally, S. V. and Matthew, H. W. Porous chitosan scaffolds for tissue engineering. *Biomaterials* **20**, 1133, 1999.
211. Glicklis, R., Shapiro, L., Agbaria, R., Merchuk, J. C. and Cohen, S. Hepatocyte behavior within three-dimensional porous alginate scaffolds. *Biotechnol Bioeng* **67**, 344, 2000.
212. Schmitz, J. P. and Hollinger, J. O. A preliminary study of the osteogenic potential of a biodegradable alloplastic-osteoinductive alloimplant. *Clin Orthop Relat Res* **245**, 1988.
213. Chen, R. R., Silva, E. A., Yuen, W. W. and Mooney, D. J. Spatio-temporal VEGF and PDGF delivery patterns blood vessel formation and maturation. *Pharm Res* **24**, 258, 2007.
214. Hao X, Silva EA, Månsson-Broberg A, Grinnemo KH, Siddiqui AJ, Dellgren G, Wårdell E, Brodin LA, Mooney DJ and Sylvén C. Angiogenic effects of sequential release of VEGF-A165 and PDGF-BB with alginate hydrogels after myocardial infarction. *Cardiovascular Research* **75**, 178, 2007.
215. Holland, T. A., Tabata, Y. and Mikos, A. G. Dual growth factor delivery from degradable oligo(poly(ethylene glycol) fumarate) hydrogel scaffolds for cartilage tissue engineering. *J Control Release* **101**, 111, 2005.
216. Sun, Q., Silva, E. A., Wang, A., Fritton, J. C., Mooney, D. J., Schaffler, M. B., Grossman, P. M. and Rajagopalan, S. Sustained release of multiple growth factors from injectable polymeric system as a novel therapeutic approach towards angiogenesis. *Pharm Res* **27**, 264, 2010.

217. Peyratout, C. S. and Dahne, L. Tailor-made polyelectrolyte microcapsules: from multilayers to smart containers. *Angew Chem Int Ed Engl* **43**, 3762, 2004.
218. Wood, K. C., Chuang, H. F., Batten, R. D., Lynn, D. M. and Hammond, P. T. Controlling interlayer diffusion to achieve sustained, multiagent delivery from layer-by-layer thin films. *Proc Natl Acad Sci U S A* **103**, 10207, 2006.
219. Jewell, C. M. and Lynn, D. M. Multilayered polyelectrolyte assemblies as platforms for the delivery of DNA and other nucleic acid-based therapeutics. *Adv Drug Deliv Rev* **60**, 979, 2008.
220. Macdonald, M. L., Rodriguez, N. M., Shah, N. J. and Hammond, P. T. Characterization of tunable fgf-2 releasing polyelectrolyte multilayers. *Biomacromolecules* **11**, 2053, 2010.
221. Su, X., Kim, B. S., Kim, S. R., Hammond, P. T. and Irvine, D. J. Layer-by-layer-assembled multilayer films for transcutaneous drug and vaccine delivery. *ACS Nano* **3**, 3719, 2009.
222. Wood, K. C., Boedicker, J. Q., Lynn, D. M. and Hammond, P. T. Tunable drug release from hydrolytically degradable layer-by-layer thin films. *Langmuir* **21**, 1603, 2005.
223. Richards Grayson, A. C., Choi, I. S., Tyler, B. M., Wang, P. P., Brem, H., Cima, M. J. and Langer, R. Multi-pulse drug delivery from a resorbable polymeric microchip device. *Nat Mater* **2**, 767, 2003.
224. Langer, R. and Tirrell, D. A. Designing materials for biology and medicine. *Nature* **428**, 487, 2004.
225. Berg, M. C., Zhai, L., Cohen, R. E. and Rubner, M. F. Controlled drug release from porous polyelectrolyte multilayers. *Biomacromolecules* **7**, 357, 2006.
226. Moskowitz, J. S., Blaisse, M. R., Samuel, R. E., Hsu, H. P., Harris, M. B., Martin, S. D., Lee, J. C., Spector, M. and Hammond, P. T. The effectiveness of the controlled release of gentamicin from polyelectrolyte multilayers in the treatment of *Staphylococcus aureus* infection in a rabbit bone model. *Biomaterials* **31**, 6019, 2010.
227. Soundrapandian, C., Datta, S. and Sa, B. Drug-eluting implants for osteomyelitis. *Crit Rev Ther Drug Carrier Syst* **24**, 493, 2007.
228. Jessel, N., Oulad-Abdelghani, M., Meyer, F., Lavalle, P., Haikel, Y., Schaaf, P. and Voegel, J. C. Multiple and time-scheduled in situ DNA delivery mediated by beta-cyclodextrin embedded in a polyelectrolyte multilayer. *Proc Natl Acad Sci U S A* **103**, 8618, 2006.

229. Ariga, K., Hill, J. P. and Ji, Q. Biomaterials and biofunctionality in layered macromolecular assemblies. *Macromol Biosci* **8**, 981, 2008.
230. Santini, J. T., Jr., Richards, A. C., Scheidt, R. A., Cima, M. J. and Langer, R. S. Microchip technology in drug delivery. *Ann Med* **32**, 377, 2000.
231. Shoji, S. and Esashi, M. Microflow Devices and Systems. *Journal of Micromechanics and Microengineering* **4**, 157, 1994.
232. Santini, J. T., Cima, M. J. and Langer, R. A controlled-release microchip. *Nature* **397**, 335, 1999.
233. Shive, M. S. and Anderson, J. M. Biodegradation and biocompatibility of PLA and PLGA microspheres. *Adv Drug Deliv Rev* **28**, 5, 1997.
234. Tamada, J. A. and Langer, R. Erosion kinetics of hydrolytically degradable polymers. *Proc Natl Acad Sci U S A* **90**, 552, 1993.
235. Kulkarni, R. K., Moore, E. G., Hegyeli, A. F. and Leonard, F. Biodegradable poly(lactic acid) polymers. *J Biomed Mater Res* **5**, 169, 1971.
236. Maloney, J. M. and Santini, J. T., Jr. Implantable microchips for controlled drug delivery. *Conf Proc IEEE Eng Med Biol Soc* **4**, 2668, 2004.
237. Prescott, J. H., Krieger, T. J., Lipka, S. and Staples, M. A. Dosage form development, in vitro release kinetics, and in vitro-in vivo correlation for leuprolide released from an implantable multi-reservoir array. *Pharm Res* **24**, 1252, 2007.
238. Jain, R. A. The manufacturing techniques of various drug loaded biodegradable poly(lactide-co-glycolide) (PLGA) devices. *Biomaterials* **21**, 2475, 2000.
239. Godin, B., Gu, J., Serda, R. E., Bhavane, R., Tasciotti, E., Chiappini, C., Liu, X., Tanaka, T., Decuzzi, P. and Ferrari, M. Tailoring the degradation kinetics of mesoporous silicon structures through PEGylation. *J Biomed Mater Res A* **94**, 1236, 2010.
240. Siepmann, J. and Gopferich, A. Mathematical modeling of bioerodible, polymeric drug delivery systems. *Adv Drug Deliv Rev* **48**, 229, 2001.
241. Saltzman, W. M. and Langer, R. Transport rates of proteins in porous materials with known microgeometry. *Biophys J* **55**, 163, 1989.
242. Gopferich, A. and Langer, R. Modeling Monomer Release from Bioerodible Polymers. *Journal of Controlled Release* **33**, 55, 1995.

243. Rothstein, S. N. and Little, S. R. A "tool box" for rational design of degradable controlled release formulations. *Journal of Materials Chemistry* **21**, 2010.
244. Cao, L. and Mooney, D. J. Spatiotemporal control over growth factor signaling for therapeutic neovascularization. *Adv Drug Deliv Rev* **59**, 1340, 2007.
245. Lalani, Z., Wong, M., Brey, E. M., Mikos, A. G. and Duke, P. J. Spatial and temporal localization of transforming growth factor-beta1, bone morphogenetic protein-2, and platelet-derived growth factor-A in healing tooth extraction sockets in a rabbit model. *J Oral Maxillofac Surg* **61**, 1061, 2003.
246. Bourque, W. T., Gross, M. and Hall, B. K. Expression of four growth factors during fracture repair. *Int J Dev Biol* **37**, 573, 1993.
247. Bostrom, M. P., Lane, J. M., Berberian, W. S., Missri, A. A., Tomin, E., Weiland, A., Doty, S. B., Glaser, D. and Rosen, V. M. Immunolocalization and expression of bone morphogenetic proteins 2 and 4 in fracture healing. *J Orthop Res* **13**, 357, 1995.
248. Yu, Y., Yang, J. L., Chapman-Sheath, P. J. and Walsh, W. R. TGF-beta, BMPS, and their signal transducing mediators, Smads, in rat fracture healing. *J Biomed Mater Res* **60**, 392, 2002.
249. Guldberg, R. E. Spatiotemporal delivery strategies for promoting musculoskeletal tissue regeneration. *J Bone Miner Res* **24**, 1507, 2009.
250. Gavrilovskaya, I. N., Gorbunova, E. E., Mackow, N. A. and Mackow, E. R. Hantaviruses direct endothelial cell permeability by sensitizing cells to the vascular permeability factor VEGF, while angiopoietin 1 and sphingosine 1-phosphate inhibit hantavirus-directed permeability. *J Virol* **82**, 5797, 2008.
251. McVerry, B. J. and Garcia, J. G. In vitro and in vivo modulation of vascular barrier integrity by sphingosine 1-phosphate: mechanistic insights. *Cell Signal* **17**, 131, 2005.
252. Greenberg, J. I., Shields, D. J., Barillas, S. G., Acevedo, L. M., Murphy, E., Huang, J., Schepke, L., Stockmann, C., Johnson, R. S., Angle, N. and Cheresch, D. A. A role for VEGF as a negative regulator of pericyte function and vessel maturation. *Nature* **456**, 809, 2008.
253. Nillesen, S. T., Geutjes, P. J., Wismans, R., Schalkwijk, J., Daamen, W. F. and van Kuppevelt, T. H. Increased angiogenesis and blood vessel maturation in acellular collagen-heparin scaffolds containing both FGF2 and VEGF. *Biomaterials* **28**, 1123, 2007.

254. Riley, C. M., Fuegy, P. W., Firpo, M. A., Shu, X. Z., Prestwich, G. D. and Peattie, R. A. Stimulation of in vivo angiogenesis using dual growth factor-loaded crosslinked glycosaminoglycan hydrogels. *Biomaterials* **27**, 5935, 2006.
255. Hasegawa M, Sudo A, Komlev VS, Barinov SM and Uchida A. High release of antibiotic from a novel hydroxyapatite with bimodal pore size distribution. *J Biomed Mater Res B Appl Biomater* **70**, 332, 2004.
256. Nunes SP and Inoue T. Evidence for spinodal decomposition and nucleation and growth mechanisms during membrane formation. *J Membr Sci* **111**, 93, 1996.
257. Shih CH, Gryte CC and Cheng LP. Morphology of membranes formed by the isothermal precipitation of polyamide solutions from water/formic acid systems. *J Appl Polym Sci* **96**, 944, 2005.
258. van de Witte P, Dijkstra PJ, van den Berg JWA and Feijen J. Phase separation processes in polymer solutions in relation to membrane formation. *J Membr Sci* **117**, 1, 1996.
259. Ye, S. H., Watanabe, J., Takai, M., Iwasaki, Y. and Ishihara, K. Design of functional hollow fiber membranes modified with phospholipid polymers for application in total hemopurification system. *Biomaterials* **26**, 5032, 2005.
260. Akhtar N, Dickerson EB and Auerbach R. The sponge/Matrigel angiogenesis assay. *Angiogenesis* **5**, 75, 2002.
261. Thurston, G., Wang, Q., Baffert, F., Rudge, J., Papadopoulos, N., Jean-Guillaume, D., Wiegand, S., Yancopoulos, G. D. and McDonald, D. M. Angiopoietin 1 causes vessel enlargement, without angiogenic sprouting, during a critical developmental period. *Development* **132**, 3317, 2005.
262. Baudelet, C., Cron, G. O., Ansiaux, R., Crockart, N., DeWever, J., Feron, O. and Gallez, B. The role of vessel maturation and vessel functionality in spontaneous fluctuations of T2*-weighted GRE signal within tumors. *NMR Biomed* **19**, 69, 2006.
263. Sinha VR and Trehan A. Biodegradable microspheres for protein delivery. *J Control Release* **90**, 261, 2003.
264. Tilakaratne HK, Hunter SK, Andracki ME, Benda JA and Rodgers VG. Characterizing short-term release and neovascularization potential of multi-protein growth supplement delivered via alginate hollow fiber devices. *Biomaterials* **28**, 89, 2007.
265. Lazzeri L, Cascone MG, Quiriconi S, Morabito L and Giusti P. Biodegradable hollow microfibres to produce bioactive scaffolds. *Polym Int* **54**, 101, 2005.

266. Kawakami O, Miyamoto S, Hatano T, Yamada K, Hashimoto N and Tabata Y. Acceleration of aneurysm healing by hollow fiber enabling the controlled release of basic fibroblast growth factor. *Neurosurgery* **58**, 355, 2006.
267. Kaplan, O., Jaroszewski, J. W., Faustino, P. J., Zugmaier, G., Ennis, B. W., Lippman, M. and Cohen, J. S. Toxicity and effects of epidermal growth factor on glucose metabolism of MDA-468 human breast cancer cells. *J Biol Chem* **265**, 13641, 1990.
268. Franca-Koh, J. and Devreotes, P. N. Moving forward: mechanisms of chemoattractant gradient sensing. *Physiology (Bethesda)* **19**, 300, 2004.
269. Doheny, J. G., Jervis, E. J., Guarna, M. M., Humphries, R. K., Warren, R. A. J. and Kilburn, D. G. Cellulose as an inert matrix for presenting cytokines to target cells: production and properties of a stem cell factor-cellulose-binding domain fusion protein. *Biochem J* **339**, 429, 1999.
270. Freeman, I. and Cohen, S. The influence of the sequential delivery of angiogenic factors from affinity-binding alginate scaffolds on vascularization. *Biomaterials* **30**, 2122, 2009.
271. Isner, J. M., Pieczek, A., Schainfeld, R., Blair, R., Haley, L., Asahara, T., Rosenfield, K., Razvi, S., Walsh, K. and Symes, J. F. Clinical evidence of angiogenesis after arterial gene transfer of phVEGF165 in patient with ischaemic limb. *Lancet* **348**, 370, 1996.
272. Okamoto, H., Takuwa, N., Yokomizo, T., Sugimoto, N., Sakurada, S., Shigematsu, H. and Takuwa, Y. Inhibitory regulation of Rac activation, membrane ruffling, and cell migration by the G protein-coupled sphingosine-1-phosphate receptor EDG5 but not EDG1 or EDG3. *Mol Cell Biol* **20**, 9247, 2000.
273. Cuvillier, O., Rosenthal, D. S., Smulson, M. E. and Spiegel, S. Sphingosine 1-phosphate inhibits activation of caspases that cleave poly(ADP-ribose) polymerase and lamins during Fas- and ceramide-mediated apoptosis in Jurkat T lymphocytes. *J Biol Chem* **273**, 2910, 1998.
274. Bergers, G. and Song, S. The role of pericytes in blood-vessel formation and maintenance. *Neuro Oncol* **7**, 452, 2005.
275. Betsholtz, C., Lindblom, P. and Gerhardt, H. Role of pericytes in vascular morphogenesis. *Exs* **115**, 2005.
276. Hellstrom, M., Gerhardt, H., Kalen, M., Li, X., Eriksson, U., Wolburg, H. and Betsholtz, C. Lack of pericytes leads to endothelial hyperplasia and abnormal vascular morphogenesis. *J Cell Biol* **153**, 543, 2001.

277. Enge, M., Bjarnegard, M., Gerhardt, H., Gustafsson, E., Kalen, M., Asker, N., Hammes, H. P., Shani, M., Fassler, R. and Betsholtz, C. Endothelium-specific platelet-derived growth factor-B ablation mimics diabetic retinopathy. *Embo J* **21**, 4307, 2002.
278. Kano MR, Morishita Y, Iwata C, Iwasaka S, Watabe T, Ouchi Y, Miyazono K and Miyazawa K. VEGF-A and FGF-2 synergistically promote neoangiogenesis through enhancement of endogenous PDGF-B-PDGFRbeta signaling. *J Cell Sci* **118**, 3759, 2005.
279. Huang, Z., Nelson, E. R., Smith, R. L. and Goodman, S. B. The sequential expression profiles of growth factors from osteoprogenitors [correction of osteroprogenitors] to osteoblasts in vitro. *Tissue Eng* **13**, 2311, 2007.
280. Facchiano, A., De Marchis, F., Turchetti, E., Facchiano, F., Guglielmi, M., Denaro, A., Palumbo, R., Scoccianti, M. and Capogrossi, M. C. The chemotactic and mitogenic effects of platelet-derived growth factor-BB on rat aorta smooth muscle cells are inhibited by basic fibroblast growth factor. *J Cell Sci* **113** (Pt 16), 2855, 2000.
281. Tengood, J. E., Kovach, K. M., Vescovi, P. E., Russell, A. J. and Little, S. R. Sequential delivery of vascular endothelial growth factor and sphingosine 1-phosphate for angiogenesis. *Biomaterials* **31**, 7805, 2010.
282. Lee, H. J., Lee, H. J., Song, G. Y., Li, G., Lee, J. H., Lu, J. and Kim, S. H. 6-(1-Oxobutyl)-5,8-dimethoxy-1,4-naphthoquinone inhibits lewis lung cancer by antiangiogenesis and apoptosis. *Int J Cancer* **120**, 2481, 2007.
283. Borges J, Müller MC, Momeni A, Stark GB and Torio-Padron N. In vitro analysis of the interactions between preadipocytes and endothelial cells in a 3D fibrin matrix. *Minimally Invasive Therapy and Allied Technologies* **16**, 141, 2007.
284. Hughes, A. D., Clunn, G. F., Refson, J. and Demoliou-Mason, C. Platelet-derived growth factor (PDGF): actions and mechanisms in vascular smooth muscle. *Gen Pharmacol* **27**, 1079, 1996.
285. Chegini, N., Rossi, M. J. and Masterson, B. J. Platelet-derived growth factor (PDGF), epidermal growth factor (EGF), and EGF and PDGF beta-receptors in human endometrial tissue: localization and in vitro action. *Endocrinology* **130**, 2373, 1992.
286. Peters, M. C., Polverini, P. J. and Mooney, D. J. Engineering vascular networks in porous polymer matrices. *J Biomed Mater Res* **60**, 668, 2002.
287. Patel, Z. S., Young, S., Tabata, Y., Jansen, J. A., Wong, M. E. and Mikos, A. G. Dual delivery of an angiogenic and an osteogenic growth factor for bone regeneration in a critical size defect model. *Bone* **43**, 931, 2008.

288. Yamamoto, M., Ikada, Y. and Tabata, Y. Controlled release of growth factors based on biodegradation of gelatin hydrogel. *J Biomater Sci Polym Ed* **12**, 77, 2001.
289. Faham, S., Hileman, R. E., Fromm, J. R., Linhardt, R. J. and Rees, D. C. Heparin structure and interactions with basic fibroblast growth factor. *Science* **271**, 1116, 1996.
290. Pellegrini, L., Burke, D. F., von Delft, F., Mulloy, B. and Blundell, T. L. Crystal structure of fibroblast growth factor receptor ectodomain bound to ligand and heparin. *Nature* **407**, 1029, 2000.
291. Pellegrini, L. Role of heparan sulfate in fibroblast growth factor signalling: a structural view. *Curr Opin Struct Biol* **11**, 629, 2001.
292. Gosain, A., Matthies, A. M., Dovi, J. V., Barbul, A., Gamelli, R. L. and DiPietro, L. A. Exogenous pro-angiogenic stimuli cannot prevent physiologic vessel regression. *J Surg Res* **135**, 218, 2006.
293. Matthies, A. M., Low, Q. E., Lingen, M. W. and DiPietro, L. A. Neuropilin-1 participates in wound angiogenesis. *Am J Pathol* **160**, 289, 2002.
294. Dang, D. T., Chun, S. Y., Burkitt, K., Abe, M., Chen, S., Havre, P., Mabweesh, N. J., Heath, E. I., Vogelzang, N. J., Cruz-Correa, M., Blayney, D. W., Ensminger, W. D., St Croix, B., Dang, N. H. and Dang, L. H. Hypoxia-inducible factor-1 target genes as indicators of tumor vessel response to vascular endothelial growth factor inhibition. *Cancer Res* **68**, 1872, 2008.
295. Heldin, C. H. and Westermark, B. Mechanism of action and in vivo role of platelet-derived growth factor. *Physiol Rev* **79**, 1283, 1999.
296. Schollmann, C., Grugel, R., Tatje, D., Hoppe, J., Folkman, J., Marme, D. and Weich, H. A. Basic fibroblast growth factor modulates the mitogenic potency of the platelet-derived growth factor (PDGF) isoforms by specific upregulation of the PDGF alpha receptor in vascular smooth muscle cells. *J Biol Chem* **267**, 18032, 1992.
297. Wang, S. J., Greer, P. and Auerbach, R. Isolation and propagation of yolk-sac-derived endothelial cells from a hypervascular transgenic mouse expressing a gain-of-function *fps/fes* proto-oncogene. *In Vitro Cell Dev Biol Anim* **32**, 292, 1996.
298. Sampath, T. K., Maliakal, J. C., Hauschka, P. V., Jones, W. K., Sasak, H., Tucker, R. F., White, K. H., Coughlin, J. E., Tucker, M. M., Pang, R. H. and et al. Recombinant human osteogenic protein-1 (hOP-1) induces new bone formation in vivo with a specific activity comparable with natural bovine osteogenic protein and stimulates osteoblast proliferation and differentiation in vitro. *J Biol Chem* **267**, 20352, 1992.

299. Wang, E. A., Rosen, V., D'Alessandro, J. S., Bauduy, M., Cordes, P., Harada, T., Israel, D. I., Hewick, R. M., Kerns, K. M., LaPan, P. and et al. Recombinant human bone morphogenetic protein induces bone formation. *Proc Natl Acad Sci U S A* **87**, 2220, 1990.
300. Wozney, J. M. The bone morphogenetic protein family and osteogenesis. *Mol Reprod Dev* **32**, 160, 1992.
301. Cheng, H., Jiang, W., Phillips, F. M., Haydon, R. C., Peng, Y., Zhou, L., Luu, H. H., An, N., Breyer, B., Vanichakarn, P., Szatkowski, J. P., Park, J. Y. and He, T. C. Osteogenic activity of the fourteen types of human bone morphogenetic proteins (BMPs). *J Bone Joint Surg Am* **85-A**, 1544, 2003.
302. Nakatsuka, S., Nakate, I. and Miyano, T. Drinking water treatment by using ultrafiltration hollow fiber membranes. *Desalination* **106**, 55, 1996.
303. Lee, K.-C. and Rittmann, B. E. Applying a novel autohydrogenotrophic hollow-fiber membrane biofilm reactor for denitrification of drinking water. *Water Research* **36**, 2040, 2002.
304. Li, J.-M., Xu, Z.-K., Liu, Z.-M., Yuan, W.-F., Xiang, H., Wang, S.-Y. and Xu, Y.-Y. Microporous polypropylene and polyethylene hollow fiber membranes. Part 3. Experimental studies on membrane distillation for desalination. *Desalination* **155**, 153, 2003.
305. Barry, R. B. and Brian, M. K. Hollow Fiber Ultrafiltration of Cottage Cheese Whey: Performance Study. *Journal of dairy science* **60**, 1379, 1977.
306. Tsuneda, S., Saito, K., Furusaki, S., Sugo, T. and Okamoto, J. Metal collection using chelating hollow fiber membrane. *Journal of Membrane Science* **58**, 221, 1991.
307. Benítez, J., Rodríguez, A. and Malaver, R. Stabilization and dewatering of wastewater using hollow fiber membranes. *Water Research* **29**, 2281, 1995.
308. Prasad, R. and Sirkar, K. K. Hollow fiber solvent extraction of pharmaceutical products: A case study. *Journal of Membrane Science* **47**, 235, 1989.
309. Rao, M. A., Acree, T. E., Cooley, H. J. and Ennis, R. W. Clarification of Apple Juice by Hollow Fiber Ultrafiltration: Fluxes and Retention of Odor-Active Volatiles. *Journal of Food Science* **52**, 375, 1987.
310. Kirk, D. E., Montgomery, M. W. and Kortekaas, M. G. Clarification of Pear Juice by Hollow Fiber Ultrafiltration. *Journal of Food Science* **48**, 1663, 1983.

311. Hong, S. P., Bae, T. H., Tak, T. M., Hong, S. and Randall, A. Fouling control in activated sludge submerged hollow fiber membrane bioreactors. *Desalination* **143**, 219, 2002.
312. Ortiz, I., Urriaga, A., Abellan, M. J. and San Roman, F. Application of hollow fiber membrane contactors for catalyst recovery in the WPO process. *Ann N Y Acad Sci* **984**, 17, 2003.
313. Liao, Z. J., Klein, E., Poh, C. K., Huang, Z. P., Lu, J. F., Hardy, P. A. and Gao, D. Y. Measurement of hollow fiber membrane transport properties in hemodialyzers. *Journal of Membrane Science* **256**, 176, 2005.
314. Labecki, M., Weber, I., Dudal, Y., Koska, J., Piret, J. M. and Bowen, B. D. Hindered transmembrane protein transport in hollow-fibre devices. *Journal of Membrane Science* **146**, 197, 1998.
315. Anderson, T. A., Yu, V., Hom, D. B. and Odland, R. M. Interstitial delivery of vascular endothelial growth factor to skin flaps. *Arch Facial Plast Surg* **12**, 326, 2010.
316. Bostrom, M. P. G., Lane, J. M., Berberian, W. S., Missri, A. A. E., Tomin, E., Weiland, A., Doty, S. B., Glaser, D. and Rosen, V. M. Immunolocalization and Expression of Bone Morphogenetic Protein-2 and Protein-4 in Fracture-Healing. *Journal of Orthopaedic Research* **13**, 357, 1995.
317. Wupper, A., Dellanna, F., Baldamus, C. A. and Woermann, D. Local transport processes in high-flux hollow fiber dialyzers. *Journal of Membrane Science* **131**, 181, 1997.
318. Locatelli, F., Manzoni, C. and Di Filippo, S. The importance of convective transport. *Kidney International* **61**, S115, 2002.
319. Kargol, A. A mechanistic model of transport processes in porous membranes generated by osmotic and hydrostatic pressure. *Journal of Membrane Science* **191**, 61, 2001.
320. Hancock, N. T. and Cath, T. Y. Solute Coupled Diffusion in Osmotically Driven Membrane Processes. *Environmental Science & Technology* **43**, 6769, 2009.
321. Kedem, O. and Katchalsky, A. A physical interpretation of the phenomenological coefficients of membrane permeability. *J Gen Physiol* **45**, 143, 1961.
322. Kedem, O. and Katchalsky, A. Thermodynamic analysis of the permeability of biological membranes to non-electrolytes. *Biochim Biophys Acta* **27**, 229, 1958.
323. Sakai, K. Determination of Pore-Size and Pore-Size Distribution .2. Dialysis Membranes. *Journal of Membrane Science* **96**, 91, 1994.

324. Andreoli, T. E., Schafer, J. A. and Troutman, S. L. Coupling of solute and solvent flows in porous lipid bilayer membranes. *J Gen Physiol* **57**, 479, 1971.
325. Rasubala, L., Yoshikawa, H., Nagata, K., Iijima, T. and Ohishi, M. Platelet-derived growth factor and bone morphogenetic protein in the healing of mandibular fractures in rats. *Br J Oral Maxillofac Surg* **41**, 173, 2003.
326. Hollinger, J. and Wong, M. E. The integrated processes of hard tissue regeneration with special emphasis on fracture healing. *Oral Surg Oral Med Oral Pathol Oral Radiol Endod* **82**, 594, 1996.